AIR FORCE INSTITUTE OF TECHNOLOGY

AIR UNIVERSITY
UNITED STATES AIR FORCE

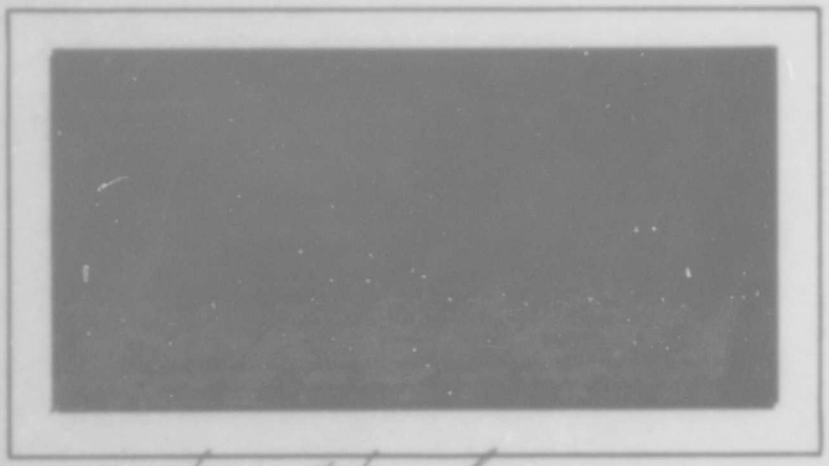

140 p $4.00 hc
$1.00 mf

SCHOOL OF ENGINEERING

WRIGHT-PATTERSON AIR FORCE BASE, OHIO

AF-WP-O-SEP 63 3M

A FEASIBILITY STUDY OF A HIGH-TEMPERATURE, LIQUID ALUMINUM COOLED, FLUIDIZED BED NUCLEAR POWER REACTOR

Lt. Kenneth R. Hooks

GNE/Phys/64-10

BLANK PAGE

A FEASIBILITY STUDY OF A HIGH-TEMPERATURE LIQUID ALUMINUM COOLED, FLUIDIZED BED NUCLEAR POWER REACTOR

THESIS

Presented to the Faculty of the School of Engineering of
the Air Force Institute of Technology
Air University
in Partial Fulfillment of the
Requirements for the Degree of
Master of Science

By
Kenneth Robert Hooks, B. A. Phys.
Lt. USAF
Graduate Nuclear Engineering
August 1964

Preface

When this feasibility study was begun, I anticipated that most of the work would be on the nuclear aspects of the design. As it turned out, more than half of my time was taken by the materials problem, which was essentially a literature search. It should be noted that the amount of information available on material properties at high temperatures is both very limited and well distributed among many unrelated journals, most of which have nothing to do with nuclear engineering. The problems of heat transfer and fluid flow also took much longer to solve than was anticipated, and so the reactor calculations were limited to the minimum amount which would indicate trends of the system.

The bibliography includes all the important references containing information on either materials or fluidized beds which I was able to find, but it does not list such sources as "Nuclear Science Abstracts" or "Chemical Abstracts", which were extensively used. The body of this report has also been shorn of much material which I felt was superfluous, including a discussion of the derivation of two-group diffusion theory.

I would like to thank both Mr. Cook and Mr. Vincze from the AFIT Library and Mrs. Denning from the Physics Department for the assistance they gave me, without which my work would have been much more difficult. Finally, I thank my wife for her help in preparing this report, and for her calm in the midst of the storm.

Kenneth R. Hooks

Contents

List of Figures

Abstract

A feasibility study of a high temperature, liquid-metal-cooled nuclear power reactor depends upon considerations of materials, heat transfer, fluid flow and nuclear parameters as well as certain design guidelines. The criteria of a coolant outlet temperature of 2000°C and a low pressure core, plus good nuclear and heat transfer properties, led to the choice of liquid aluminum as the coolant. A compatibility study determined that only aluminum mononitride is inert to aluminum at 2000°C, and must be used for constructing the core. Since no uranium or plutonium compounds are inert to liquid aluminum at 2000°C, fuel elements of uranium mononitride were chosen on the basis of probable compatibility with the required aluminum nitride cladding. Consideration of the heat transfer effects led to the choice of micron-size coated fuel particles in a cylindrical fluidized bed core. Three methods of determining the parameters of the fluidized bed were used to indicate the best particle size and aluminum flow rate in the core for any desired power level. The nuclear parameters of the system were studied using two-group diffusion theory and an infinitely reflected spherical geometry. The results predict a fast core with a critical mass above ten kilograms, and indicate that the reactor may be made inherently stable by correct design of the core.

I. Introduction

The great variety in both type and purpose of nuclear reactors requires that any attempt to design such a system must start with the establishment of the criteria which the reactor must meet. These guide lines perform the functions of: (1) defining the purpose of the design study, (2) suggesting ways in which the problem may be attacked, and (3) providing a check upon the value of the results.

Problem

This report presents the results of a feasibility study of a very high temperature, liquid-metal-cooled nuclear power reactor, based upon the following criteria. First, the reactor should be capable of operation with a coolant outlet temperature of about 2000°C. Second, a liquid-metal heat-transfer agent should be used to cool the core, to eliminate the problems of pressurization.

The temperature requirement reflects the desire to improve heat transfer characteristics in the power cycle (heat exchanger) of the system, where efficiency improves with increasing temperature. The use of a normal liquid or gaseous coolant at the proposed outlet temperature would result in very high operating pressures, and this consideration led to the second criterion.

Current liquid-metal-cooled reactors, using coolants such as sodium or NaK, achieve peak fuel temperatures of about 600°C, with maximum coolant temperatures at the outlet of about 500°C. (4: 444-449). Reactors have been proposed which would be fueled with a liquid uranium (or plutonium) metal alloy or a slurry of liquid-metal coolant and refractory fuel. These reactors are expected to operate with coolant outlet temperatures near 1000°C. In particular, one design for a slurry-fueled reactor specifies a peak fuel temperature of 1500°C and a maximum outlet temperature

of 1100°C (9: 1-3). In general, little consideration has been given to liquid (metal or otherwise) cooled reactors for use above 1000°C.

Scope

The problem was treated in as general a fashion as possible, within the limits imposed by the guide lines and available time. No experimental work was performed, so all the results are based upon literature searches and theoretical calculations. Where no generally accepted property values or defining relationships were available, extrapolations were made. The main effort was given to the materials problem and core design, with little attention given to pumping, heat exchange or technical problems of flow systems outside the core.

Method of Attack

The design problem was attacked by first considering the materials requirements, then heat transfer and probable core geometry, and finally determining the nuclear parameters of the reactor under operating conditions (steady state). Since each step is almost completely dependent upon the particular solution of the previous step, it was necessary to select only one "best" answer to each problem and base each successive answer upon the previous one.

Selection of the liquid-metal coolant was accomplished by elimination on the basis of nuclear properties, melting points and vapor pressures followed by comparison of the heat transfer properties of the remaining possibilities. Once the coolant was selected, a study of the compatibility of possible construction and fuel materials with the coolant was performed.

When the materials selection was completed, further comparison of the thermodynamic and thermochemical properties of the materials led to a particular type of fuel element. Consideration of the necessary heat output of the reactor (megawatts of thermal power) and the probable thermal stresses in the fuel elements resulted in the determination of a core configuration.

Lack of time limited the nuclear parameters study, resulting in the use of a simplified geometry and an analytical rather than a numerical solution to the flux equations. Although the results could not be checked against a known solution, they indicate that the final design selected will be inherently stable and controllable.

Summary

In the next three chapters of this report, a detailed discussion of the solutions to the problems of materials selection, heat transfer and core geometry, and determination of the nuclear parameters of the reactor are presented. The last chapter lists the conclusions which may be drawn from this feasibility study and some recommendations of areas for further study.

II. Selection of Materials

The materials which are selected for use in the core region of the reactor will be one of the deciding factors in the overall design. Their physical and nuclear properties will influence the core geometry, the coolant rate of flow, the fuel loading--and whether or not the design is practical. The materials problem consists of three parts: (1) the selection of the liquid-metal coolant, (2) determining which materials are inert to the selected coolant at 2000°C, and (3) the choice of the construction material(s) and fuel material.

A great many simplifying assumptions were made during the course of selecting materials, due to the lack of information and time. It should be noted that the lack of information is not peculiar to this report, but is inherent in any study of materials at very high temperatures.

Coolant

The first requirement of any coolant being considered for use in a nuclear reactor is a low neutron absorption cross section. Almost equally important are its heat transfer properties, including heat capacity, thermal conductivity, density and viscosity. To fit the criteria set forth in Chapter I, any coolant must have a low vapor pressure at 2000°C. Finally, if the coolant has a short activated product half-life, it will present less hazard in handling or repairs.

Aluminum was suggested as a possible coolant for a high temperature, low-pressure nuclear reactor by a design study performed in 1962 (1; 3). The nuclear properties of aluminum are excellent, as is evident by its use in reactors as a fuel matrix or cladding, and for structural purposes. Its heat transfer characteristics are not as well known, but it does have a high boiling temperature and a low density.

In order to justify the use of aluminum as the coolant, before spending time to determine its properties at 2000°C, four rather arbitrary criteria were selected by which other possible coolants could be compared to aluminum. First, all metal alloy systems were discarded for the following reasons: (1) the number of possible molten alloy systems is simply too great to consider, (2) the thermochemical relationships of a system are much easier to determine with a pure (single) metal coolant, and (3) a quick survey indicated that no alloy systems which would be good coolants at 2000°C have been discovered. Second, all elements with neutron absorption cross sections greater than one barn at either 0.025 eV or 1 MeV were eliminated. Third, metals with a melting temperature above 1000°C were discarded, and fourth, those metals which have a vapor pressure of more than one atmosphere at 2000°C were eliminated. Since the neutron cross sections and melting and boiling points of the elements are all well tabulated, and in fairly good agreement regardless of the source, the application of these criteria was simple.

Aluminum. The only liquid metal coolant which passed all of the above tests was aluminum. It has neutron absorption cross sections of 0.23 barns at 0.025 eV and 0.37 millibarns at 1 MeV. The activated product of Al^{27} (the only isotope) is Al^{28}, with a half life of 2.3 minutes (5: 2-13, 29). Aluminum melts at 660°C and has a vapor pressure of less than 100 mm Hg. at 2000°C. On the basis of the above results, molten aluminum was selected as the "best" coolant.

The heat transfer properties of liquid aluminum are neither well tabulated nor in agreement, with the exception of the values of heat capacity, C_p, and (usually) thermal conductivity, k. To determine the most likely values of these properties, an extensive literature survey was performed, supplemented by correspondence with laboratories and individual researchers (Appendix A).

Appendix B contains graphs of density, ρ, vapor pressure, p, and dynamic viscosity, μ, of molten aluminum as a function of temperature, and an explanation of the methods of extrapolation employed in each case. Values of the other physical properties of liquid aluminum which were not required for the calculations of fluid flow and nuclear parameters can also be found in the references noted on the graphs.

Although some attempts have been made to define a heat transfer number which would differentiate between good and not-so-good heat transfer agents, these methods are usually hedged by experimental results. In the Liquid-Metals Handbook, for instance, the heat transfer properties of sodium, NaK, bismuth, etc. are compared by plots of the change in heat content as a function of temperature (Btu/ 100°F) versus velocity in a one-inch tube, and also by plots of the heat transfer coefficient, h (Btu/ hr-ft^2 $^{\circ}$F) versus velocity in a one-inch tube (20: 18).

Murray (22: 156-157) states that a good coolant should have a high specific heat, high thermal conductivity and a high heat transfer coefficient to achieve maximum heat flow at minimum coolant flow rates and temperature. The heat transfer coefficient, h, is the rate at which heat can be transferred per unit area per degree difference in temperature between the heating surface and the fluid. The heat transfer coefficient is defined differently depending on the flow situation, and for liquid metals flowing in circular tubes or between parallel plates is

$$h = \frac{k}{D}\left[A + B\left(\frac{D\overline{u}_f \rho C_p}{k}\right)^C\right] \qquad (1)$$

where $\overline{u}_f$ is the average fluid velocity, D is the diameter of the pipe or twice the distance between the plates, A, B, and C are constants determined by conditions such as constant temperature, constant heat flux, etc. It is thus apparent that viscosity is not rate-determining in liquid metal heat transfer for tubes or parallel plates (4: 246-256).

Since h depends on D and $\overline{u_f}$ in the equations above, and will have another form for other geometries, no attempt was made to define an h which would prove aluminum to be a "good" heat transfer agent. Instead, a comparison between some of the property values of liquid aluminum at 2000°C and two other typical liquid-metal heat transfer agents at their probable maximum operating temperatures is offered in Table I as a method of determining the value of liquid aluminum as a coolant.

Vapor pressure is the only value in which liquid aluminum at 2000°C differs greatly from the other two liquid metals, and vapor pressure should not be a strong factor in determining the heat transfer in the system. Thus it appears that liquid aluminum will probably be an acceptable, if not a good heat-transfer agent at the desired temperature.

Table I

Comparison of Property Values*

	Aluminum (2000°C)	Sodium (500°C)	Bismuth (600°C)
Density (g/ cc)	2.0**	0.829	9.66
Dynamic Viscosity (centipoise)	2.0**	0.226	1.00
Heat Capacity (cal/ gm°C)	0.259	0.301	0.0359
Thermal Conductivity (cal/ sec cm^2 °C/cm)	0.2	0.016	0.037
Vapor Pressure (mm Hg)	50**	1.0	1.0

* (34: 613-640)

** Appendix B

Once the coolant has been selected, and its properties determined, a material(s) which is inert to attack by liquid aluminum at 2000°C must be found. If this cannot be done, or the material has nuclear properties which exclude it from consideration in the construction of the core region, the whole process of selecting a coolant must be repeated with differing criteria.

Compatibility

The compatibility of materials is an area in which a great deal of experimental work has been carried out, but without the development of a broad theory capable of accurate predictions of the interactions of different compounds (metallic or otherwise). The best tool available for theoretical predictions of reactions between compounds is the Gibbs' free energy equation, which is based upon experimentally obtained thermochemical data.

The criterion that a system of compounds (or elements) will not react is

$$\Sigma (n \Delta G)_{\text{products}} - \Sigma (n \Delta G)_{\text{reactants}} = \Delta G^{\circ} > 0 \qquad (2)$$

where ΔG is the Gibbs' free energy of formation of the compounds and n is the number of moles involved. ΔG is defined by

$$\Delta G \equiv \Delta H - T \Delta S$$

where ΔH is the change in enthalpy with temperature, ΔS is the change in entropy with temperature, and T is the absolute temperature at which the reaction takes place. The change in enthalpy and the change in entropy are defined by

$$\Delta H = \Delta H_{298} + \int_{298}^{T} \Delta C_p \, dT$$

$$\Delta S = \Delta S_{298} + \int_{298}^{T} \frac{\Delta C_p}{T} \, dT$$

with the change in heat capacity as a function of temperature denoted by ΔC_p (29: 34).

Thus the use of equation (2) requires a knowledge of the enthalpy, entropy and heat capacity of the reactants and products, and how they vary with temperature. There are usually uncertainties in the values which will lead to a possible error of 5 to 20% or more in the calculation of the Gibbs' free energy at higher temperature. An example of this variation in ΔG^o depending upon the source of the values of ΔH_{298}, ΔS_{298} and ΔC_p is given in Table II.

Table II

Comparison of Gibbs' Free Energy of Formation for Two Compounds (kilocalories/ mole)

Compound	Temperature	(34: 587)	(21: 8)	(29: 71, 72)
AlN	500°K	-47. 2	-63. 05	----
AlN	1000	-35. 0	-50. 2	----
UN	500	-57. 2	----	-69. 8
UN	1000	-47. 0	----	-49. 5

The use of equation (2) is further limited by the requirement of having to know the possible product compounds resulting from a reaction of the materials being compared. Finally, even if ΔG_o is negative, a reaction may not take place, since $\Delta G_o > 0$ is only a sufficient condition and does not account for the formation of protective films or other mechanisms which may prevent a reaction.

The experimental data available on the compatibility of liquid metals with other materials is mainly limited to the alkali metals such as sodium, potassium and lithium, although some information

is available on lead, mercury, and bismuth (4: 434). In particular, almost no work has been done concerning the erosion-corrosion (flow corrosion) effects of any other molten metals upon possible containment materials.

At temperatures below 1000°C a number of materials are fairly resistant to attack by liquid aluminum, including graphite, alumina (Al_2O_3), beryllia (BeO), and zirconia (ZrO_2). No metals are compatible at this temperature, although iron, chromium and nickle exhibit some resistance to attack below 800°C. Graphite is generally considered to be usable up to 1800°C, due to the formation of Al_4C_3 as a protective surface film (20: 126-170). At 1800°C, aluminum reacts to completion with carbon and graphite, and at 2000°C alumina and molten aluminum combine to form volatile Al_2O. The only material which appears to be inert to aluminum at 2000°C is aluminum mononitride (18: 53).

Aluminum mononitride (AlN) consists of 65. 81% aluminum and 34. 19% nitrogen, and is a white crystal having hexagonal wurtzite structure. It has a theoretical density of 3. 26 g/ cc and appears to disassociate (rather than melt) at about 2450°C. Hot pressed AlN is a better conductor of heat than alumina, and has a thermal expansion coefficient slightly higher than that of silicon carbide which exhibits excellent resistance to thermal shock and good dimensional stability at 1000°C. It also appears that AlN is stable in contact with graphite, tungsten and molybdenum at 1800-2000°C (18: 425).

On the basis of mechanical (physical) properties, aluminum mononitride seems to be as good a material for high temperature construction as most other ceramics, although the problems of forming large articles from AlN by hot-pressing or slip-casting may require the use of a "firebrick" or furnace-wall-type construction for the core. Its nuclear properties will depend upon those of

aluminum and nitrogen. Nitrogen has an absorption cross section of 1.88 barns at 0.025 eV, for N^{14}, which is 99.63% abundant (5: 13-18). Although this absorption cross section is greater than that specified for the coolant, it is small enough to be acceptable, since the only other alternative is the selection of another coolant. No information on radiation damage to AlN is available, but in general ceramics tend to be fairly insensitive to radiation damage and heal quickly at high temperatures.

Fuel Materials

Unless the reactor is to be a liquid-fuel type, the fuel material chosen must be a solid at 2000°C. There is almost no information available on the compatibility of materials with molten uranium, or plutonium alloys above 1000°C. For this reason the use of a fluid fuel was excluded.

Due to the lack of information on high-temperature properties of plutonium and its compounds, the search for a fuel material was restricted to uranium compounds. The nuclear properties of Pu^{239} (fast or thermal fuel) are no better than those of U^{235} at thermal energies (σ_f greater, but σ_f/σ_a smaller). For a fast reactor Pu^{239} offers a slightly higher fission cross section and number of neutrons per fission with about the same parasitic capture cross section (average values). Since the spectrum of the reactor is not yet determined, the use of U^{235} in preference to Pu^{239} seems reasonable. The temperature requirement limits the possible fuel materials to oxides, nitrides and carbides of uranium.

The results of the search for a material inert to aluminum at 2000°C indicate that no uranium compounds are available which will resist attack by liquid aluminum. In particular, it has been shown that uranium monocarbide (UC), uranium dicarbide (UC_2) and uranium mononitride (UN) all react with aluminum above 600°C to

form UAl_3 and UAl_4 (14: 174, 175). All uranium-aluminum compounds are completely soluable in aluminum above 1600°C (41: 143). This being the case, it is evident that any fuel material used must be coated or clad with AlN to protect it from contact with the liquid aluminum coolant.

The requirement that the fuel material be coated with AlN means that it must be a compound which is likely to be stable in contact with AlN. Among UC, UC_2, UO_2, and UN, it is likely that UN would be the most stable in contact with AlN, since there would be no tendency for any other compounds to form. Aluminum mononitride appears to be the only nitride of aluminum (10: 161) and of the nitrides of uranium, only the mononitride is stable above 1100°C (6: 43-46). Finally, the driving force for formation of any uranium-aluminum compounds at high temperature is much less than that for the formation of nitrides.

Having selected aluminum mononitride and uranium mononitride as the construction and fuel materials, and having determined that the fuel elements for the reactor must be coated or clad, it is necessary to consider the type of fuel element which could be used. Ceramics are usually brittle, possessing low tensile strength and high compressive strength with little change in these properties over large temperature ranges. They are not subject to much radiation damage, and tend to heal quickly at high temperatures, although suffering some loss in strength. Also, most ceramics have low diffusion coefficients for volatile fission products (26: 49-50).

Hot-pressed UN has a very low coefficient of thermal expansion and it is about eight times more effective than UO_2 in transferring heat. Irradiated UN exhibits good dimensional stability and low fission gas release, plus an increase in hardness (37: 1). It thus appears that the use of UN as a coated fuel material would be likely

to result in little stress upon the coating material. No information is available on the changes in physical properties which occur in AlN under irradiation, but they should be small as in other ceramics.

Testing on micron-size coated-particle fuels has been carried out for several years, and has demonstrated that the 100-500 micron-size fuel particles, coated with a layer of ceramic material at least 150 microns thick, exhibit excellent integrity under thermal stress and high burnup. For particle sizes from 200 to 500 microns, thermal stresses from self-heating are small. Stress resulting from differences in the thermal expansion coefficient of the coating and the fuel will not cause cracking if (a) the coefficient of thermal expansion of the fuel is greater than that of the coating and (b) the particles are used at temperatures below the coating temperature (36: 43-45). These requirements are due to the ability of ceramics to withstand very large compressive forces, but only small tensile forces. The coatings which have been tested do not include AlN, but there is no reason to suppose that it would not perform as well as pyrolytic graphite or Al_2O_3, two of the most tested coatings.

In order to give a basis for comparison of the properties of UN particles coated with AlN, Table III compares the properties of these two materials with those of UO_2 and Al_2O_3, which are a typical coated fuel combination. The comparison of values in Table III indicates that AlN coated UN particles would not perform as well as Al_2O_3 coated UO_2 particles, since the difference in the temperature coefficients of expansion is greater. However, the temperature coefficients of expansion of all the carbides of uranium are greater than that of UN, so that using either UO_2 or a carbide of uranium (UC, UC_2, U_2C_3) would not improve performance.

The problem of using the particles at temperatures below that at which they were coated is difficult to solve, as the best coating

Table III

Property Values of Two Ceramic Fuels and Two Possible Ceramic Coatings

	AlN	Al_2O_3	UN	UO_2
Theoretical Density (g/ cc)	3.26(35)	3.98(10)	14.32(6)	10.96(6)
Melting or Sublimation Temperature (^{o}C at 1 atm.)	2450(35)	2000(10)	2650(6)	2750(6)
Uranium Content (wt. %)	----	----	71(6)	53(6)
Thermal Conductivity (cgs units at 400^{o}C)	0.060(35)	0.054(10)	0.042(37)	0.012(37)
Coefficient of Linear Expansion (10^{-6}/ ^{o}C)	5.64(35) (25-1000^{o}C)	8.5(11) (20-800^{o}C)	9.9(37) (20-1600^{o}C)	10.52(37) 26-1000^{o}C)
Heat Capacity (cal/ gm ^{o}C)	.20-.28(10) (20-1000^{o}C)	.20-.30(10) (20-1000^{o}C)	---- ----	.06-.08(10) (20-1000^{o}C)

BLANK PAGE

temperature can be ascertained only by experiment (2: 377). However, the limited data available indicates that AlN may be deposited above 1500°C at atmospheric pressure, so that it is entirely possible that coating temperatures of better than 2000°C could be attained (27: 97).

Summary

The materials problem appears to be solvable through the selection of liquid aluminum as the heat transfer agent, with aluminum mononitride as the core construction material (possibly in the form of small interlocking bricks) and micron-size uranium mononitride fuel particles coated with AlN. The solution presented is obviously based on many assumptions, including the exclusion of metal-alloy coolants, fluid (liquid metal) fuel and plutonium compounds, which were necessary due to lack of time and information.

The main justification for these assumptions is that they have made it possible to go on to the problems of heat transfer within the core and the selection of a core geometry and flow system.

III. Liquid Fluidized Beds

The selection of AlN clad UN particles for the fuel elements leaves two types of fuel loading systems to be considered. One is particulate with the coolant in direct contact with the particles. The other is a system using the particles in a matrix of AlN, perhaps in fixed fuel rods.

The large fuel elements (rods) would be subject to the thermal stresses mentioned in the preceding chapter, which are essentially proportional to size. Such an arrangement (fixed elements) would also result in "hot spots" in the core, with temperatures appreciably above the average core temperature. A system involving direct contact of the coolant with the fuel particles will provide a greater heat transfer area per unit volume of fuel and should result in lower peak temperatures in the fuel.

If the particles are fixed in a solid mass, with the coolant flowing in the spaces between them (fixed bed) there will still be temperatures above the bed average at any points where the flux peaks. In addition, either the coolant flow rate must be low or large particles must be used, since the pressure drop in a fixed bed increases as the average size of the particles (average size of the interstices) decreases.

Probably the best configuration from the heat transfer standpoint is a fluidized bed in which the particles are supported by the flow of coolant and undergo rapid mixing both vertically and horizontally. This system allows for a high coolant flow rate and a small temperature gradient within the mass of particles, and the mixing effect will insure uniform fuel burnup. The pressure drop in a fluidized bed will be much less than that in a fixed bed for fluid velocities above the minimum velocity required to fluidize the bed.

Fluidized Bed (25: 1-5)

A fluidized bed results when a fluid (liquid or gas) is flowed upward through a bed of solid particles with sufficient velocity to buoy the particles and give them a highly turbulent, fluid-like motion. The fluid velocity can vary from a minimum value, which is just sufficient to buoy the particle bed, to the velocity which will flush the particles out of their container. With suitable sizes and densities of particles and the correct fluid velocity, a stable bed can be maintained which has a definite separation between the top of the bed and the escaping fluid, and has little carryover of particles.

Most fluidized beds contain a baffle plate or screen on which the particles rest prior to the onset of fluidization, much as if they were in a fixed configuration. This plate also acts to break up the fluid stream and distribute it over the total area of the inlet.

In liquid fluidized beds, the solid particles are normally dispensed individually and uniformly, giving the whole bed an ordered structure (homogeneous or particulate fluidization). Gaseous fluidized beds, on the other hand, usually have spots where the particles form solid masses with some of the gas flowing through the bed as bubbles (aggregative fluidization).

Both types of fluidized beds are characterized by very high thermal conductivity compared to that of the carrier fluid, and by transport of heat from one part of the bed to the other by the movement of the solid particles. This leads to a nearly uniform bed temperature, both axially and radially, even if there are localized zones in the bed which produce heat at a rate far above the average for the bed.

Heat Transfer

There are three aspects of heat transfer in a fluidized bed which must be considered: the heat transfer from the fuel particles to the fluid, the heat transfer from the fluid to the walls of the container,

and the heat transfer from one region of the bed to another. Ideally, the rate of heat transfer from the fluid to the walls of the bed would be low, and that from the particles to the fluid high, resulting in low temperature gradients in the particles (low thermal stress) and low heat loss through the walls of the core. For a nuclear reactor, good heat transfer from region to region is also desirable.

Basically, the first two types of heat transfer will involve conduction and convection through a thin film (boundary layer) of fluid immediately adjacent to the surface of the wall or particle. This may be expressed by

$$q = \frac{k}{\delta'} \Delta t \tag{3}$$

where q is the heat flux from the wall to the fluid, k is the thermal conductivity of the liquid, δ' is the thickness of the boundary layer and Δt is the temperature difference between the wall and the average fluid temperature. This equation is normally expressed by

$$q = h \Delta t \tag{4}$$

where h is called the heat transfer coefficient. Thus, for a given Δt, q will be a direct function of h, or an inverse function of δ' for a given fluid (a given value of k).

Experiments indicate that extremely high coefficients of heat transfer exist between a fluidized bed of small particles and its containing walls, and that these coefficients are normally much higher than for a fixed bed of particles. These high coefficients may be due to the scouring action of the particles on the walls, resulting in a very thin boundary layer at the wall. In any event, although the data on bed to wall (or wall to bed) heat transfer is extensive and agrees qualitatively, it contains many discrepancies, and no consistent method of predicting the heat transfer rates has been found (39: 737-740).

Some of the problems involved in setting up a theoretical method for predicting heat transfer in a fluidized bed are shown in a report by Carr and Amundson (3: 1856-1862). Even with the assumptions of complete random motion of the particles and complete mixing of the fluid only qualitative values of heat transfer rates could be computed.

Almost all the data available on particle to fluid heat transfer is for gaseous fluidized beds, where the heat transfer coefficients are orders of magnitude lower than for most liquid fluidized systems (liquid metals in particular). The work on gaseous fluidized systems indicates that the heat transfer coefficients for particle to fluid heat transfer are lower than for bed to wall transfer for the same fluidising agent. However, the rate of heat transfer from the particles to the fluid is high due to the small size of the particles (large area to volume ratio) (25: 47-48).

Very little data is available on the temperature gradients within the particles themselves, since it appears to be standard practice to assume a uniform temperature throughout the particle. Calculations performed after the fluidization and reactor calculations were completed indicate that for particles 0. 1 centimeters or less in diameter, the probable temperature rise across the particles will be less than 20°C. For particles 1. 0 centimeters in diameter, the temperature rise is on the order of 200°C for the same rate of heat generation in the fuel. The detailed calculations are given in Appendix E.

The rate of heat transfer from one spot to another within a fluidized bed is always at such a high rate that temperature gradients are negligible. The small gradients are due to the rapid circulation of the solid particles in liquid fluidized beds (25: 20-23).

Leva presents some graphs of vertical and radial temperature gradients in fluidized beds which indicate an almost flat temperature profile (less than 5% rise or drop) starting within a very small

distance from the bed entrance (baffle plate) and walls, respectively (16: 185-190). Although this data is for gaseous fluidized systems, it should be valid for liquid systems also, where the lower turbulence of the bed would be offset by the higher thermal conductivity of the fluids.

The heat transfer rates in a fluidized bed are so impressive that several reactor designs based upon fluidized systems have been performed since 1955. One of the first such studies was done at the Oak Ridge School of Reactor Technology. Several designs were considered, including fast and thermal systems (8). One of the best recent fluidized bed designs was performed by the Martin Nuclear Division, based on a low temperature water-fluidized system with refractory uranium fuel particles (7). All of these design studies used standard sources such as Leva (16) or Lewis and Bowerman (15) for their predictions on heat transfer and fluidization, and contributed little new information on either subject.

Particulate Fluidization

When a fluid is forced upward through a bed of particles at a low velocity, it flows through the interstices, experiencing a drop in pressure due to film friction. If the fluid velocity is increased, a flow rate will be reached at which the upward drag forces on the particles exactly equal the weight of the particles and the bed is effectively weightless. Any further increase in fluid velocity will increase the upward drag on the particles and lift them, thus causing the bed to expand. The expansion of the bed increases the area for flow between the particles, resulting in a decrease of the interstitial velocity to the point where the upward drag force again exactly equals the gravitational force on the particles. Perturbations to the ideal picture are caused by wall friction in the bed, which gives a minimum fluid velocity at the walls. Thus the particles rise at the center of

the bed and fall at the walls in a pattern superimposed on the local turbulent motion (40: 230). This total flow pattern is called particulate or homogeneous fluidization.

The pressure drop through a homogeneously-fluidized bed is a function of the drag forces coupling the fluid and the particles, and the drag forces are a function of the interstitial fluid velocity. The interstitial velocity depends on the effective cross sectional area for flow, which in turn depends on the average fluid volume per unit volume of the bed (that is, total bed volume at a given flow rate minus the total particle volume). This volume ratio is called the voidage of the bed.

The minimum value of voidage occurs when the particles in the bed have the loosest possible configuration in which they all touch (equivalent to the maximum fixed bed dispersion). This value of voidage is determined experimentally, and depends on particle size and shape but not on the fluidizing agent. The maximum theoretical value of voidage is +1.0, which means that no particles are in the bed.

Extensive experimental data has shown that for particulate fluidization, a plot of the logarithm of average fluid velocity in the bed versus the logarithm of the voidage results in a straight line. This result is true for both liquid and gaseous fluidizing agents and for a large range of sizes, shapes (including both spheres and cubes) and densities of particles. Some of the best examples of these experimental results are presented in a report published in 1954 by J. F. Richardson and W. N. Zaki (32: 35-53).

Unfortunately, there is no valid (generally accepted) way to determine the initial point, minimum voidage and minimum fluid velocity, or the slope of this straight line except by experimental testing. Since such experimentation was not within the scope of this report, it was necessary to find some other (theoretical) method of

determining the size and density of a liquid aluminum fluidized bed for various combinations of particles and fluid velocities.

Both the size of the core (total bed volume) and the mass of fuel per unit volume of the core depend on the voidage of the bed. Thus an accurate method of determining voidage as a function of fluid velocity is the basis of any critical calculations of the reactor.

Three separate nonexperimental methods of determining the relationship between voidage and average fluid velocity were selected for use in this report. Two of them are attempts to correlate experimental values by means of a set of formulas, which may then be used to predict the parametric values of other fluidized beds. The third method performs essentially the same function but uses graphical techniques rather than analytical equations. All three methods result in values of voidage as a function of fluid velocity which fit the experimental criterion of a straight line log-log plot, but each method results in a different straight line.

The more widely known (circulated) of the three methods is that devised by Dr. Max Leva, which will be presented below. The other two methods are presented in Appendix C, along with a digital computor program used to calculate the values used in this report.

Leva's Method (16: 21-94)

If it is assumed (or specified) that the terminal free-fall velocity of a spherical particle in still fluid, u_t, is a single-valued function of any fluid-particle system, just as is the minimum voidage, then the relationship between voidage, ϵ, and average fluid velocity, $\overline{u_f}$, may be written as

$$\frac{\overline{u_f}}{u_t} = \epsilon^n \tag{5}$$

where u_t is a constant, k'. Then

$$\frac{\overline{u_f}}{k'} = \epsilon^n$$

and letting mf indicate the value of a variable at minimum fluidization

$$\frac{\overline{u}_{mf}}{k'} = \epsilon_{mf}^{n}$$

where both $\overline{u}_{mf}$, ϵ_{mf} and n are determined by the physical properties of the system. Then

$$k' = \frac{\overline{u}_{mf}}{\epsilon_{mf}}$$

and substituting into the defining equation

$$\overline{u}_f = \epsilon^{n} \frac{\overline{u}_{mf}}{\epsilon_{mf}^{n}}$$

Solving for the voidage as a function of average fluid velocity gives the working equation for predicting voidage:

$$\epsilon = \epsilon_{mf} \left(\frac{\overline{u}_f}{u_{mf}} \right)^{1/n}$$

Leva has developed a set of four equations to give values of n for various values of the particle Reynold's number at minimum fluidization. The particle Reynold's number is a standard dimensionless group used in fluidization work which indicates the flow pattern of the fluid (laminar, turbulent, etc.) and is defined by

(7) $$Re_p = \frac{D_p \overline{u}_f \rho_f}{\mu}$$

where D_p is the particle diameter, ρ_f is the fluid density, and μ is the dynamic viscosity of the fluid.

The value of Re_p at minimum fluidization, Re_{mf}, is obtained from

$$Re_{mf} = \frac{D_p \overline{u}_{mf} \rho_f}{\mu} = \frac{D_p G_{mf}}{\mu}$$

where G_{mf} is the mass flow rate at minimum fluidization, given by

(9) $$G_{mf} = \frac{668 D_p^{1.82} \left[\rho_f (\rho_p - \rho_f) \right]^{0.94}}{\mu^{0.88}}$$

with ρ_p the density of the particle. Depending upon the value of Re_{mf} a new value of G_{mf} is determined by multiplying the first number by the correction factor C_f, where

$$
\begin{aligned}
C_f &= 1.0 && Re_{mf} < 10 \\
C_f &= 1.39 - 0.422 \log_{10} Re_{mf} && 10 < Re_{mf} < 250 \\
C_f &= 0.898 - 0.2162 \log_{10} Re_{mf} && 250 < Re_{mf} < 1000
\end{aligned} \tag{10}
$$

A new value of Re_{mf} is then determined and used in selecting the value of n, where the defining equations for n are

$$
\begin{aligned}
n &= \left(4.35 + 17.5 \frac{Dp}{D_t}\right) Re_{mf}^{-0.03} && 0.2 < Re_{mf} < 1.0 \\
n &= \left(4.45 + 18 \frac{D_p}{D_t}\right) Re_{mf}^{-0.1} && 1.0 < Re_{mf} < 200 \\
n &= 4.45\, Re_{mf}^{-0.1} && 200 < Re_{mf} < 500 \\
n &= 2.39 && Re_{mf} > 500
\end{aligned} \tag{11}
$$

with D_t the diameter of the tube in which the fluidized bed is contained. For values of D_t much greater than D_p the preceding equations simplify to

$$
\begin{aligned}
n &= 4.35\, Re_{mf}^{-0.03} && 0.2 < Re_{mf} < 1.0 \\
n &= 4.45\, Re_{mf}^{-0.1} && 1.0 < Re_{mf} < 500 \\
n &= 2.39 && Re_{mf} > 500
\end{aligned} \tag{12}
$$

which are the equations used in this report.

Now the following procedure may be followed to determine the values of ϵ as a function of $\overline{u_f}$:

(a) Using equation (9), determine G_{mf}.

(b) Determine Re_{mf} and $\overline{u}_{mf}$ using equation (8) and multiply these values by the correct C_f.

(c) Using the corrected Re_{mf}, select the correct equation for n from equations (12) and calculate n.

(d) Select a value of ϵ_{mf} from theory or previous experiments ($\epsilon_{mf} \sim 0.4$ for micron-size spheres).

(e) Use equation (6) to obtain values of ϵ as a function of the average fluid velocity, $\overline{u}_f$.

This method is mainly based on the experimental data of Richardson and Zaki (32: 35-53), and is probably most accurate for values of ϵ less than 0.75: its accuracy will depend in part on the value of ϵ_{mf} which is used.

Figure 1 shows the values of ϵ as a function of the mass flow rate, $G_f = \overline{u}_f \rho_f$, obtained using Leva's method and those of Zenz and Othmer and Lewis and Bowerman (Appendix C). The lines are for three sets of particles, fluidized by liquid aluminum of density 2 g/ cc and viscosity 2 centipoise. The heavy solid line is from the graphical method by Zenz and Othmer, which was taken as the standard since it does not involve any guessed values such as ϵ_{mf}. The other two lines were assumed to indicated the maximum probable margin of error, so that the real values lie in the region defined by the three lines.

If the thermal power output of the reactor is defined as the heat gained by the liquid aluminum coolant between entering and leaving the core, then for a fixed inlet and exit temperature, the thermal power will be a direct function of the flow rate. For temperatures of 1700°C at the entrance and 2000°C at the exit, the thermal power output (kilowatts/ ft^2 core cross sectional area) is about 0.041 times the mass flow rate, G_f (see Appendix C).

The probable effects of a variation in particle size (and/ or density) and the relative smoothness and shape of the walls surrounding the bed should also be considered. Leva (16: 63-69) indicates that the effect of size differences in the particles will be small, and that use of a composite or average particle diameter will give acceptable results in voidage computations.

Figure 1

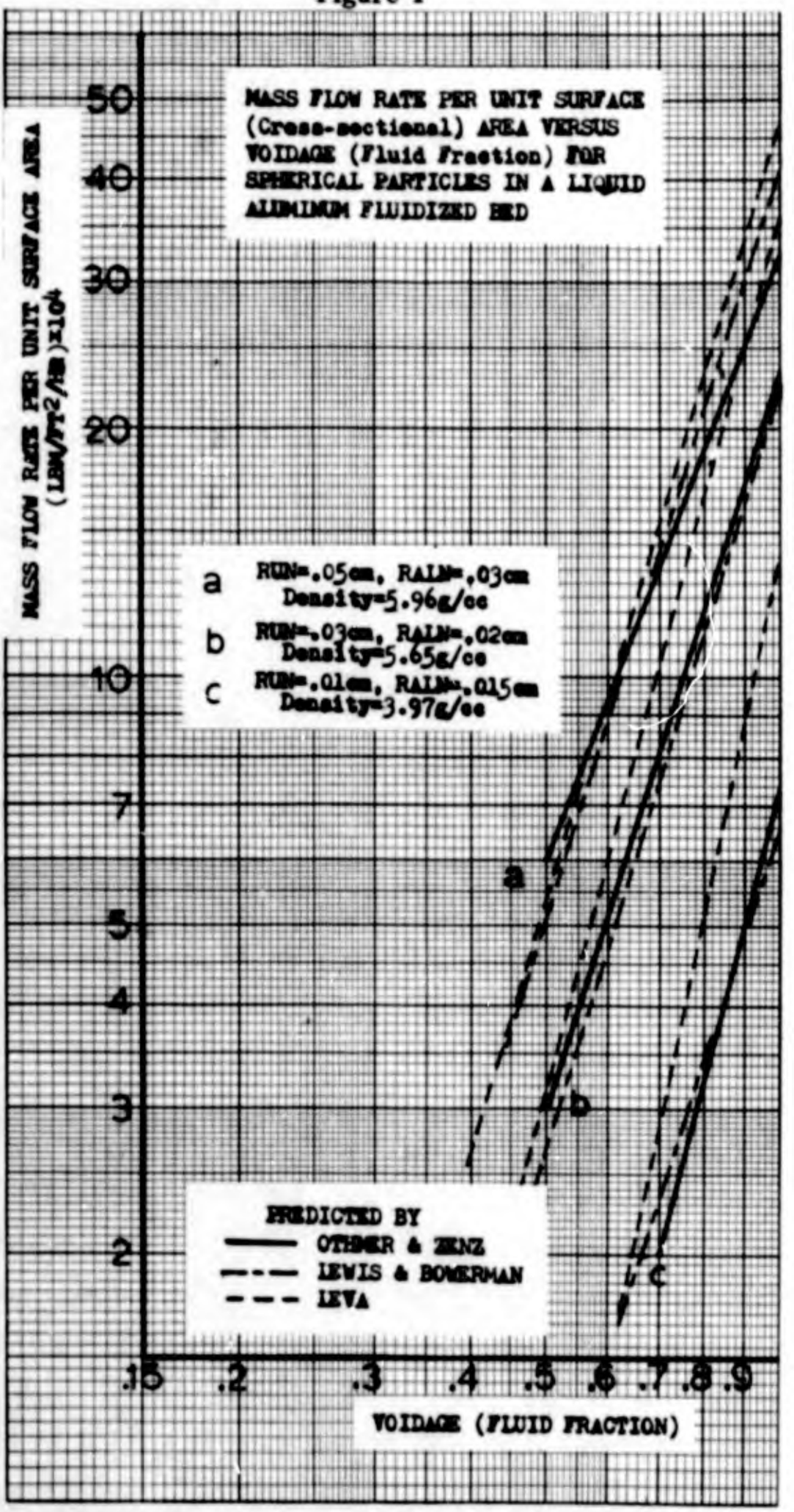
MASS FLOW RATE PER UNIT SURFACE (Cross-sectional) AREA VERSUS VOIDAGE (Fluid Fraction) FOR SPHERICAL PARTICLES IN A LIQUID ALUMINUM FLUIDIZED BED
MASS FLOW RATE PER UNIT SURFACE AREA (LBM/FT²/HR)x10⁴
50
40
30
20
10
7
5
4
3
2
a RUN=.05cm, RALN=.03cm Density=5.96g/cc
b RUN=.03cm, RALN=.02cm Density=5.65g/cc
c RUN=.01cm, RALN=.015cm Density=3.97g/cc
PREDICTED BY
OTHMER & ZENZ
LEWIS & BOWERMAN
LEVA
.15
.2
.3
.4
.5
.6
.7
.8
.9
VOIDAGE (FLUID FRACTION)

The effects of wall drag on fluidization appear to be small, and for channel diameters much greater than particle diameter, the size of the channel is unimportant (see equations (11) and (12)). The limited data which is available indicates that beds whose height is of the same order of magnitude as their diameter are the most stable, and that for heavy particles and dense fluids, tapering the bed from top to bottom with the greatest cross section at the top will improve stability.

Summary

It is evident that accurate predictions of either heat transfer rates or voidage in a liquid fluidized bed of spherical particles are impossible, but good qualitative estimates can be obtained. All indications are that the temperature gradients in the bed are negligible, with a high rate of heat transfer through the bed walls. Thermal gradients in the particles will be essentially negligible, and variations in particle size and density will not affect voidage appreciably. The size and shape of the containment vessel will have little influence on the bed parameters, as long as it is approximately cylindrical. Therefore the use of "firebrick" construction for the bed walls should be practical. Finally, good stability may be expected for a vessel with height the same order of magnitude as diameter, which is also the best ratio for neutron conservation.

Thus the best core design at this point appears to be a cylindrical core, with the height about the same as the diameter, containing a very large number of microspheres of AlN coated UN, fluidized by liquid aluminum. The walls of the core might be constructed of small interlocking bricks, to eliminate the problems of forming large objects from ceramic materials. The problem of a baffle plate or similar device at the bed entrance has not been solved, but it will be considered in the final chapter.

IV. Nuclear Parameters

The nuclear parameters study was based on two-group diffusion theory calculations, using fast group cross sections obtained from the GAM-I program written at Atomics International. The thermal group cross sections were obtained from both the multigroup cross section sets and standard tables of cross sections, as explained below. An infinitely reflected spherical geometry was assumed with an enrichment of 1. The general flux distribution in the core and reflector was determined, and the effects of changes in voidage (average fluid velocity) and the fuel particle size and composition on the critical radius of the core were studied.

Cross Sections

Prior to any study of the nuclear parameters of a system, the neutron cross sections to be used must be selected. All of the values which are calculated will depend upon these cross sections, so every effort must be made to pick the "best" values.

The lack of data on N^{14} cross sections between thermal energies and intermediate energies greatly limited the choice of values. As it turned out, no self-consistent set of values for U^{235}, Al^{27} and N^{14} over the desired energy range could be found, so a composite set was created. A list of all cross sections used is included in Appendix D.

Fast Group. The GAM-I program developed by Atomics International may be used to calculate flux-weighted cross sections for as many as sixty-eight energy groups, with a lower limit of 0.414 eV (lethargy of 17.0). Inputs are the nuclei densities of the materials (assumed homogeneous), the neutron spectrum to be used (of six available in the code), the width of the group intervals, and a guess at the value of buckling. The output consists of both microscopic and macroscopic cross sections for each group, the group fluxes, and the neutron age to each group.

This code apparently assumes a uniform source distributed through the specified media, and calculations are not dependent upon geometry, except in the case of U^{238} resonance absorption. The age is calculated for an infinite system, starting above 10 MeV and going to 0.414 eV. There is a dependence of the cross sectional values on the specified buckling, but it is small.

Use of GAM-I prior to obtaining the fast group cross sections for the diffusion equations indicated that, for all reasonable voidages and coating thicknesses on the fuel particles, the core spectrum would be very hard (see Figure 2 for an example). The age to 0.414 eV in AlN as given by GAM-I is 268.25 cm^{-2}, as compared to 321.65 for graphite, which indicates that AlN is a fairly good moderator.

Thus, even before determining the flux distribution by the use of two-group diffusion theory it is possible to predict a fast core with very little slowing down of neutrons, and a thermal flus peaking in the reflector. This qualitative picture of the probable flux distribution was used in determining what approximations were valid in solving the diffusion equations.

The fast group was considered to extend to 1.125 eV (lethargy 16) based on the assumption that the neutrons would obey Maxwell-Boltzman statistics (average energy 0.25 eV at 2000°C). An approximate Maxwell-Boltzman distribution for 2000°C is shown as part of Figure 2. The flux units for this distribution are arbitrary, and do not indicate the size (amount) of the thermal flux.

Thermal Group. It was assumed that even though a "pool" of thermal neutrons might not exist in either the reflector or core, or have a Maxwell-Boltzman distribution, the 1.125 eV cutoff would still include most of the thermal group.

The thermal group cross sections for aluminum and uranium 235 were obtained from those given in the LASL 16-group fast reactor

Figure 2

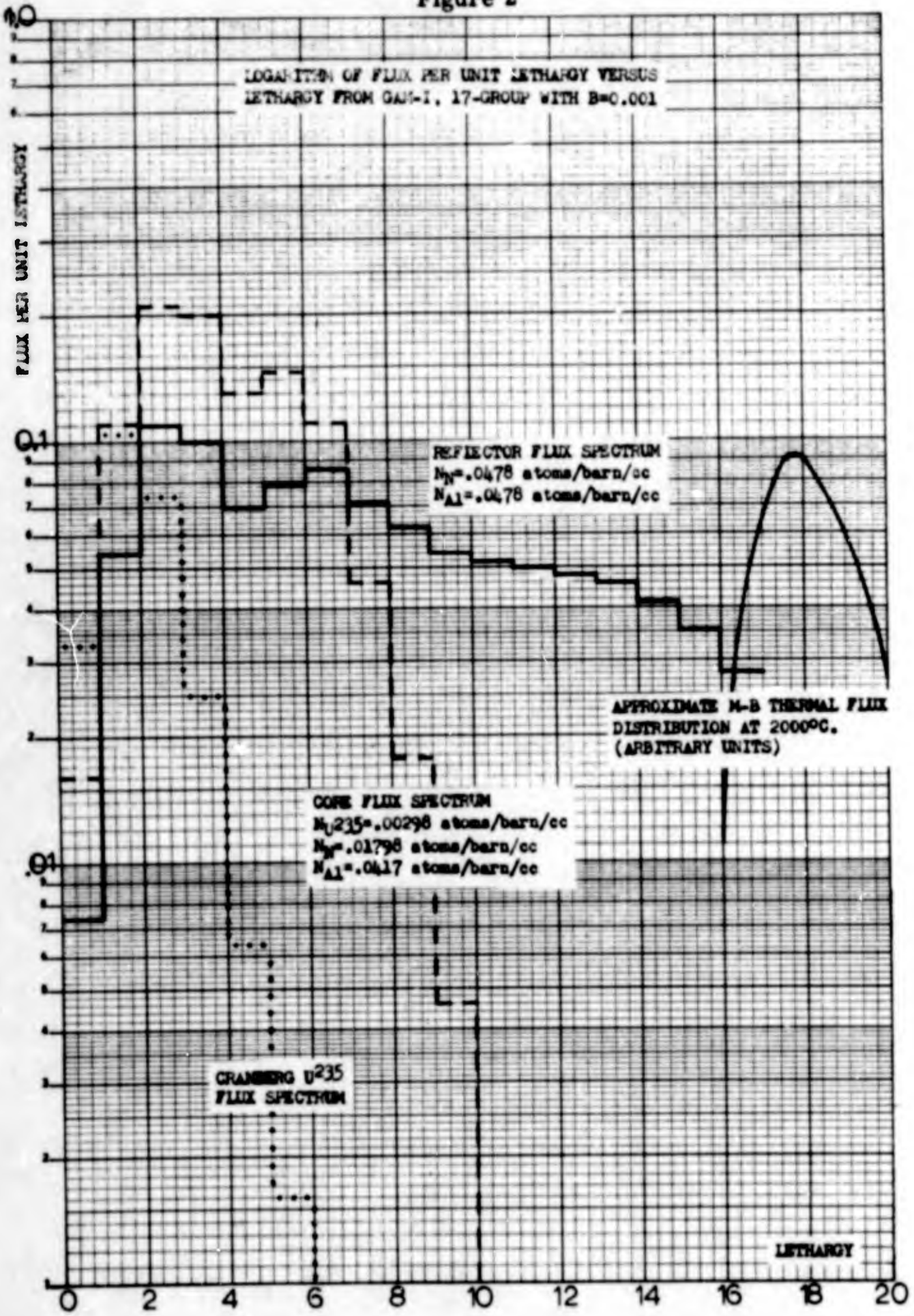
LOGARITHM OF FLUX PER UNIT LETHARGY VERSUS
LETHARGY FROM GAM-I, 17-GROUP WITH B=0.001
FLUX PER UNIT LETHARGY
1.0
0.1
.01
REFLECTOR FLUX SPECTRUM
N_N=.0478 atoms/barn/cc
N_{Al}=.0478 atoms/barn/cc
APPROXIMATE M-B THERMAL FLUX
DISTRIBUTION AT 2000°C.
(ARBITRARY UNITS)
CORE FLUX SPECTRUM
$N_{U^{235}}$=.00298 atoms/barn/cc
N_N=.01798 atoms/barn/cc
N_{Al}=.0417 atoms/barn/cc
CRANBERG U^{235}
FLUX SPECTRUM
LETHARGY
0
2
4
6
8
10
12
14
16
18
20

cross section set in ANL-5800 (31: 568-576), using the average of the last three groups (14 through 16). Since no multigroup cross sections for N^{14} could be found which extend to the energy levels of the thermal group, the thermal cross sections for nitrogen were taken from BNL-325 (24: 4, 98-101). The absorption cross sections were modified by

$$\frac{\overline{\sigma}(T)}{\overline{\sigma}(T_o)} = \sqrt{\frac{T_o}{T}}$$

and the transport cross section found by

$$\sigma_{tr} = \sigma_t - \overline{\mu_o}\ \sigma_s$$

Table IV

Thermal Group Cross Section

	U^{235}	N^{14}	Al^{27}
$\overline{\nu}$	2.43	0	0
$\overline{\sigma_f}$	257	0	0
$\overline{\sigma_c}$	48	0.64	0.11
$\overline{\sigma_{tr}}$	315	10.16	1.49

One set of critical and flux calculations was made with the cutoff between fast and thermal groups set at 3.059 eV, for $\epsilon = 0.6$, RUN = 0.03, RALN = 0.02. The flux distribution was approximately the same, and the critical radius was increased. Since raising the energy cutoff lowers the fission cross section in both groups, this is the logical result (parasitic capture << fission).

Reactor Calculations

The standard time-independent two-group equations were written for the core

$$(13)\quad D_{fc} \nabla^2 \phi_{fc} - \Sigma_{fc}^{s,re} \phi_{fc} - \Sigma_{fc}^{a} \phi_{fc} + \chi_f (\nu_f \Sigma_{fc}^{f} \phi_{fc} + \nu_t \Sigma_{tc}^{f} \phi_{tc}) = 0$$

$$(14)\quad D_{tc} \nabla^2 \phi_{tc} - \Sigma_{tc}^{a} \phi_{tc} + \Sigma_{fc}^{s,re} \phi_{fc} + \chi_t (\nu_f \Sigma_{fc}^{f} \phi_{fc} + \nu_t \Sigma_{tc}^{f} \phi_{tc}) = 0$$

and for the reflector

$$(15)\quad D_{fR} \nabla^2 \phi_{fR} - \Sigma_{fR}^{s,re} \phi_{fR} - \Sigma_{fR}^{a} \phi_{fR} = 0$$

$$(16)\quad D_{tR} \nabla^2 \phi_{tR} - \Sigma_{tR}^{a} \phi_{tR} + \Sigma_{fR}^{s,re} \phi_{fR} = 0$$

where fc = fast group in core, tR = thermal group in reflector, etc.

The following assumptions were made to simplify the calculations

$\Sigma_{fc}^{c} \sim 0$ (Re-introduced later - see Appendix D for details)

$\chi_t = 0$

$\Sigma_{fc}^{s,re} \sim 0$ (Both removal scatter cross section and parasitic capture cross section were several orders of magnitude less than the parasitic capture in the core).

$\Sigma_{fR}^{c} \sim 0$

These simplifications allowed the core equations to be decoupled, and resulted in the following set of equations to be solved.

$$(13a)\quad D_{fc} \nabla^2 \phi_{fc} + (\nu_f - 1) \Sigma_{fc}^{f} \phi_{fc} + \nu_t \Sigma_{tc}^{f} \phi_{tc} = 0$$

$$(14a)\quad D_{tc} \nabla^2 \phi_{tc} - \Sigma_{tc}^{a} \phi_{tc} = 0$$

$$(15a)\quad D_{fR} \nabla^2 \phi_{fR} - \Sigma_{fR}^{s,re} \phi_{fR} = 0$$

$$(16a)\quad D_{tR} \nabla^2 \phi_{tR} - \Sigma^{a}_{tR} \phi_{tR} + \Sigma^{s,re}_{fR} \phi_{fR} = 0 \ .$$

The solution of this set of equations for both critical radius and flux distribution was carried out in standard textbook fashion, following the notation in Murray's book (23: 111-133), and is given in detail in Appendix D along with a flow diagram, listing and sample output of the digital computer program used for the calculations. The four flux equations developed are

$$(17)\quad \phi_{tc}(r) = C_1 \frac{\sinh (B_{tc} r)}{r}$$

$$(18)\quad \phi_{fc}(r) = C_3 \frac{\sin (B_{fc} r)}{r} - \frac{m}{B^2_{fc} + B^2_{tc}} \phi_{tc}(r)$$

$$(19)\quad \phi_{fR}(r) = A_2 \frac{e^{-k_{fR} r}}{r}$$

$$(20)\quad \phi_{tR}(r) = E_2 \frac{e^{-k_{tR} r}}{r} + \frac{m'}{K^2_{tR} - K^2_{fR}} \phi_{fR}(r)$$

and a typical flux plot is shown in Figure 3, page 34.

Results

The values of critical radius as a function of voidage for three different particles are shown in Figure 4. The size of the UN pellet was held constant in order to give an indication of the effect to be expected when aluminum nitride replaces liquid aluminum (coating thickened, voidage reduced).

Figure 4 indicates that for a given particle, an increase in voidage (increase in fluid flow rate) will make the reactor subcritical, while a decrease in voidage will make the reactor supercritical. The displacement of the curves from left to right for increasing coating thickness is due to replacing UN with AlN while the amount of liquid aluminum remains constant.

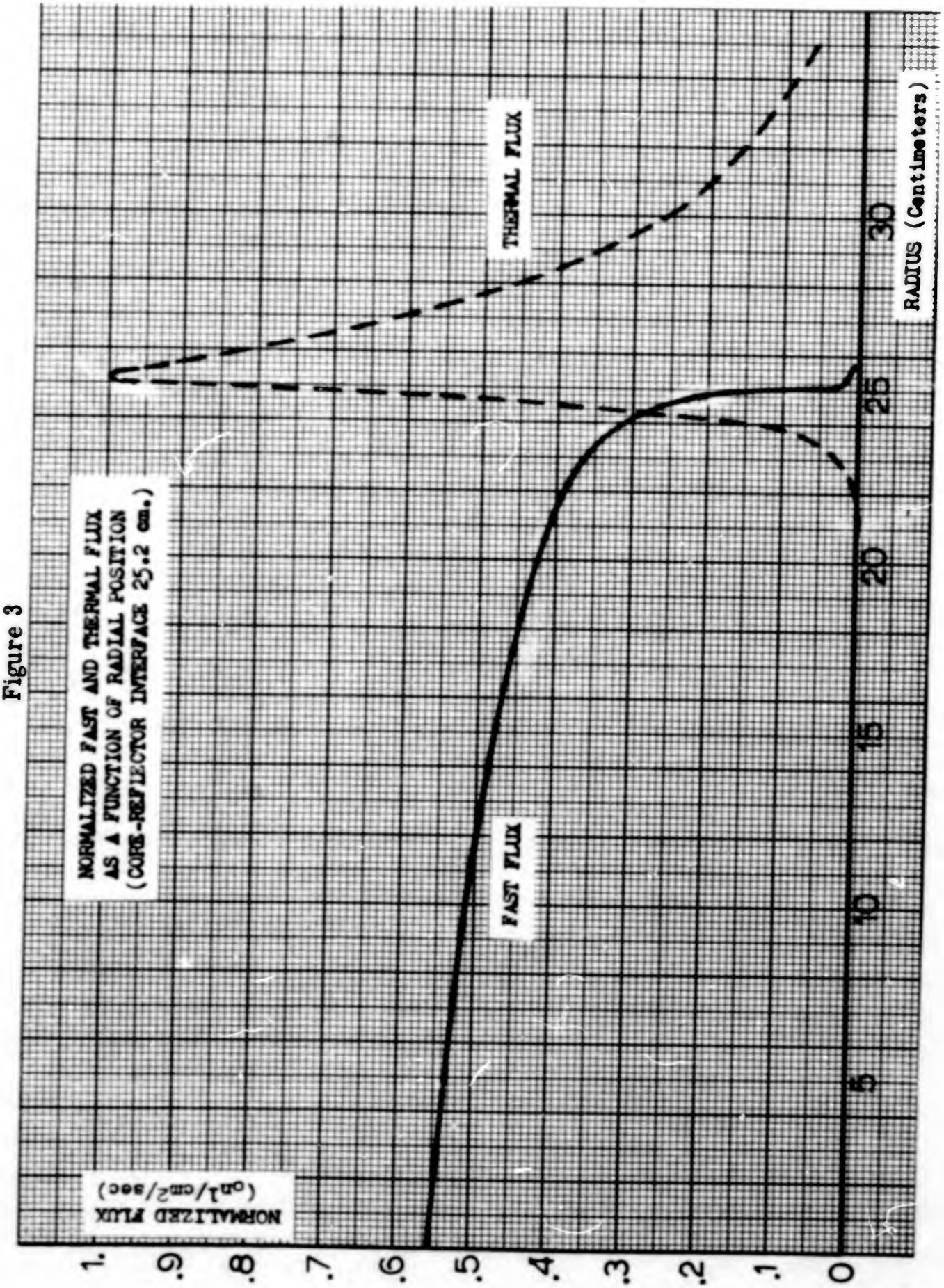
NORMALIZED FLUX AND THERMAL FLUX
AS A FUNCTION OF RADIAL POSITION
(CORE-REFLECTOR INTERFACE 25.2 cm.)
NORMALIZED FLUX
(on1/cm2/sec)
THERMAL FLUX
FAST FLUX
RADIUS (Centimeters)
1.
.9
.8
.7
.6
.5
.4
.3
.2
.1
0
5
10
15
20
25
30

Figure 3

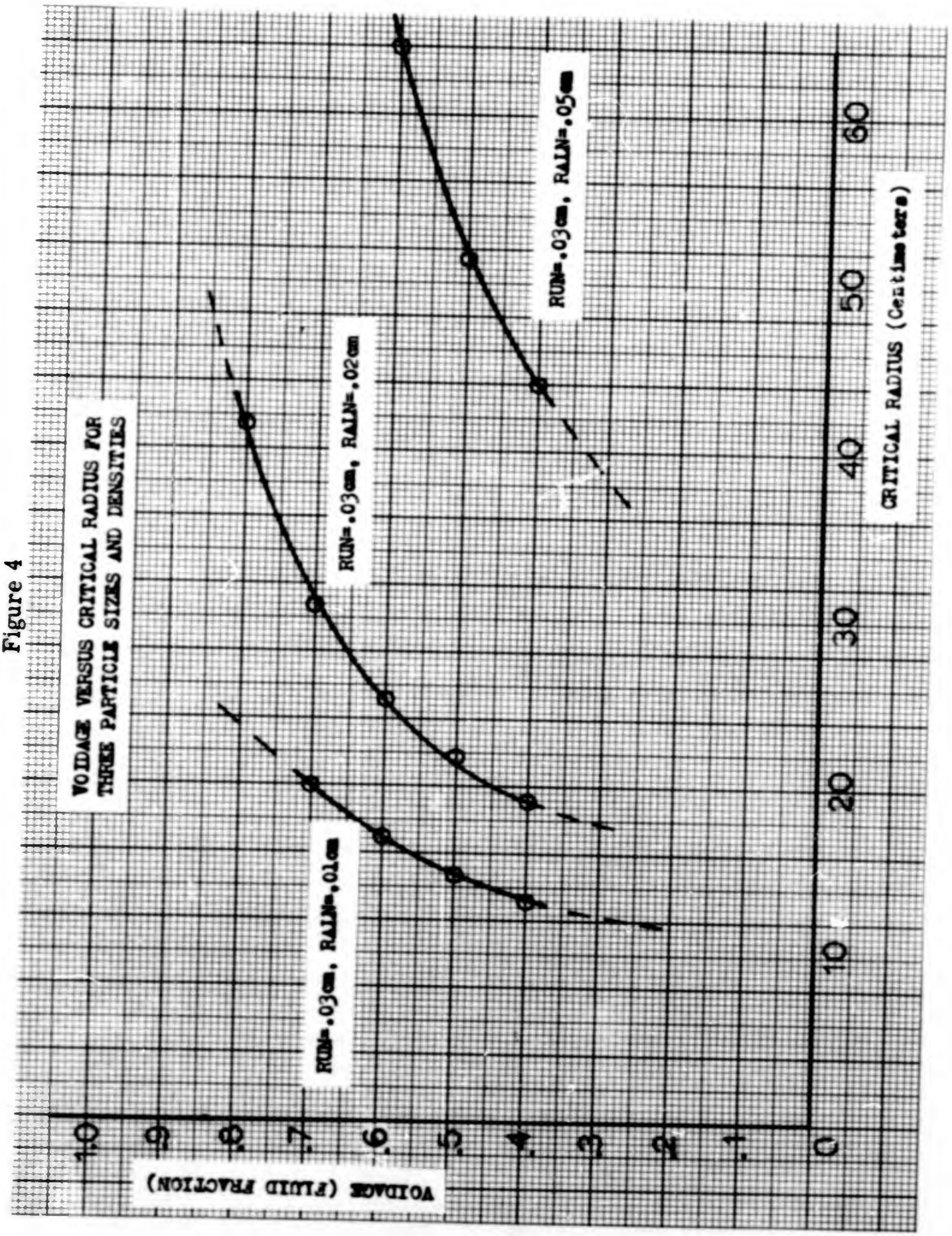
VOIDAGE VERSUS CRITICAL RADIUS FOR
THREE PARTICLE SIZES AND DENSITIES
RUN=.03cm, RAIN=.05cm
RUN=.03cm, RAIN=.02cm
RUN=.03cm, RAIN=.01cm
VOIDAGE (FLUID FRACTION)
CRITICAL RADIUS (Centimeters)
1.0
.9
.8
.7
.6
.5
.4
.3
.2
.1
0
10
20
30
40
50
60

Figure 4

If the solid lines in Figure 5 may be legitimately extended, they would indicate that the same critical radius may be obtained by replacing a given amount of liquid aluminum with AlN, or vice versa, for a constant U^{235} atom ratio (not necessarily a constant volume of U^{235} per unit volume).

It begins to appear that AlN and liquid aluminum may be essentially interchanged in the reactor without affecting criticality. If this is true, then the introduction of voids of AlN into the core would make up for a loss of coolant and prevent a supercritical condition.

Figure 6 confirms this guess, showing that the important factor affecting critical radius is the total mass of U^{235} in the system, not the ratio between AlN and liquid aluminum. Another observation from this figure is that an increase in effective volume (thus radius) of the core by the introduction of a nonfissionable material (AlN) leaving the mass of U^{235} constant, will result in a subcritical configuration.

Three-Component Graphs. The three-component graphs are an attempt to correlate the important parts of the preceding three graphs into one system. Molecular fractions of each component, UN, AlN, and Al (liquid) are read either from the sides or the cross-hatching lines perpendicular to the sides. At the upper vertex, the molecular fraction of UN is 1.0, that of AlN is 1.0 at the right-hand vertex, and that of Al (liquid) is 1.0 at the left-hand vertex. Points in between the vertices represent various ratios of these three components. Moving along a line parallel to one side means that the fraction of the component represented by the opposite vertex remains constant, while the fractions of the other two components change.

Lines of constant voidage for any coating thickness (for the same UN spheres) and lines of constant critical radius (heavy lines) are

BLANK PAGE

Figure 5

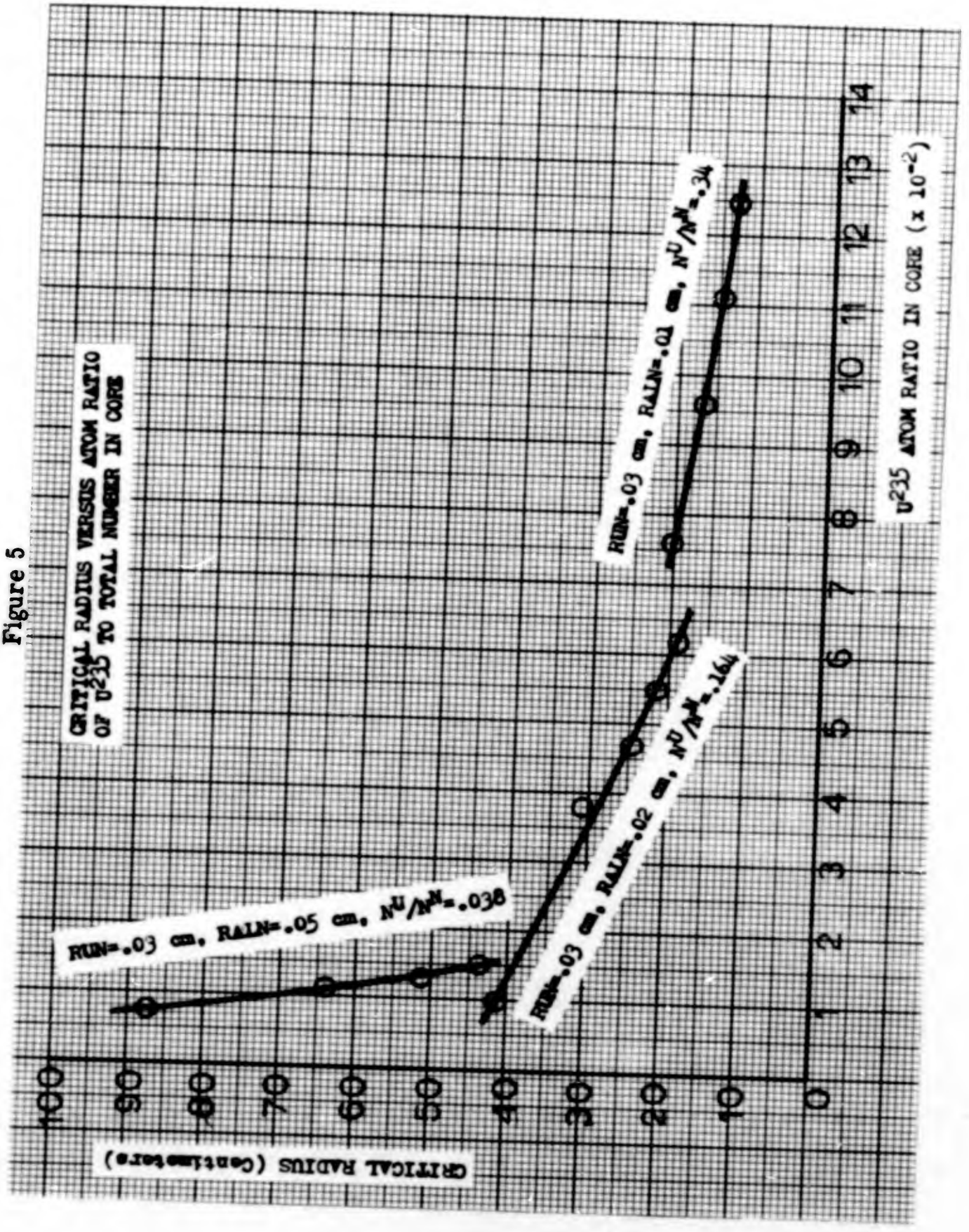
CRITICAL RADIUS VERSUS ATOM RATIO OF U235 TO TOTAL NUMBER IN CORE
RUN=.03 cm, RALN=.05 cm, N^U/N^N=.038
RUN=.03 cm, RALN=.02 cm, N^U/N^N=.164
RUN=.03 cm, RALN=.01 cm, N^U/N^N=.34
CRITICAL RADIUS (Centimeters)
U235 ATOM RATIO IN CORE (x 10^{-2})
100
90
80
70
60
50
40
30
20
10
0
1
2
3
4
5
6
7
8
9
10
11
12
13
14

Figure 6

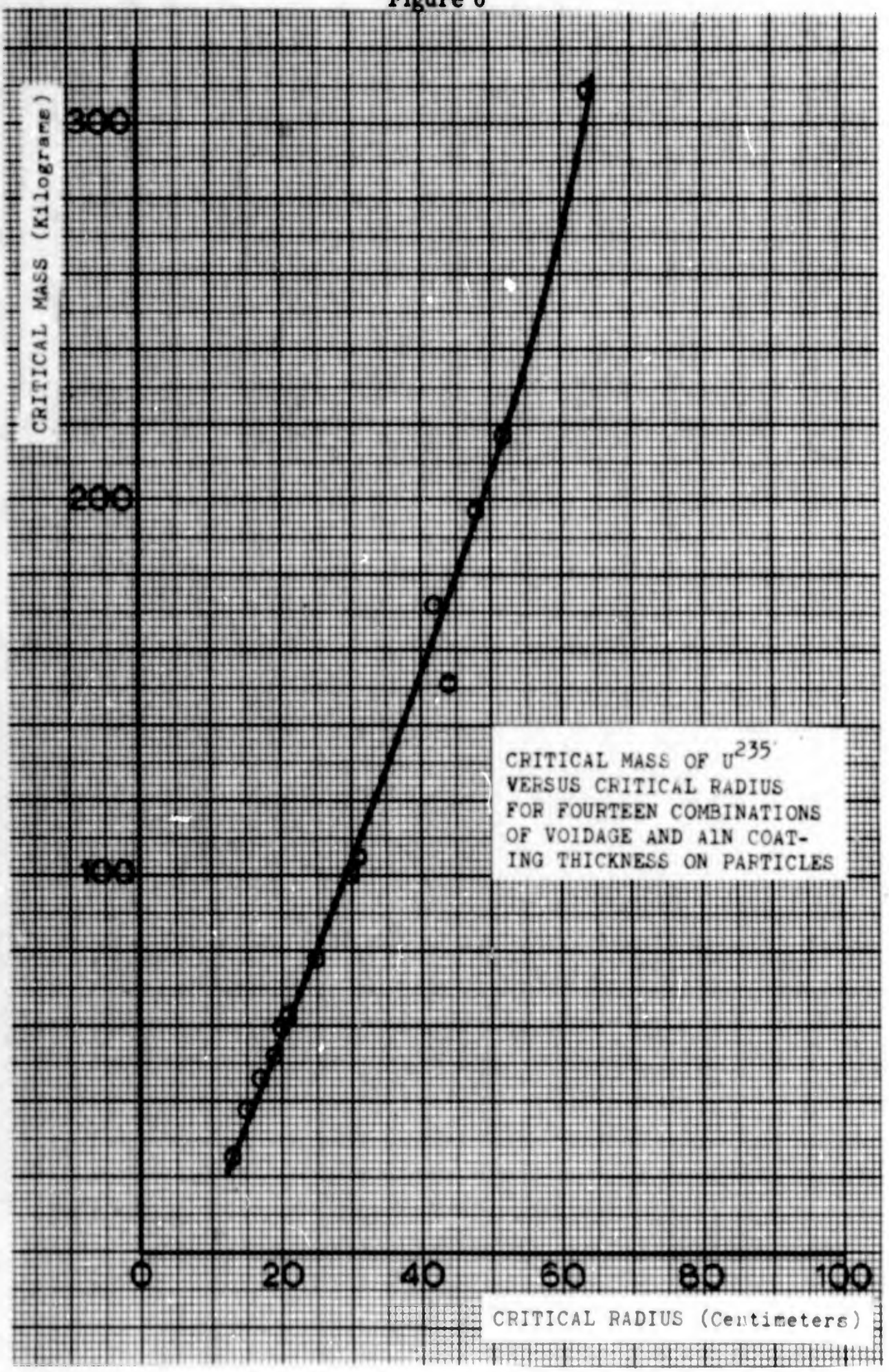
CRITICAL MASS (Kilograms)
300
200
100
0
20
40
60
80
100
CRITICAL RADIUS (Centimeters)
CRITICAL MASS OF U^{235} VERSUS CRITICAL RADIUS FOR FOURTEEN COMBINATIONS OF VOIDAGE AND AlN COATING THICKNESS ON PARTICLES

Figure 7

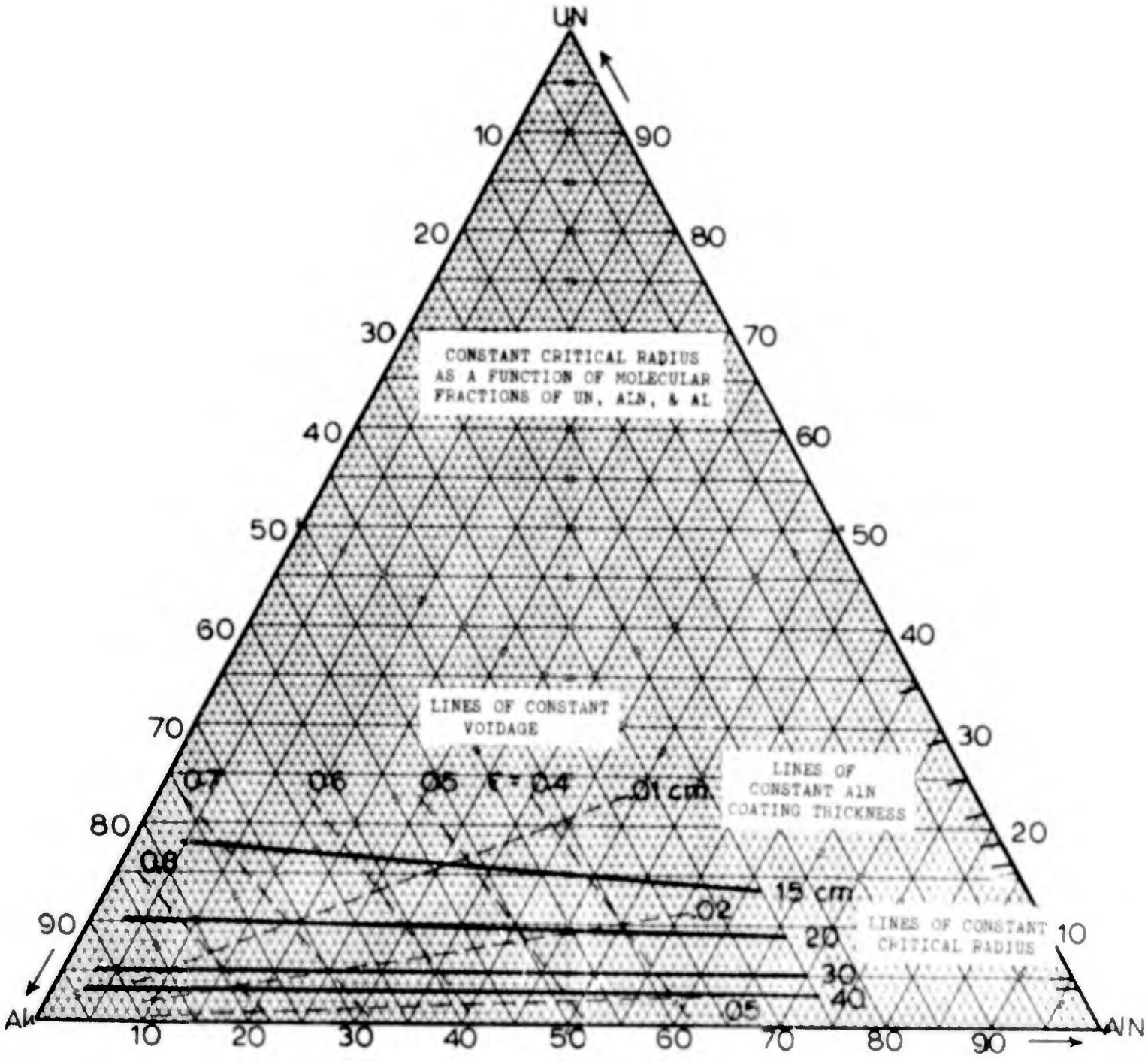
UN
AlN
Al
CONSTANT CRITICAL RADIUS AS A FUNCTION OF MOLECULAR FRACTIONS OF UN, AlN, & Al
LINES OF CONSTANT VOIDAGE
LINES OF CONSTANT AlN COATING THICKNESS
LINES OF CONSTANT CRITICAL RADIUS
.01 cm
.02
.05
.06
.07
.08
ε = 0.4
15 cm
20
30
40
10
20
30
40
50
60
70
80
90

plotted on these graphs. Figure 8 is simply a "times two" reproduction of the important portion of the preceding Figure 7.

To use the graph in predicting the operation at the reactor, choose an operating point, for example $\epsilon = 0.6$, coating thickness = 0.02 cm, and draw a straight line from that point to any other point. Each line represents a path along which a change in the molecular fraction of one component results in a precisely defined change in the fractions of the other two components, and the system parameters.

Moving along a line to the Al vertex will show the changes in system parameters as the voidage changes. Alternately, a line to the AlN vertex shows the effect of increasing the coating thickness on the particles.

Finally, looking at Figure 8, it is evident that a path exists (some line, not necessarily straight)along which a decrease in voidage (Al fraction) could be offset by the introduction of voids of AlN (increase AlN fraction) and an increase in the effective volume of the core (decrease UN fraction). Thus the reactor may be made stable by the correct placing of chunks of AlN and diverging channels.

Summary

Two-group diffusion theory calculations, based upon cross sections from the GAM-I code and BNL-325, have given values of critical radius and flux distribution, and have shown how these values change with changes in both the fuel particles and voidage. A study of these relationships indicates that a stable core configuration is possible. A tentative design for the core region will be presented in the following chapter.

Figure 8

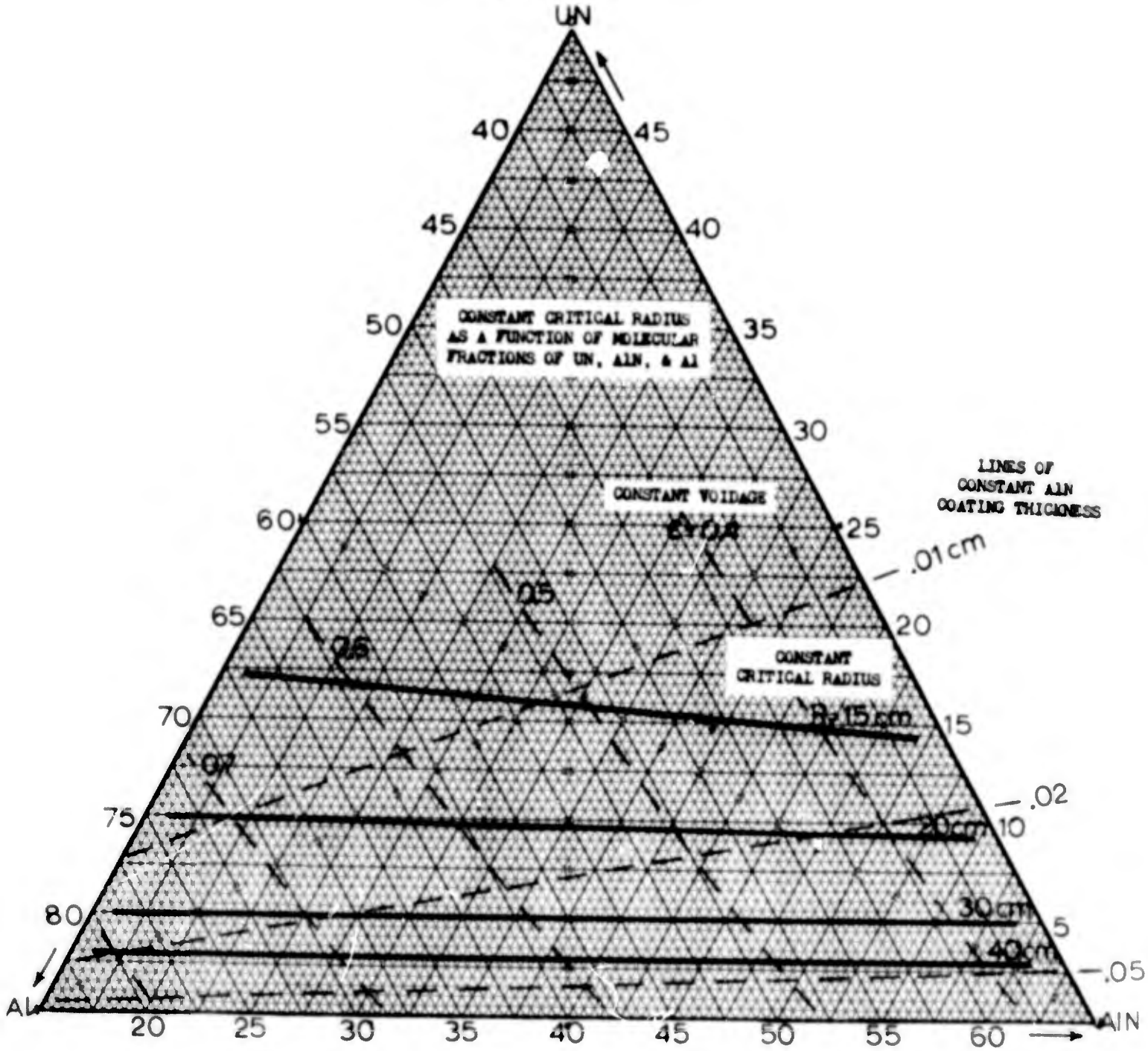
UN
40
45
45
40
50
35
55
30
60
25
65
20
70
15
75
10
80
5
Al
20
25
30
35
40
45
50
55
60
AlN
CONSTANT CRITICAL RADIUS AS A FUNCTION OF MOLECULAR FRACTIONS OF UN, AlN, & Al
CONSTANT VOIDAGE
.05
.06
.07
CONSTANT CRITICAL RADIUS
R=15cm
20cm
30cm
40cm
LINES OF CONSTANT AlN COATING THICKNESS
.01cm
.02
.05

V. Summary

A solution to the problem of materials selection was obtained by excluding metal-alloy coolants, liquid-metal fuels and refractory compounds of plutonium from consideration, for the reasons stated in Chapter II. These exclusions led to the selection of aluminum as the coolant, aluminum nitride as the core construction material, and uranium mononitride clad with aluminum nitride as the fuel material.

Consideration of the heat transfer requirements for a high thermal-power-output from the reactor (at 2000°C) resulted in the selection of a cylindrical, fluidized bed core, with spherical AlN coated UN fuel particles 0.1 cm. in diameter fluidized by liquid aluminum.

Once the materials and the general core configuration were selected, a nuclear parameters study was performed using two-group diffusion calculations for an infinitely reflected spherical geometry. The reactor calculations indicate that the core can be made critical without an excessive fuel inventory (for a fast reactor) and that a stable, controllable core configuration is possible.

With the problem of control apparently solvable, it is possible to determine a complete core configuration. The tentative design from Chapter III, which specified a cylindrical core with a height-to-diameter ratio of about 1.0 and a "firebrick" type of core wall is still valid, but the following additions may be made.

In place of a baffle plate, diverging circular channels with an increasing cross-sectional area will be used. The fuel particles will be introduced to the core region through these channels at a high flow rate. The increasing cross-sectional area at the core entrance will lower the fluid velocity sufficiently to achieve a voidage of about 0.6 to 0.7 in the core, with very few of the particles still contained in the entrance channels. Since the channels diverge rapidly away from

BLANK PAGE

the core entrance, any decrease in flow rate which collapses the bed into the channels will also increase the effective volume (radius) of the core and render it subcritical. That such a system is possible is evident from Figure 8, although the exact shape of the channels will have to be determined.

Some fine control will be possible either by changing the flow rate slightly or by introducing more fuel particles to the core. For shutdown, the flow rate may be increased to blow the particles from the core, or decreased to let the bed collapse back into the entrance channels.

Figure 9 shows a possible core configuration which incorporates the results of the nuclear parameters study with the tentative design from Chapter III. If it is assumed that the reactor calculations for the infinitely reflected, spherical geometry are also valid for this configuration, then some idea of the parameters of the core at criticality may be obtained.

If a core radius of twenty-five centimeters and a voidage of 0.6 are chosen, the critical mass of U^{235} in the core will be about eighty kilograms (Figures 4 and 5). Assuming particles with a UN core 0.03 cm. in diameter, coated with 0.02 cm. of AlN, the mass flow rate for a voidage of 0.6 will be between 45,000 and 60,000 $lbm/ft^2/hr$ per square foot of core cross sectional area (Figure 1). For an inlet temperature of 1700°C and an outlet temperature of 2000°C, the thermal power at the outlet will be between 1.8 and 2.5 megawatts per square foot of bed cross sectional area, with an average fluid velocity of 0.1 to 0.13 feet per second (Appendix C).

The above procedure indicates in a qualitative manner what could be expected from the final design. Although many details have been ignored, the feasibility of the design is evident.

Figure 9

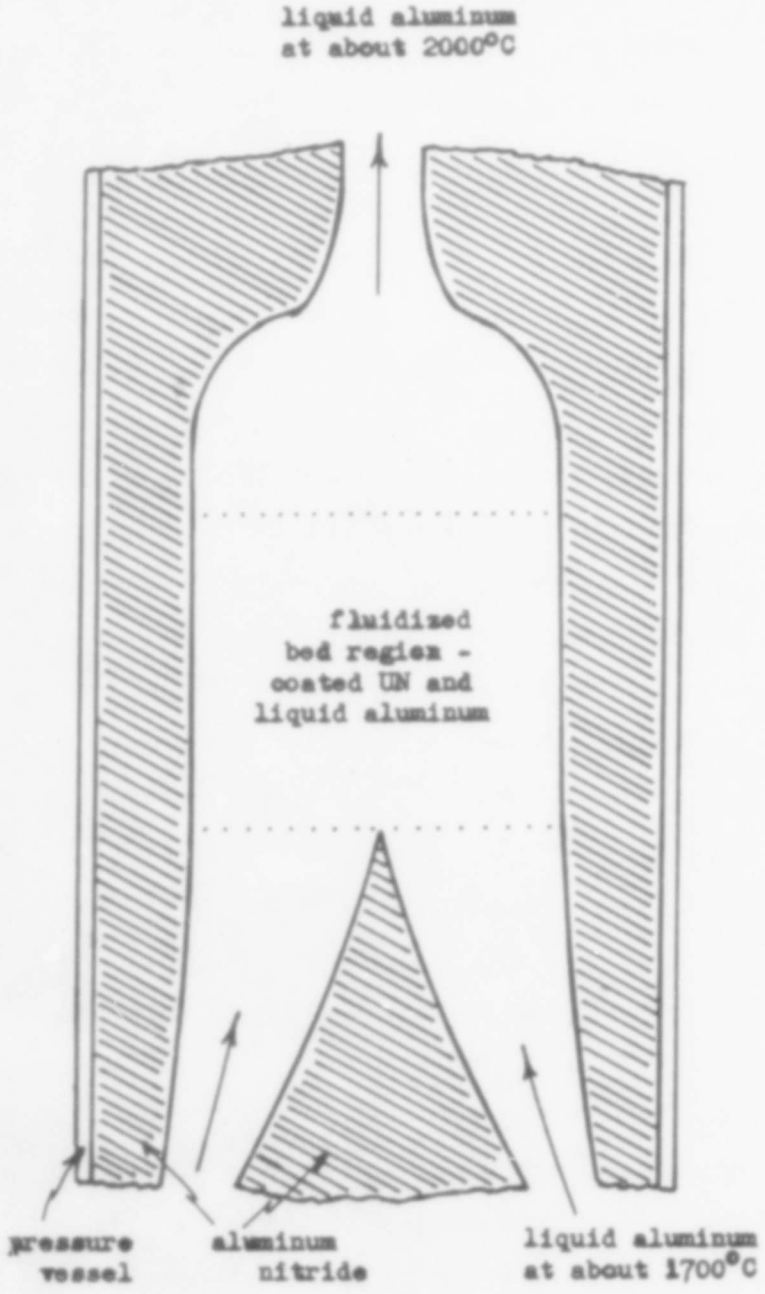

Schematic Cross-section of Liquid Aluminum Fluidized Bed Nuclear Reactor

Recommendations

It is probable that the major value of this report lies in the questions which could not be answered. A surprisingly small amount of experimental data on high-temperature properties of materials is available, although more is being generated all the time. The field of liquid metals is almost completely restricted to work below 1000°C, and what data is available for higher temperatures is inconsistent. Finally, the compatibility of materials is obviously extremely difficult to predict even at low temperatures. At high temperatures (above 1000°C), experimentation will be necessary in order to determine compatibility.

Since the feasibility of the design presented in this report is based upon the materials study, any further work should start with a much closer look at materials and should include experimental work on compatibility.

Bibliography

1. Anders, William A. et. al. Feasibility Study of a High Temperature Fluidized Bed Nuclear Reactor. Prepared for Physics 393, Nuclear Systems Engineering, Air Force Institute of Technology, 4 August 1962.

2. Blocher, J. M. et. al. "Properties of Ceramic-Coated Nuclear Fuel Particles." Transactions of the American Nuclear Society, 6:377-378 (November 1963).

3. Carr, Norman L. and Amundson, Neal R. "Heat Transfer and Heat Release in Fluidized Beds." Industrial and Engineering Chemistry, 43:1856-1862 (1951).

4. El-Wakil, M.M. Nuclear Power Engineering. New York: McGraw-Hill Book Company, 1962.

5. Etherington, Harold. Nuclear Engineering Handbook. New York: McGraw-Hill Book Company, 1958.

6. Evans, P. E. and Davies, T. J. "Uranium Nitrides." Journal of Nuclear Materials, 10:43-54 (1963).

7. -----. Fluidized Bed Reactor Study, Phase I - Feasibility. Martin Nuclear Division, MND-FBR-1696 (February 1959).

8. -----. Fluidized Bed Reactor Study - Reactor Design and Feasibility Study. Oak Ridge School of Reactor Technology, CF-57-8-14 (August 1957).

9. Gronroos, H. G. Critical Calculations for a Fast Liquid-Metal-Cooled Reactor - Phase I. Jet Propulsion Laboratory, Technical Report No. 32-512 (15 November 1963).

10. Hague, J. R. et. al. Refractory Ceramics of Interest in Aerospace Structural Applications - A Materials Selection Handbook. Technical Documentary Report No. ASD-TDR-63-4102 (October 1963).

11. Hauck, Jack E. "Guide to Refractory Ceramics." Materials in Design Engineering:85-95 (July 1963).

12. Jackson, Carey. Liquid-Metals Handbook - Sodium (NaK) Supplement (Third Edition). United States Atomic Energy Commission, July 1955.

13. Jones, W.R.D. and Bartlett, W.L. "The Viscosity of Aluminum and Binary Aluminum Alloys." The Journal of the Institute of Metals, 6:145-152 (1952).

14. Katz, Seymour. "High Temperature Reactions Between refractory Uranium Compounds and Metals." Journal of Nuclear Materials, 6:172-181 (1962).

15. Lewis, E. W. and Bowerman, E. W. "Fluidization of Solid Particles in Liquids." Chemical Engineering Progress, 48:603-610 (1952).

16. Leva, Max. Fluidization. New York: McGraw-Hill Book Company, 1959.

17. -----. Literature Survey - Uranium Mononitride. Atomics International, NAA-SR-TDR-7208 (March 1962).

18. Long, George and Foster, L. M. "Aluminum Nitride, A Refractory for Aluminum to 2000°C." Journal of the American Ceramic Society, 42:53-59 (1 February 1959).

19. Long, George and Foster, L. M. "Aluminum Nitride Containers for Vacuum Evaporation of Aluminum." Ceramic Bulletin, 40: 423-425 (1961).

20. Lyon, Richard N. et. al. Liquid-Metals Handbook (Second Edition). Office of Naval Research, 1952.

21. Mah, Alla D. et. al. "Thermodynamic Properties of Aluminum Nitride." Bureau of Mines Report of Investigations #5716 (1961).

22. Murray, R. L. Introduction to Nuclear Engineering (Second Edition). Englewood Cliffs, N. J.: Prentice-Hall, Inc., 1961.

23. Murray, R. L. Nuclear Reactor Physics. Englewood Cliffs, N. J.: Prentice-Hall, Inc., 1957.

24. -----. Neutron Cross Sections. Brookhaven National Laboratory, BNL-325, 1 July 1958.

25. Othmer, Donald F. Fluidization. New York: Reinhold Publishing Corporation, 1956.

26. Paulsen, F. R. "Ceramics and Cermats for Nuclear Fuels." Chemical and Process Engineering:49-52 (February 1960).

27. Powell, C. F. et. al. Vapor Plating. New York: John Wiley and Sons, Inc., 1955.

28. Quill, Laurence L. The Chemistry and Metallurgy of Miscellaneous Compounds. New York: McGraw-Hill Book Company, 1950.

29. Rand, M. H. and Kubaschewski, O. The Thermochemical Properties of Uranium Compounds. New York: Interscience Publishers, 1963.

30. ----. "Raw Materials for High Temperature Ceramics." Ceramic Industry: 86-92 (January 1963).

31. ----. Reactor Physics Constants (Second Edition). Argonne National Laboratory, ANL-5800. United States Atomic Energy Commission, July 1963.

32. Richardson, J. F. and Zaki, W. N. "Sedimentation and Fluidization: Part I." Transactions of the Institute of Chemical Engineers, 32: 35-53 (1954).

33. Shvidkovsky, E. G. "Certain Problems Relating to the Viscosity of Liquid Metals." NASA Technical Translation F-88, 1962.

34. Smithells, Colin J. Metals Reference Book (Second Edition). New York: Interscience Publishers, 1955.

35. Taylor, L. M. and Lenie, Camille. "Some Properties of Aluminum Nitride." Journal of the Electrochemical Society, 107:308-314 (April 1960).

36. Townley, C. W. et. al. "In-Pile Performance of Ceramic Coated-Particle Fuels." Nucleonics, 22: 43-48 (February 1964).

37. Wullaert, Richard A. et. al. Radiation Stability of Uranium Mononitride. Battelle Memorial Institute, BMI-1638 (28 June 1963).

38. Yao, T. P. and Kondic, V. "The Viscosity of Molten Tin, Lead, Zinc, Aluminum, and Some of Their Alloys." The Journal of the Institute of Metals, 81: 17-24 (1952).

39. Zabrodsky, S. S. "Heat Transfer by a Fluidized Bed." International Developments in Heat Transfer, Part IV - Mass Transfer, Packed and Fluidized Beds. ASME, 1961.

40. Zenz, Frederick A. and Othmer, Donald F. Fluidization and Fluid-Particle Systems. New York: Reinhold Publishing Corporation, 1960.

41. Hansen, Max. The Constitution of Binary Alloys (Second Edition). New York: McGraw-Hill Book Company, 1958.

42. Frank, W. B. Personal Correspondence, 6 November 1963 (Appendix A).

Appendix A

Personal Correspondence

Copies of six of the eleven letters which were received during the course of collecting property values of materials are included in this appendix. They contain references to physical properties of liquid aluminum at high temperatures, to materials which might be inert to liquid aluminum, and to thermochemical properties of various uranium compounds. The inclusion of these six letters is intended to give examples of the sources which were contacted and to underline the lack of high-temperature data on both physical and thermochemical properties. The letters are in order of date received.

Defense Metals Information Center

Battelle Memorial Institute
505 KING AVENUE
COLUMBUS 1, OHIO
AREA CODE 614. TELEPHONE 299-3191

ZIP CODE 43201
October 18, 1963

Lt. Kenneth Hooks
Air Force Institute of Technology
Wright-Patterson Air Force Base
Ohio

Dear Lt. Hooks:

Enclosed is a list of references on the compatibility of materials with molten aluminum as discussed by phone with you recently.

There are no known metals or alloys completely resistant to attack by molten aluminum(1)*. Plated chromium is reported to be resistant to aluminum near its melting point(2) while stainless steels become embrittled under similar exposure conditions(3). The high melting refractory metals would offer little advantage at temperatures much above the aluminum melting point as evidenced by binary phase diagrams(4). For example, tungsten is readily dissolved by molten aluminum at temperatures of 1300 to 1600 C(5).

Only the refractory oxides and graphite apparently are resistant to molten aluminum. Graphite has good resistance up to 1200 C, but can be used up to 1700 and 1800 C. Ceramics which may be useful are Al_2O_3, BeO, ThO_2, MgO, and ZrO_2.(1)

We hope this information will be of value to you.

Very truly yours,

WK. Boyd

Walter K. Boyd
Acting Chief
Corrosion Research Division

WKB:bcw

Enc.

*Please refer to enclosed List of References.

REFERENCES

1. R. N. Lyon, "Liquid Metals Handbook", AEC and BuShip Dept of Navy, NAVEXOS P-733 (Rev) June 1952.

2. M. Kolodney, "Industrial Applications of Chrome Plating - A Review"

3. F. R. Morrall, "Corrosion of Materials of Construction by Molten Metals", Wire and Wire Products 23, 484, 571 (1948).

4. M. Hansen, "Constitution of Binary Alloys", McGraw-Hill Book Co., Inc., New York, 1958.

5. W. D. Clark, "The Aluminum-Tungsten Equilibrium Diagram", J. Inst. Metals 66, 271-286 (1940).

ALUMINUM COMPANY OF AMERICA

P. O. BOX 772 · NEW KENSINGTON, PA.

ALCOA RESEARCH LABORATORIES

November 6, 1963

Lt. Kenneth R. Hooks
Box 3035, AFIT
Wright-Patterson AFB
Dayton, Ohio

Dear Mr. Hooks:

Your letter of October 28, 1963, to Mr. George Long requesting information on the high temperature properties of liquid aluminum has been directed to my attention. Neither Mr. Long nor Dr. Foster, the coauthor of the paper to which you referred, is now associated with Alcoa Research Laboratories.

Few of the properties of molten aluminum have been measured in the temperature interval 1500-2000°C. Estimates of the values of most properties at these temperatures must be obtained from extrapolations of measurements at considerably lower temperatures. There is no reason to believe that such extrapolations of the physical properties of liquid aluminum are not valid at the elevated temperatures.

A good source of thermochemical data for liquid aluminum is JANAF THERMOCHEMICAL TABLES, The Dow Chemical Company, Midland, Michigan. The vapor pressure of molten aluminum, as calculated from the thermodynamic data of the JANAF TABLES is presented in the following table:

°K	°C	P (atm.)
1800	1527	0.0010
1900	1627	0.0030
2000	1727	0.0079
2100	1827	0.0188
2200	1927	0.0410
2300	2027	0.0818

The density of aluminum above its melting point has been reported by Belyaev, et al. (Metallurgie Des Aluminiums, I, VEB Verlag Technik, Berlin, 1956, p. 20). The

values are presented in the following table:

Temperature °C	Density g/cm^3
658.7	2.382
700	2.371
800	2.343
900	2.316
1000	2.289
1100	2.262

These values can be represented by the linear equation,

$$D = 2.382 - 0.000273\ (t - 659)$$

where D is the density in g. per cc
and t is the temperature in °C.

The values of electrical resistivity of aluminum reported by Roll and Motz [Z. Metallkunde, 48, 272 (1957)] are given in the following table:

Temperature °C	Electrical Resistivity 10^{-6} Ω cm
700	24.7[s]
800	26.2[s]
900	27.7[s]
1000	29.2
1100	30.6[s]
1200	32.1[s]

A linear extrapolation of these values to the temperatures of interest would appear to be valid.

Recent experience in these Laboratories has shown that molten aluminum reacts rapidly with carbon or graphite above 1500°C and that the aluminum carbide formed does not inhibit further attack on the graphite.

Some possible refractory materials for liquid aluminum above 1500°C are the oxides of beryllium, magnesium, and aluminum. Limitations of these materials are thermal shock, workability, and the formation of aluminum suboxide at elevated temperatures. You are familiar with the literature on the refractory properties of aluminum nitride. We have no information on the compatibility of the nitrides of uranium and plutonium with aluminum at 1500-2000°C. However, the thermochemical stability of these materials (See Campbell, I.E., "High Temperature Technology," p. 172, John Wiley and Sons, 1956) suggests that they may be inert to attack by molten aluminum at high temperatures.

I hope that this information will be helpful to you in your thesis on reactor design.

Very truly yours,

ALUMINUM COMPANY OF AMERICA
Alcoa Research Laboratories

W. B. Frank

W. B. Frank
Physical Chemistry Division

WBF:jg

GNE/Phys/64-10

RESEARCH INSTITUTE OF TEMPLE UNIVERSITY
4150 Henry Avenue
Philadelphia 44, Pa.

OFFICE OF THE PRESIDENT

TELEPHONES
GERMANTOWN 8-5100
VICTOR 8-8000

November 6, 1963

Kenneth R. Hooks, 2/Lt., USAF
AFIT Box 3035
Wright-Patterson AFB
Dayton, Ohio

Dear Lt. Hooks:

In reply to your letter of October 31, 1963, I can provide you with the literature references listed below dealing with the physical properties of liquid aluminum.

Viscosity

E. Gebhardt, M. Becker and S. Dorner, Z. Metallk., 44, 510 (1953).

E. G. Shvidkovsky, "Certain Problems Relating to the Viscosity of Liquid Metals", NASA Technical Translation F-88, 1962.

Liquid Metals Handbook, NAVEXOS P-733 (Rev.), Washington (1952).

T. P. Yao and V. Kondic, J. Inst. Metals, 81, 17 (1952).

W. R. D. Jones and W. L. Bartlett, J. Inst. Metals, 81, 145 (1952).

E. Polack and S. V. Sergueiev, Doklady Akad. Nauk., S.S.S.R., 30, 137 (1941).

C. J. Smithells, Metals Reference Book, Butterworths Scientific Publications, London (1955).

Surface Tension

International Critical Tables, McGraw-Hill Book Co., Inc., New York (1933).

U. A. Kliachko, Zavadskaya Lab., 6., 1376 (1937).

A. Portevin and P. Bastien, Compt. rend., 202, 1072 (1936).

E. Pelzel, Berg-und Hüttenmannische Monatsheft, 93, 248 (1948).

V. N. Eremenko and Yu. V. Naidich, Fiz. Metal i. Metalloved Akad. Nauk. S.S.S.R., 11, 883 (1961).

A. M. Korolkov, Izvest. Akad. Nauk. S.S.S.R., Odtel. Tekl. Nauk., 1956, No. 2, 35.

Density

J. D. Edwards and T. A. Moorman, Chem. and Met. Eng., 24, 61 (1921).

E. Gebhardt, M. Becker and S. Dorner, Z. Metallk., 44, 573 (1954).

E. Pelzel, Z. Metallk., 32, 7 (1940).

K. Bornemann and F. Sauerwald, Z. Metallk., 14, 145 (1922).

Few if any of the data mentioned in these articles refer to temperatures in excess of 1000°C. However, in many cases reasonable extrapolations are possible but many of the data are conflicting. I cannot guarantee that the above is a complete list of available references.

Boron nitride and aluminum nitride will contain aluminum above 1500°C.; graphite and alumina may possibly serve. Offhand, I don't know of anyone who is actually working on the high-temperature properties of aluminum.

Best of luck in your studies.

Sincerely,

A. V. Grosse

AVG:etc

GNE/Phys/64-10

THE LIBRARY OF CONGRESS

WASHINGTON 25, D. C.

REFERENCE DEPARTMENT
NATIONAL REFERRAL CENTER
FOR SCIENCE AND TECHNOLOGY

November 12, 1963

Lieutenant Kenneth R. Hooks
AFIT Box 3035
Wright-Patterson Air Force Base
Dayton, Ohio

Dear Lieutenant Hooks:

This is in reply to your letter of November 4, in which you asked for information about corrosion resistant materials for liquid aluminum above 1500°C.

The National Referral Center directs inquirers to sources of information, rather than providing bibliographic reference services or answering specific questions. Depending upon their capabilities, the information resources to which you are referred will provide one or both of these services. A brochure further describing our functions is enclosed.

The following information resources and those indicated on the attached sheet may be able to assist you:

Aluminum Association
420 Lexington Avenue
New York, New York 10017

The Association provides special state-of-the-art reports and answers technical questions.

American Die Casting Institute, Inc.
366 Madison Avenue
New York, New York 10017

The Institute collects and disseminates information on aluminum castings.

Aluminum Smelters Research Institute
20 North Wacker Drive
Chicago, Illinois 60606

The Institute provides answers to technical questions relating to secondary aluminum and alloys.

American Foundrymen's Society
Golf and Wolf Roads
Des Plaines, Illinois

The Society collects and makes available information relating to the casting industry. It provides answers to technical questions and limited technical consultant services.

American Society for Metals (ASM)
Metals Park
Novelty, Ohio

This Society provides current and retrospective searching services for a fee on subjects specified by the subscriber. The Society also publishes and sells a monthly periodical, ASM Review of Metal Literature.

Engineering Societies Library
United Nations Plaza
345 East 47th Street
New York, New York 10017

Open to the public, the ESL will answer requests in all fields of engineering and related sciences. Questions involving readily available information are answered free but fees are charged for literature searches and translating services. Photoprint or microfilm copies of articles in the Library including all items indexed by Engineering Index are supplied on order.

You can also refer to the following publications for additional information:

Aluminium Abstracts, published and distributed for the Centre International de Developpement de l'Aluminium, 6 rue Bertie Albrecht, Paris 8e by British Aluminum, Norfolk House, St. James's Square, London S.W.1, England. Biweekly.

Abstract Bulletin of Aluminum Laboratories, Ltd., published and distributed gratis by the Laboratories, Box 84, Kingston, Canada. Monthly.

Chemical Abstracts, published and sold by the American Chemical Society, Washington, D. C. 20006. Biweekly.

The Wright-Patterson Air Force Base Technical Library may be of assistance in making available to you these and other publications pertinent to your needs.

We have purposely omitted a resource at Wright-Patterson Air Force Base, the Materials Central, assuming that you are already familiar with the services provided by this organization. However, if you are not acquainted with it, we will be glad to provide you with appropriate details.

The foregoing citations include only those we have thus far identified as relevant to your need. Our listings are not yet as definitive, quantitatively or qualitatively, as those we expect to furnish when we achieve increased knowledge of more specific information resources.

Any comments you care to give us on the usefulness of the resources we have cited will be most helpful in improving the effectiveness of our referral service.

Sincerely,

Charles E. McCabe, Head
Referral Services Section

Enclosures

GNE/Phys/64-10

THE DOW CHEMICAL COMPANY

MIDLAND, MICHIGAN

December 12, 1963

2/Lt. Kenneth R. Hooks
AFIT Box 3035
Wright-Patterson AFB
Ohio

Dear Mr. Hooks:

The JANAF Thermochemical Tables are designed to serve the rocket industry, and have studied chiefly the "light elements" plus some special additive elements. Thus, neither plutonium or uranium are included in our mission.

A table of the thermodynamic properties of uranium to 3000°K. may be found in "The Thermodynamic Properties of the Elements" by Stull & Sinke [No. 18 in the Advances in Chemistry Series] Publ. by the American Chemical Society, Washington, D. C., 1956, $5.

For additional thermodynamic information on uranium, plutonium, and their compounds, you might contact the U. S. Atomic Energy Commission, or consult the open (or classified) literature.

Very truly yours,

Daniel R. Stull

Daniel R. Stull
Thermal Research Laboratory
574 Building

DRS:ndl

U. S. DEPARTMENT OF COMMERCE
NATIONAL BUREAU OF STANDARDS
WASHINGTON 25

ADDRESS REPLY TO
NATIONAL BUREAU OF STANDARDS

December 26, 1963

IN YOUR REPLY
REFER TO FILE
15.01

2/Lt. Kenneth R. Hooks
AFIT Box 3035
Wright-Patterson AFB
Ohio

Dear Lt. Hooks:

Your request for thermochemical properties of uranium, plutonium, and thorium compounds has been transferred to the Thermochemistry Section. We are not aware of any NBS reports on the thermochemical properties of uranium, plutonium and thorium compounds above 1000°C. However information on the elements and some of their compounds may be found in Kelley, Contributions to the data on theoretical metallurgy. XIII High-temperature heat content, heat capacity, and entropy data for the elements and inorganic compounds, U.S. Bur. of Mines Bull. 584 (1960). Information on the elements may also be found in Hultgren, Orr, Anderson and Kelley, Selected values of thermodynamic properties of metals and alloys (John Wiley and Sons, Inc., New York, 1963).

Sincerely yours,

Vivian B. Parker

Vivian B. Parker, Chemist
Thermochemistry Section
Division of Physical Chemistry

Appendix B

Physical Properties of Liquid Aluminum

Vapor pressures of elements are usually represented by an equation of the type

(21) $$\log_{10} p = \frac{A}{T} + B + C \log_{10} T + DT$$

where $A >> B >> C \sim D$ (34: 613), and are ordinarily plotted as logarithm of vapor pressure in mm Hg. versus temperature for work in liquid metals (12: 42). This procedure results in a curve which is a straight line in the middle temperature ranges and concave downward at the ends, if extended sufficiently.

Figure 10 is a plot of the logarithm of the vapor pressure of molten aluminum versus temperature in degrees Centigrade. All of the values are for "pure" or 99+ % pure aluminum, but since some of the values are from 1955 or earlier, the actual purity may be questionable in some cases.

The graph of density as a function of temperature ($^{\circ}$C) on page 66 Figure 11, is obviously lacking in data above 1200°C. The straight line equation

(22) $$D = 2.382 - 0.000273 (T - 659^{\circ}C)$$

is from a letter by Dr. Frank (Appendix A) and applies up to 1100°C. A possible justification for the extension of this straight line to 2000°C is that other liquid metals, sodium and NaK for instance, have densities which are straight line functions of temperature up to their boiling points (12: 39).

It was impossible to determine an accurate value for the viscosity of liquid aluminum above 1300°C. The five sets of points in Figure 12, page 66, are all for 99+ % pure aluminum if the sources are to be believed. There is reason to believe that the viscosity of aluminum decreases markedly as it approaches 99. 99+ % purity (38: 18). The

lowest set of points is from work performed in Russia after 1958 and is for "pure, unoxidized" aluminum (33: 182).

The accepted method for extrapolation of viscosity data to higher temperatures is a straight line extension of a logarithm of μ versus $1/T$ (^{o}K) plot. This method is usually good for 50 or 100^{o}K, but it is certainly liable to error over nearly 1000^{o}K. Since plots of experimental points for liquid metals usually show a decreasing slope at higher temperatures, it is probably safe to pick $\mu > 1$ at 2000^{o}C for aluminum of reasonable purity.

Figure 10

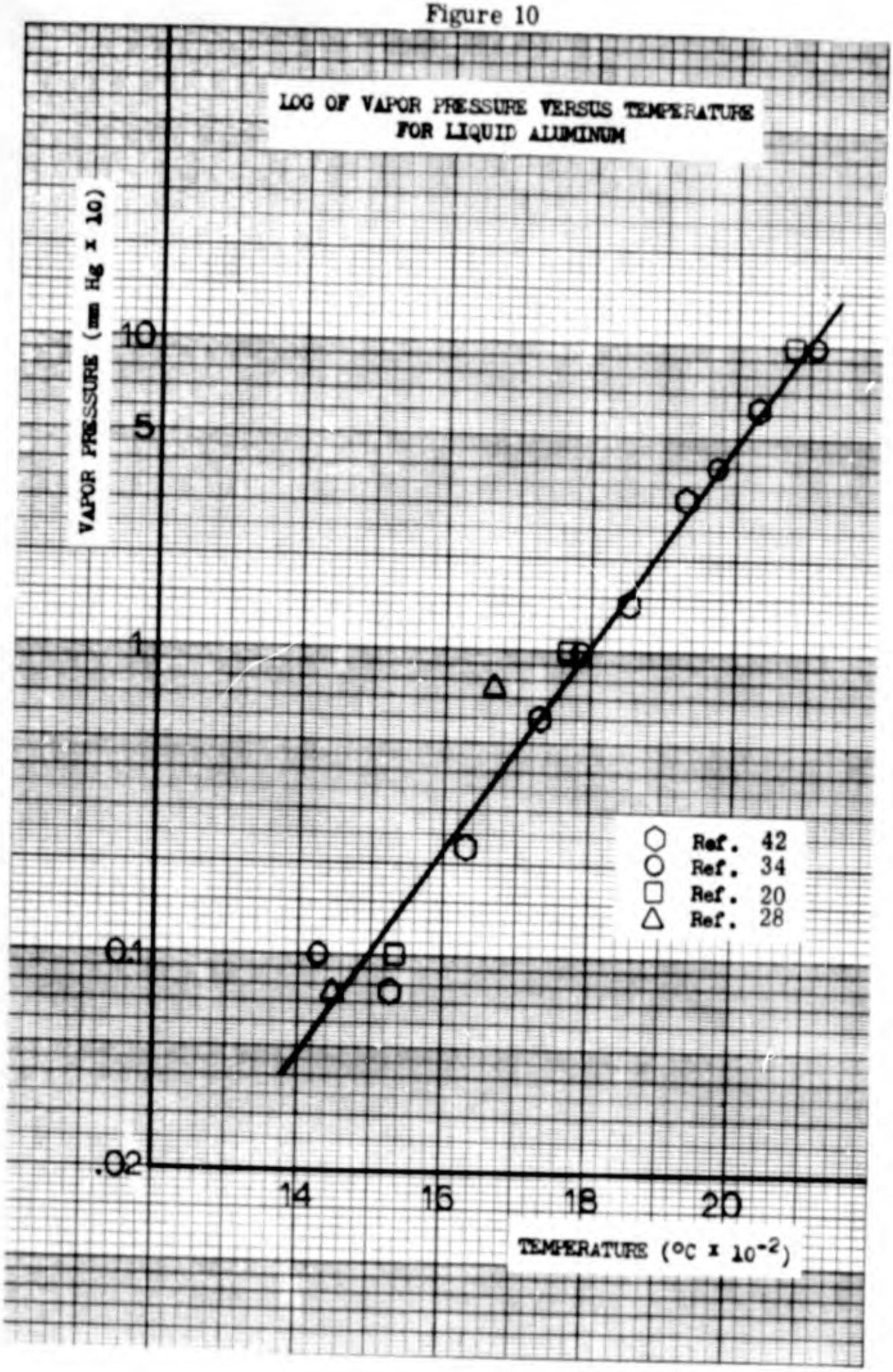
LOG OF VAPOR PRESSURE VERSUS TEMPERATURE
FOR LIQUID ALUMINUM
VAPOR PRESSURE (mm Hg x 10)
10
5
1
0.1
.02
14
16
18
20
TEMPERATURE (°C x 10⁻²)
Ref. 42
Ref. 34
Ref. 20
Ref. 28

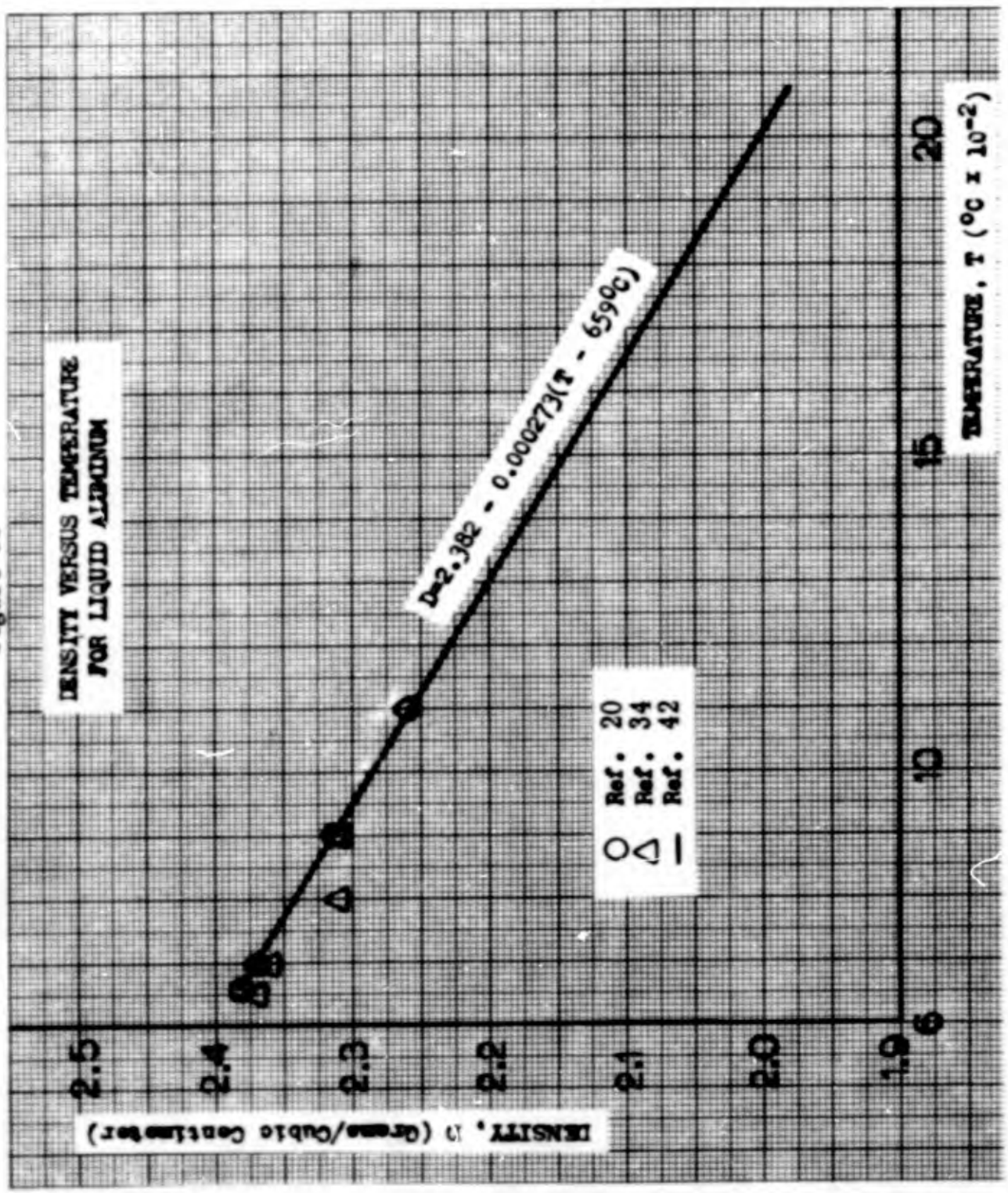
DENSITY VERSUS TEMPERATURE
FOR LIQUID ALUMINUM
D=2.382 - 0.000273(T - 659°C)
○ Ref. 20
△ Ref. 34
— Ref. 42
DENSITY, D (Grams/Cubic Centimeter)
2.5
2.4
2.3
2.2
2.1
2.0
1.9
TEMPERATURE, T (°C x 10⁻²)
6
10
15
20

Figure 11

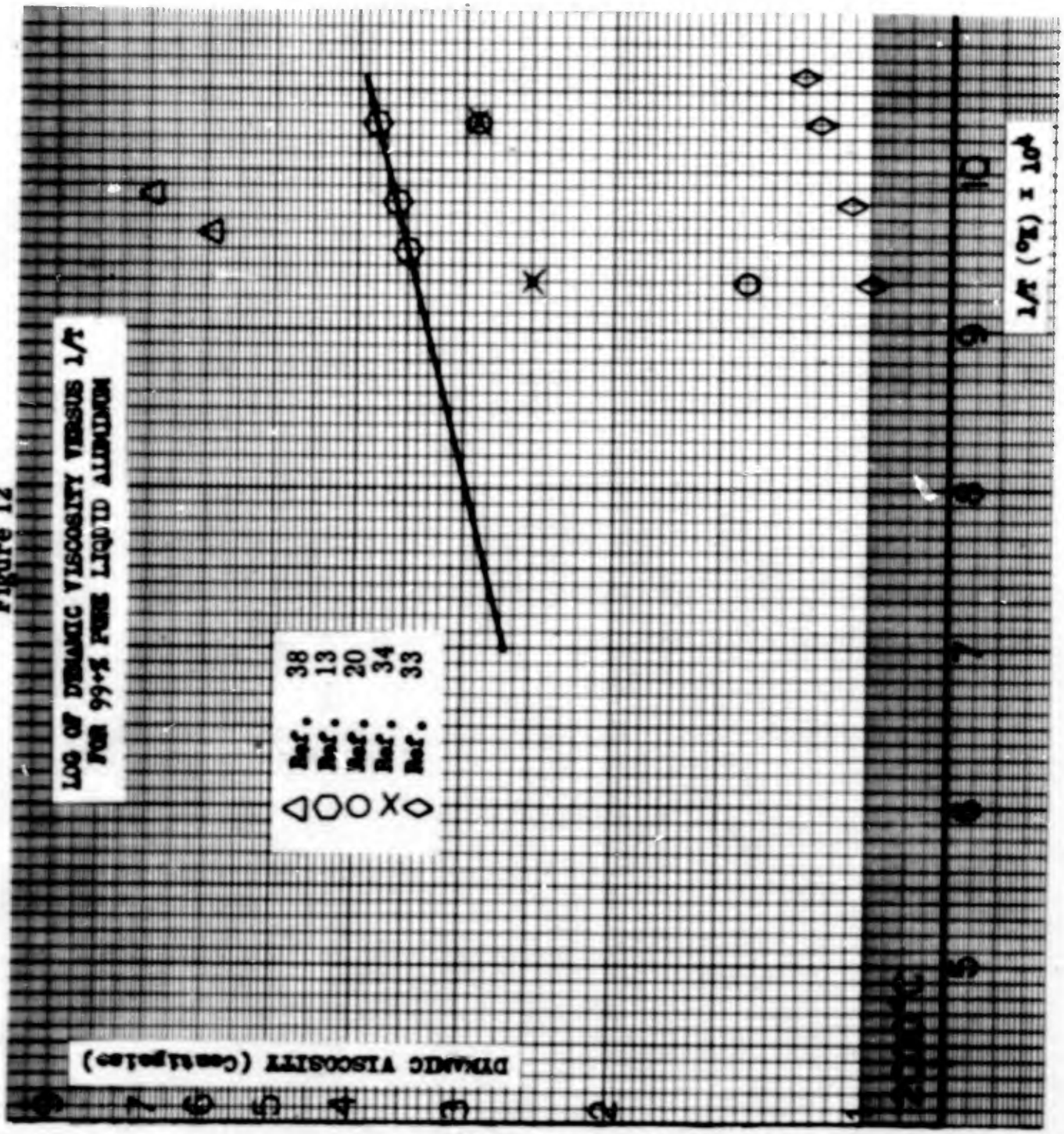
LOG OF DYNAMIC VISCOSITY VERSUS 1/T
FOR 99+% PURE LIQUID ALUMINUM
38 Ref.
13 Ref.
20 Ref.
34 Ref.
33 Ref.
DYNAMIC VISCOSITY (centipoise)
1/T (°K) x 10⁴

Figure 12

Appendix C

Methods of Computing Voidage

Two methods for predicting voidage in a particulate fluidized bed of spherical particles as a function of the average fluid velocity in the bed are presented in an abbreviated form in this appendix. It also includes the flow chart, listing and a sample output of the computer program used to calculate voidage by all three of the methods discussed in this report (Figure 1).

Lewis and Bowerman (15:603-610)

Lewis and Bowerman devised an analytical method for predicting voidage which is quite similar to Leva's method. The functional relationship is

$$\epsilon = A\left(\frac{\overline{u_f}}{u_t}\right)^b \tag{23}$$

which is analogous to equation (5) in Chapter III, with A and b constants to be determined on the basis of the particle Reynold's number at terminal velocity.

The value of the terminal velocity, u_t, is given by one of the equations (24)

$$u_t = \frac{g D_p^2}{18\mu}(\rho_p - \rho_f) \qquad Re_t < 2$$

$$u_t = 0.153\, D_p^{1.14}\left(\frac{\rho_f}{\mu}\right)^{0.43}\left[g\left(\frac{\rho_p}{\rho_f} - 1\right)\right]^{0.71} \qquad 2 < Re_t < 500 \tag{24}$$

$$u_t = 1.74\left[g D_p\left(\frac{\rho_p}{\rho_f} - 1\right)\right]^{1/2} \qquad 500 < Re_t < 2 \times 10^5$$

and the selected value of u_t is used in one of the equations

$$\epsilon = 0.99\left(\frac{\overline{u_f}}{u_t}\right)^{0.118} \qquad Re_t < 2$$

(25) $$\epsilon = 1.04\left(\frac{\overline{u_f}}{u_t}\right)^{0.336} \qquad 2 < Re_t < 500$$

$$\epsilon = 1.15\left(\frac{\overline{u_f}}{u_t}\right)^{0.43} \qquad 500 < Re_t < 2 \times 10^5$$

The values of ϵ as a function of $\overline{u_f}$ are then obtained.

One small problem inherent in this method is that u_t must be known in order to pick the proper defining equation for u_t. For purposes of this report, an approximation to Re_t was obtained using either of the other two methods of calculating $\epsilon = f(\overline{u_f})$, and then $\overline{u_f}$ was calculated and checked against the approximate value.

This particular method of calculating voidage was used in the Martin Company's feasibility study of a fluidized bed nuclear reactor using water as the fluidizing agent (7: II-5-II-16). The system of notation used above was taken from the Martin Company Report, as it is much clearer than that used in the original article. For the region of turbulent flow ($Re_t > 500$) the agreement between the formula values and the experimental values obtained in the feasibility study was excellent. Leva states (16: 89) that in general the formulation of Lewis and Bowerman is most accurate in the turbulent region, and unsatisfactory in the laminar-flow region ($Re_t < 2$).

Zenz and Othmer (40: 230-237)

A graphical method of predicting voidage which covers a wide range of experimental variables was devised by Zenz and Othmer. In this system, a velocity dependent variable

$$\log_{10}\left[\overline{u_f} \Big/ \left(\frac{4}{3}\,\frac{\mu(\rho_p - \rho_f)g}{\rho_f^2}\right)^{1/3}\right]$$

was plotted as abscissa and a particle diameter dependent variable was plotted as the ordinate.

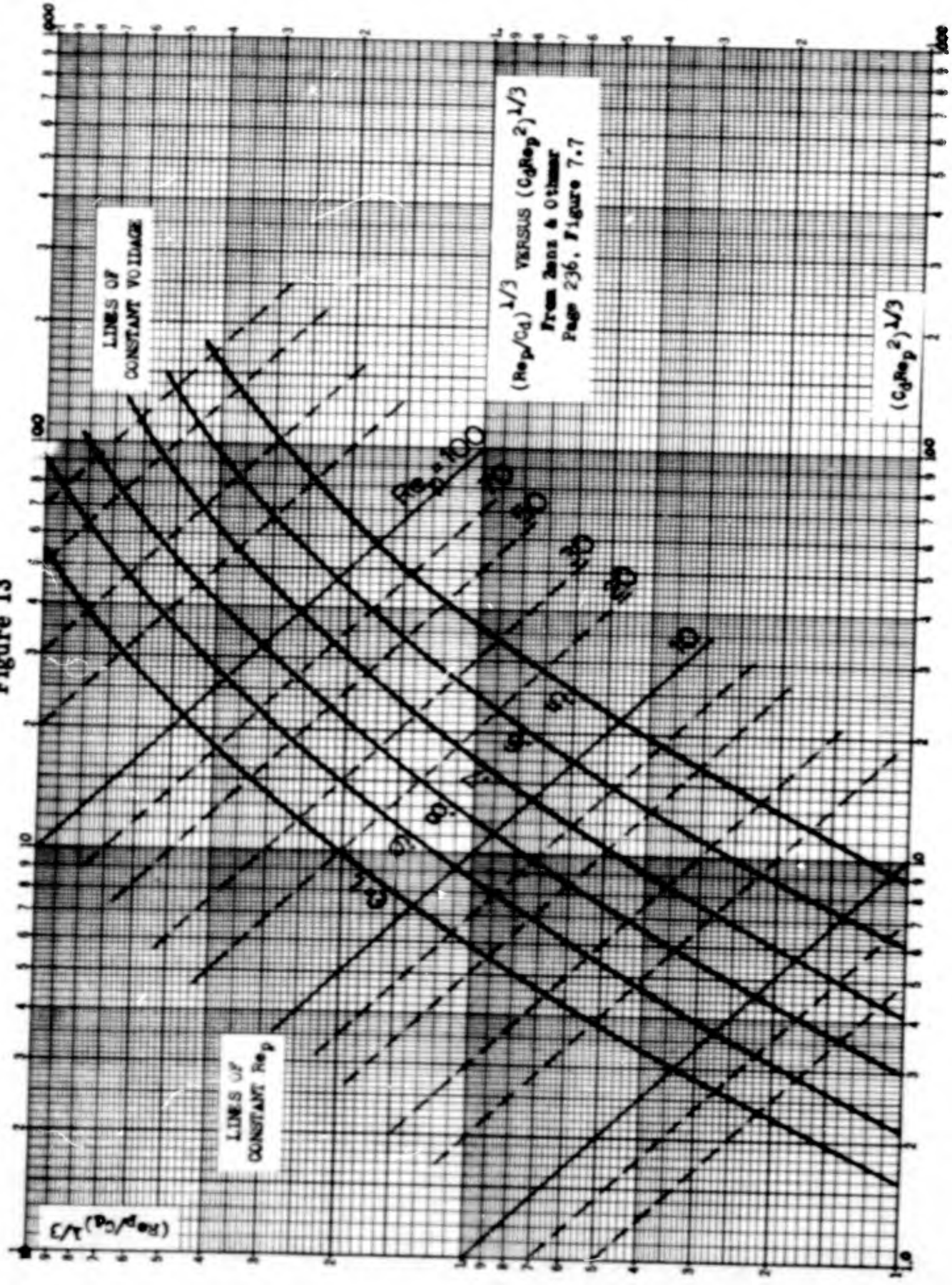
LINES OF CONSTANT VOIDAGE
LINES OF CONSTANT Re_p
$(Re_p/C_d)^{1/3}$ VERSUS $(C_d Re_p^2)^{1/3}$
From Zenz & Othmer
Page 236, Figure 7.7
$(C_d Re_p^2)^{1/3}$
$\epsilon/\pi^{(P_b/d_{eq})}$
Re = 100
80
60
40
30
20
10
8
6
4
2
1
1000
800
600
400
300
200
100
80
60
40
30
20
10
8
6
4
2
1

Figure 13

BLANK PAGE

$$\log_{10}\left[D_p \Big/ \left(\frac{3}{4}\,\frac{\mu^2}{(\rho_p - \rho_f)\,g}\right)^{1/3}\right]$$

If a modified particle drag coefficient is defined as

$$C_d \equiv 4\,g\,D_p\,(\rho_p - \rho_f) \Big/ 3\rho_f\,\overline{u}_f^{\,2}$$

and the particle Reynold's number

$$Re_p \equiv \frac{D_p\,\overline{u}_f\,\rho_f}{\mu}$$

are used in place of the previous two equations, the result is $\log_{10}\ (Re_p/\,C_d)^{1/3}$ plotted on the abscissa and $\log_{10}\ (C_d\,Re_p^{\,2})^{1/3}$ on the ordinate, as in Figure 13. For any given system all the values except $\overline{u}_f$ may be considered constant, and approximate values of $\epsilon = f(\overline{u}_f)$ taken from a straight line parallel to the abscissa.

Data from both liquid and gaseous fluidized systems of approximately spherical particles of many densities and diameters was used to obtain the graphs on which the smoothed correlation in Figure 13 is based. It should be noted that this correlation is valid only for systems exhibiting particulate fluidization.

Although Zenz and Othmer's system does not give the value of $\overline{u}_f$ at minimum fluidization, it does not depend on a guess as to minimum voidage of terminal velocity in predicting the voidage as a function of average fluid velocity. Also, this method uses a continuous (graphical) method of determining ϵ, rather than substituting three or four line segments (individual equations) depending upon the value of the particle Reynold's number.

Flow Chart. This flow chart details the major steps in an AFIT FORTRAN program which computes voidage and mass flow rates for a liquid aluminum fluidized bed.

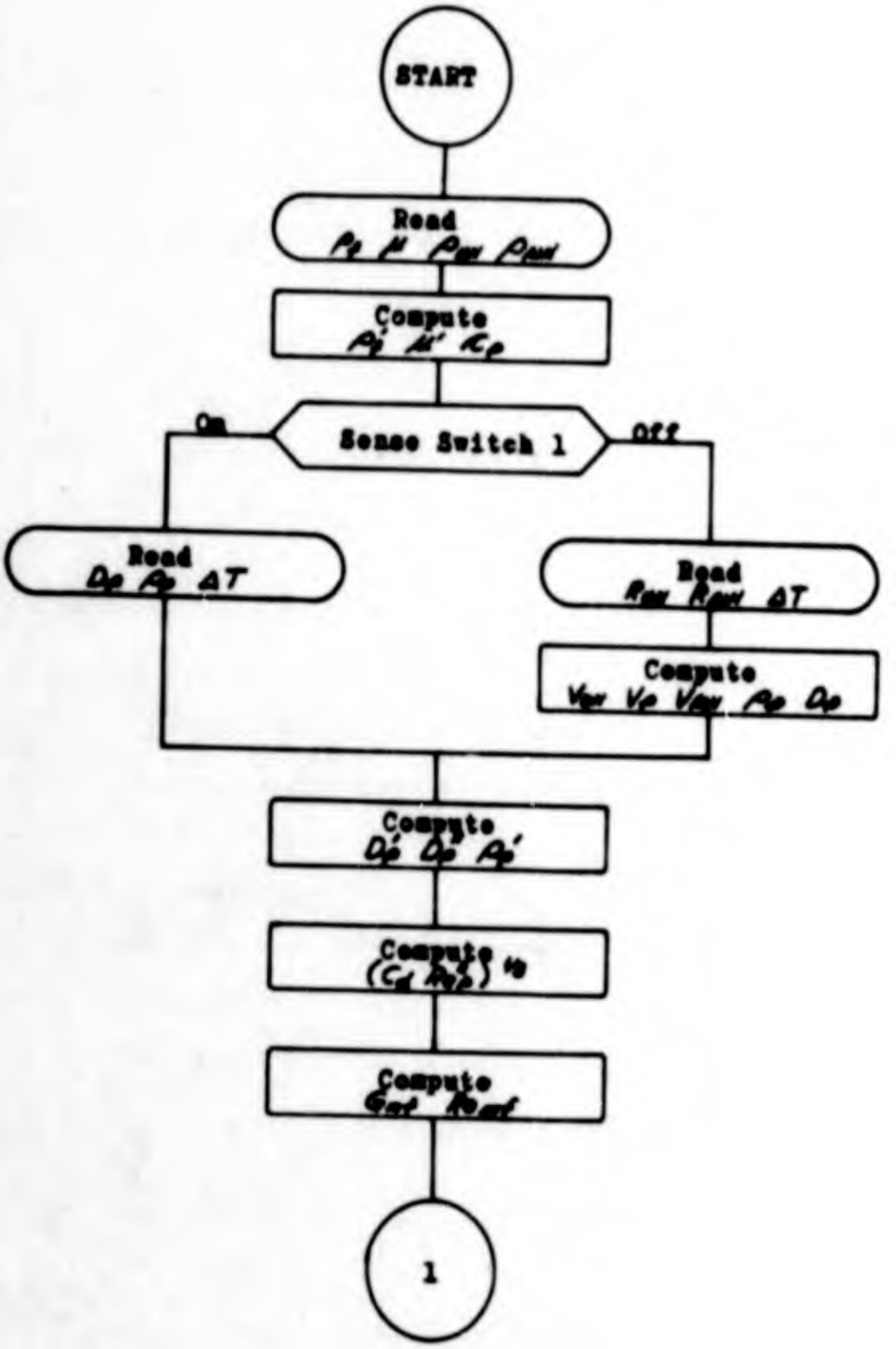

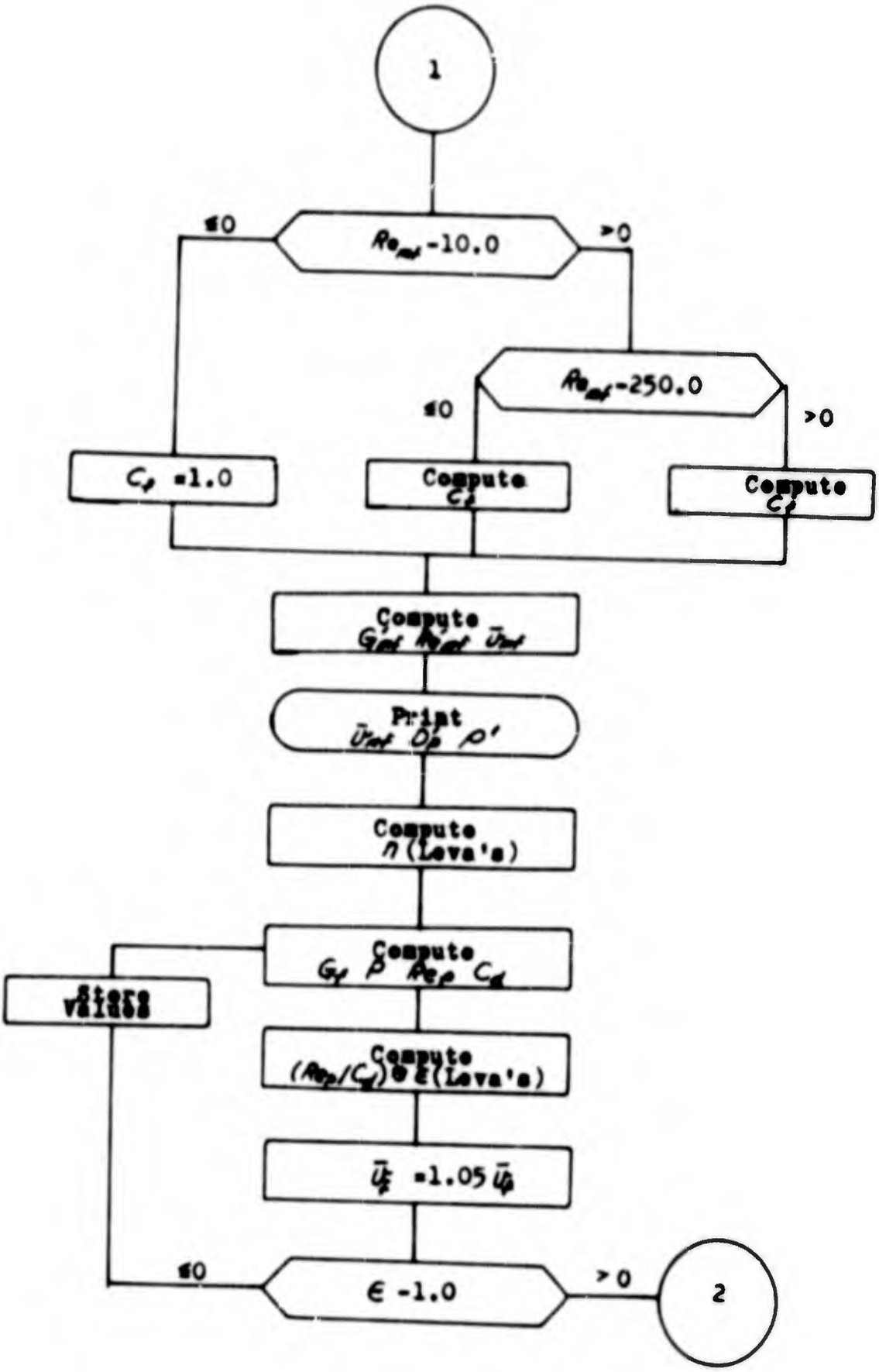
1
≤0
Re_{ref} -10.0
>0
Re_{ref} -250.0
≤0
>0
C_f =1.0
Compute C_f
Compute C_f
Compute G_{ref} R_{ref} $\bar{U}_{ref}$
Print $\bar{U}_{ref}$ δ_p^* ρ'
Compute η (Leva's)
Compute G_f β Re_p C_d
Compute (Re_p/C_d) ε (Leva's)
$\bar{U}_f$ =1.05 $\bar{U}_p$
≤0
ϵ -1.0
>0
2

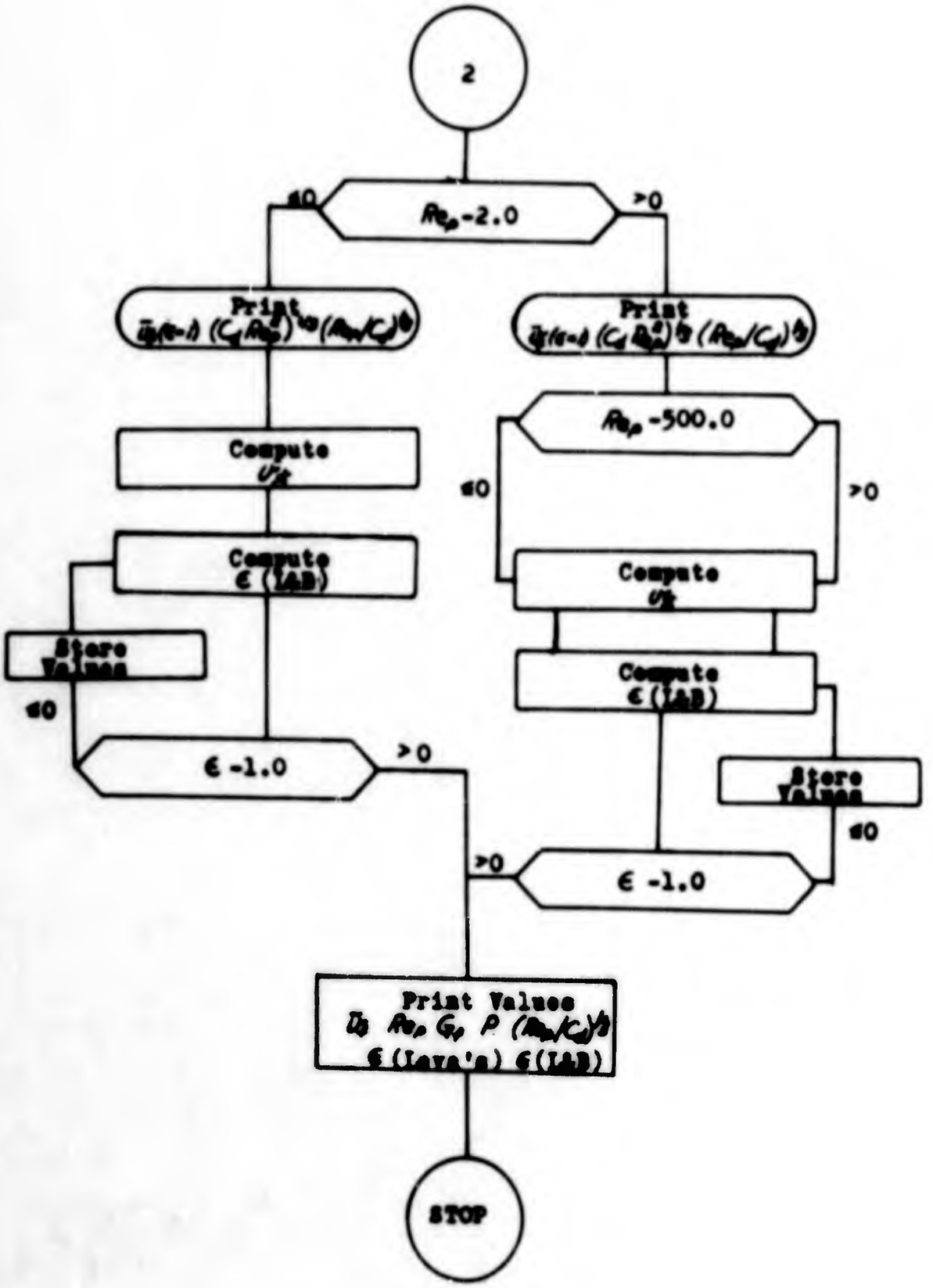
2
≤0
Re_p -2.0
>0
Print
Compute
Compute
Store
≤0
ϵ -1.0
>0
Re_p -500.0
≤0
>0
Compute
Compute
Store
≤0
>0
ϵ -1.0
Print Values
STOP

```
C       AFIT FORTRAN PROGRAM TO COMPUTE PARTICLE REYNOLD'S NUMBER,
C       THERMAL POWER AND VOIDAGE OF A FLUIDIZED BED AS A FUNCTION
C       OF AVERAGE FLUID VELOCITY (THREE METHODS OF COMPUTING VOIDAGE)


        DIMENSION YABSC(150), VOID(150), VMND(150)
        DIMENSION VELFL(150), RENPT(150), GFL2(150), POWER(150)
        PRINT 95
        PRINT 96
  100   READ 1, DFL1, VIFL1, DUN, DALN
        PRINT 3, DFL1, VIFL1, DUN, DALN
C       DFL1=FLUID DENSITY IN GRAMS/CUBIC CENTIMETER
C       VIFL1=FLUID DYNAMIC VISCOSITY IN CENTIPOISE
C       DUN=DENSITY OF URANIUM MONONITRIDE IN GRAMS/CUBIC CENTIMETER
C       DALN=DENSITY OF ALUMINUM MONOTRIDE IN GRAMS/CUBIC CENTIMETER
        DFL2=DFL1*62.24
C       DFL2=FLUID DENSITY IN LBM/CUBIC FOOT
        VIFL2=VIFL1*0.000672
C       VIFL2=DYNAMIC VISCOSITY OF FLUID IN LBM/SEC FT
        C1=1.0/3.0
        CP=1.8*(7.0/26.98)
C       CP=SPECIFIC HEAT OF LIQUID ALUMINUM IN BTU/LBM DEG CENTIGRADE
  105   PRINT 91
        PAUSE
              IF(SENSE SWITCH 1)120,110
  110   READ 2, RUN, RALN, DELT
        PRINT 4, RUN, RALN, DELT
C       RUN=RADIUS OF URANIUM NITRIDE PARTICLE IN CENTIMETERS
C       RALN=RADIAL THICKNESS OF ALUMINUM NITRIDE COATING IN CENTIMETERS
C       DELT=TEMPERATURE DROP FROM BOTTOM TO TOP OF FLUIDIZED BED, DEG CENT
        VUN=(4.0/3.0)*3.1416*(RUN**3.0)
C       VUN=VOLUME OF URANIUM MONOTRIDE PER PARTICLE IN CUBIC CENTIMETERS
        VPT=(4.0/3.0)*3.1416*((RUN+RALN)**3.0)
C       VPT=TOTAL VOLUME OF COATED PARTICLE IN CUBIC CENTIMETERS
        VALN=VPT-VUN
C       VALN=VOLUME OF ALUMINUM MONOTRIDE PER PARTICLE IN CUBIC CENTIMETERS
        DPT1=(DUN*VUN+DALN*VALN)/VPT
C       DPT1=TOTAL PARTICLE DENSITY IN GRAMS/CUBIC CENTIMETER
        DIPT1=2.0*(RUN+RALN)
C       DIPT1=TOTAL PARTICLE DIAMETER IN CENTIMETERS
        GO TO 130
  120   READ 2, DIPT1, DPT1, DELT
        PRINT 5, DIPT1, DPT1, DELT
  130   DIPT2=DIPT1*0.3937
C       DIPT2=TOTAL PARTICLE DIAMETER IN INCHES
        DIPT3=DIPT2/12.0
C       DIPT3=TOTAL PARTICLE DIAMETER IN FEET
        DPT2=DPT1*62.42
C       DPT2=TOTAL PARTICLE DENSITY IN LBM/CUBIC FOOT
        C2=DPT2-DFL2
```

```
C       BEGIN FLUIDIZATION CALCULATIONS, LEVA, ZENZ AND OTHMER

        XORD=DIPT3/((3.*VIFL2**2.)/(4.*DFL2*C2*32.2))**C1
C       XORD=(DRAG/(REMPT SQUARED)) TO THE 1/3, ZENZ AND OTHMER
C       DRAG=ZENZ AND OTHMERS DRAG COEFFICIENT
        BSC=((4.*VIFL2*C2*32.2)/(3.*DFL2**2.))**C1
        C3=DIPT3/DFL2
        C4=C2*(4.0/3.0)*32.2*C3
        C5=DIPT3/(VIFL2*3600.0)
        C6=DFL2*3600.0
        GMF1=688.0*(DIPT2**1.82)*((DFL2*C2)**0.94)/(VIFL1**0.88)
C       GMF1=UNCORRECTED MASS FLOW RATE FOR MINIMUM FLUIDIZATION, LEVA
        REMF1=C5*GMF1
C       REMF1=UNCORRECTED PARTICLE REYNOLDS NUMBER FOR MINIMUM FLUIDIZATION
        IF(REMF1-10.0)10,10,15
 10     CMF=1.0
C       CMF=LEVA'S CORRECTION FACTOR BASED ON REMF1
        GO TO 20
 15     IF(REMF1-250.0)16,16,17
 16     CMF=1.39-(0.422/2.30259)*LOGF(REMF1)
        GO TO 20
 17     CMF=0.898-(0.2162/2.30259)*LOGF(REMF1)
 20     REMF2=CMF*REMF1
C       REMF2=CORRECTED PARTICLE REYNOLDS NUMBER FOR MINIMUM FLUIDIZATION
        GMF2=CMF*GMF1
C       GMF2=CORRECTED MASS FLOW RATE FOR MINIMUM FLUIDIZATION
        VELFL(1)=GMF2/C6
C       VELFL=AVERAGE (OR BULK) FLUID VELOCITY IN FEET/SECOND
        PRINT 6, VELFL(1), DIPT2, DPT2
        SLOPE=4.45/(REMF2**0.1)
C       SLOPE=SLOPE OF MASS FLOW RATE VERSUS VOIDAGE PLOT, LOG-LOG
        XINV=1.0/SLOPE
        I=1
 145    GFL2(I)=C6*VELFL(I)
C       GFL2=MASS FLOW RATE THROUGH BED IN LBM/SQ FT HOUR
        POWER(I)=GFL2(I)*CP*DELT*0.0002931
C       POWER=THERMAL POWER OUT OF BED IN KILOWATTS PER SQUARE FOOT
C       OF CROSS SECTIONAL AREA PERPENDICULAR TO FLOW
        REMPT(I)=C5*GFL2(I)
C       REMPT=REYNOLDS NUMBER BASED ON PARTICLE DIAMETER
        YABSC(I)=VELFL(I)/BSC
C       YABSC=(REMPT/DRAG) TO THE 1/3, ZENZ AND OTHMER
 155    YDIST=REMPT(I)/REMF2
        VOID(I)=0.41*(YDIST**XINV)
C       VOID=CALCULATED VOIDAGE (FUNCTION OF MASS FLOW RATE), LEVA
        J=I
        I=I+1
 140    VELFL(I)=1.05*VELFL(J)
        IF(VOID(J)-1.0)145,145,160
 160    IF(REMPT(J)-2.0)165,170,170
```

```
C       VOIDAGE CALCULATIONS USING LEWIS AND BOWERMAN'S FORMULATION

 165    UT=32.2*(DIPT3**2.0)*C2/(18.0*VIFL2)
C       UT=TERMINAL VELOCITY OF FREE-FALLING SPHERE IN FLUID, FT PER SEC
        GO TO 186
 170    PRINT 94, J, REMPT(J), XORD, YABSC(J)
C       CHANGE REYNOLD'S NUMBER AT WHICH TURBULENT FLOW FORMULA IS USED
              IF(SENSE SWITCH 2)166,167
 166    PRINT 93
        ACCEPT 92, TLIM
C       TLIM=PARTICLE REYNOLDS NUMBER AT WHICH TURBULENT FLOW BEGINS
        GO TO 174
 167    TLIM=500.0
 174    IF(REMPT(J)-TLIM)175,180,180
 175    UT=.153*DIPT3**1.14*(DFL2/VIFL2)**.43*(32.2*((DPT2/DFL2)-1.))**.71
        GO TO 188
 180    UT=1.74*((32.2*DIPT3)*((DPT2/DFL2)-1.0))**0.5
        M=1
 185    VMND(M)=1.15*((VELFL(M)/UT)**0.43)
C       VMND=VOIDAGE AT MINIMUM FLUIDIZATION, LEWIS AND BOWERMAN
        M=M+1
        IF(VMND(M-1)-1.0)185,185,190
 186    M=1
 187    VMND(M)=0.99*((VELFL(M)/UT)**0.118)
        M=M+1
        IF(VMND(M-1)-1.0)187,187,190
 188    M=1
 189    VMND(M)=1.04*((VELFL(M)/UT)**0.337)
        M=M+1
        IF(VMND(M-1)-1.0)189,189,190
 190    PRINT 7
        PRINT 8
        M=M-1
        DO 200 L=1,M
        PUNCH9,VELFL(L),REMPT(L),GFL2(L),POWER(L),YABSC(L),VOID(L),VMND(L)
              IF(SENSE SWITCH 3)105,200
 200    CONTINUE
```

```
1     FORMAT(2F8.4,2F9.4)
2     FORMAT(2F7.4,F7.2)
3     FORMAT(/5HDFL1=F8.4,4X,6HVIFL1=F8.4,4X,4HDUN=F9.4,4X,5HDALN=F8.4/)
4     FORMAT(/1X,4HRUN=F7.4,6X,5HRALN=F7.4,4X,5HDELT=F7.2/)
5     FORMAT(/6HDIPT1=F7.4,5X,5HDPT1=F7.4,4X,5HDELT=F7.2/)
6     FORMAT(/6HVELFL=F7.4,4X,6HDIPT2=F8.5,3X,5HDPT2=F9.4/)
7     FORMAT(/2X,5HVELFL,4X,5HRENPT,7X,4HGFL2,7X,5HPOWER)
8     FORMAT(5X,5HYABSC,4X,4HVOID,4X,4HVWND/)
9     FORMAT(F7.4,2X,F7.2,2X,F10.2,2X,F10.2,3X,F7.2,2X,F6.3,2X,F6.3)
91    FORMAT(/37HSWITCH 1 ON TO READ DIPT1, DPT1, DELT)
92    FORMAT(F8.2)
93    FORMAT(23HENTER XLIM IN F8.2 FORM)
94    FORMAT(/3X,2HJ=I4,8X,6HRENPT=F8.2,3X,5HXORD=F6.2,6X,6HYABSC=F6.2/)
95    FORMAT(/10X,45HAFIT FORTRAN PROGRAM TO ESTIMATE VOIDAGE IN A)
96    FORMAT(/11X,43HLIQUID FLUIDIZED BED OF SPHERICAL PARTICLES/)
            IF(SENSE SWITCH 2)105,100
      END
```

AFIT FØRTRAN PRØGRAM TØ ESTIMATE VØIDAGE IN A
LIQUID FLUIDIZED BED ØF SPHERICAL PARTICLES

DFL1= 2.0000 VIFL1= 2.0000 DUN= 14.3200 DALN= 3.2600

SWITCH 1 ØN TØ READ DIPT1, DPT1, DELT
RUN= .0300 RALN= .0200 DELT= 300.00

VELFL= .0338 DIPT2= .03937 DPT2= 352.6081

J= 66 RENPT= 245.51 XØRD= 28.77 YABSC= 8.53

VELFL	RENPT	GFL2	PØWER	YABSC	VØID	VMND
.0338	10.29	15187.96	623.68	.35	.410	.404
.0355	10.81	15947.36	654.86	.37	.415	.411
.0373	11.35	16744.73	687.61	.39	.421	.418
.0392	11.92	17581.97	721.99	.41	.427	.425
.0411	12.51	18461.07	758.09	.43	.433	.432
.0432	13.14	19384.12	795.99	.45	.439	.439
.0454	13.80	20353.33	835.79	.47	.445	.446
.0476	14.49	21370.99	877.58	.50	.451	.454
.0500	15.21	22439.54	921.46	.52	.458	.461
.0525	15.97	23561.52	967.54	.55	.464	.469
.0552	16.77	24739.60	1015.91	.58	.470	.477
.0579	17.61	25976.58	1066.71	.61	.477	.485
.0608	18.49	27275.41	1120.04	.64	.484	.493
.0639	19.41	28639.18	1176.05	.67	.490	.501
.0671	20.39	30071.14	1234.85	.70	.497	.509
.0704	21.41	31574.69	1296.59	.74	.504	.518
.0739	22.48	33153.43	1361.42	.78	.511	.526
.0776	23.60	34811.10	1429.49	.82	.518	.535
.0815	24.78	36551.65	1500.97	.86	.526	.544
.0856	26.02	38379.24	1576.02	.90	.533	.553
.0899	27.32	40298.20	1654.82	.94	.540	.562
.0944	28.69	42313.11	1737.56	.99	.548	.571
.0991	30.12	44428.76	1824.44	1.04	.555	.581
.1041	31.63	46650.20	1915.66	1.09	.563	.590
.1093	33.21	48982.71	2011.44	1.15	.571	.600
.1147	34.87	51431.85	2112.01	1.21	.579	.610
.1205	36.61	54003.44	2217.61	1.27	.587	.620
.1265	38.44	56703.61	2328.50	1.33	.595	.631
.1328	40.37	59538.79	2444.92	1.40	.604	.641
.1395	42.39	62515.73	2567.17	1.47	.612	.652
.1464	44.51	65641.52	2695.53	1.54	.621	.662
.1538	46.73	68923.60	2830.30	1.62	.629	.673
.1614	49.07	72369.78	2971.82	1.70	.638	.685
.1695	51.52	75988.27	3120.41	1.79	.647	.696
.1780	54.10	79787.68	3276.43	1.87	.656	.708
.1869	56.80	83777.06	3440.25	1.97	.665	.719
.1962	59.64	87965.92	3612.26	2.07	.674	.731
.2061	62.63	92364.21	3792.88	2.17	.684	.743
.2164	65.76	96982.42	3982.52	2.28	.693	.756
.2272	69.05	101831.55	4181.65	2.39	.703	.768

.2385	72.50	106923.13	4390.73	2.51	.713	.781
.2505	76.12	112269.28	4610.27	2.64	.723	.794
.2630	79.95	117882.75	4840.78	2.77	.733	.807
.2762	83.95	123776.89	5082.82	2.91	.743	.820
.2900	88.12	129965.73	5336.96	3.06	.753	.834
.3045	92.53	136464.02	5603.81	3.21	.764	.848
.3197	97.16	143287.22	5884.00	3.37	.775	.862
.3357	102.01	150451.58	6178.20	3.54	.785	.876
.3525	107.11	157974.16	6487.11	3.72	.796	.891
.3701	112.47	165872.87	6811.47	3.90	.807	.906
.3886	118.09	174166.52	7152.04	4.10	.819	.921
.4080	124.00	182874.84	7509.64	4.30	.830	.936
.4284	130.20	192018.59	7885.13	4.52	.842	.951
.4499	136.71	201619.51	8279.38	4.75	.853	.967
.4724	143.55	211700.49	8693.35	4.98	.865	.983
.4960	150.72	222285.51	9128.02	5.23	.877	1.000

Appendix D

Two-Group Calculations

(13a) $$D_{fc} \nabla^2 \phi_{fc} + (\nu_f - 1) \Sigma_{fc}^{c} \phi_{fc} + \nu_t \Sigma_{tc}^{f} \phi_{tc} = 0$$

(14a) $$D_{tc} \nabla^2 \phi_{tc} - \Sigma_{tc}^{a} \phi_{tc} = 0$$

(15a) $$D_{fR} \nabla^2 \phi_{fR} - \Sigma_{fR}^{s,re} \phi_{fR} = 0$$

(16a) $$D_{tR} \nabla^2 \phi_{tR} - \Sigma_{tR}^{a} \phi_{tR} + \Sigma_{fR}^{s,re} \phi_{fR} = 0$$

For spherical geometry with no angular dependence,

$$\nabla^2 = \frac{d^2}{dr^2} + \frac{2}{r} \frac{d}{dr}$$

and making the following substitution

$$\phi(r) = \frac{u(r)}{r}$$

$$\frac{d}{dr}\left(\frac{u}{r}\right) = \frac{1}{r} \frac{du}{dr} - \frac{u}{r^2}$$

$$\frac{d^2}{dr^2}\left(\frac{u}{r}\right) = \frac{1}{r} \frac{d^2u}{dr^2} - \frac{2}{r^2} \frac{du}{dr} + \frac{2u}{r^3}$$

the thermal flux in the core may be described by

$$\frac{1}{r} \frac{d^2u}{dr^2} - \frac{\Sigma_{tc}^{a}}{D_{tc}} \frac{u}{r} = 0$$

$$\frac{d^2u}{dr^2} - \frac{\Sigma_{tc}^{a}}{D_{tc}} u = 0$$

$$B_{tc}^2 = \frac{\Sigma_{tc}^{a}}{D_{tc}}$$

$$u(r) = C_1 \sinh(B_{tc} r) + C_2 \cosh(B_{tc} r)$$

$$(26) \qquad \phi_{tc}(r) = C_1 \frac{\sinh(B_{tc} r)}{r} + C_2 \frac{\cosh(B_{tc} r)}{r}$$

For $\phi_{tc}(r)$ finite as $r \to 0$,

$$C_2 \equiv 0$$

$$\lim_{r \to 0} \frac{\sinh(B_{tc} r)}{r} = \frac{0}{0}$$

$$\lim_{r \to 0} B_{tc} \frac{\cosh(B_{tc} r)}{1} = B_{tc}$$

$$(17) \qquad \phi_{tc}(r) = C_1 \frac{\sinh(B_{tc} r)}{r}$$

and in an exactly similar manner

$$(27) \qquad \phi_{fR}(r) = A_1 \frac{e^{+k_{fR} r}}{r} + A_2 \frac{e^{-k_{fR} r}}{r}$$

$$k_{fR}^2 = \frac{\Sigma_{fR}^{s,re}}{D_{fR}}$$

For $\phi_{fR}(r)$ finite as $r \to \infty$,

$$A_1 \equiv 0$$

$$\lim_{r \to \infty} \frac{e^{-k_{fR} r}}{r} = 0$$

$$(19) \qquad \phi_{fR}(r) = A_2 \frac{e^{-k_{fR} r}}{r}$$

Solving the homogeneous part of equation (13a),

$$\frac{d^2 u}{dr^2} + B_{fc}^2 u = 0,$$

where $$B_{fc}^2 = (\nu_f - 1)\frac{\Sigma_{fc}^f}{D_{fc}}$$

$$u_h(r) = C_3 \sin(B_{tc} r) + C_4 \cos(B_{fc} r)$$

and solving for the particular solution,

$$\frac{d^2u}{dr^2} + B_{fc}^2 u = -m C_1 \sinh(B_{tc} r)$$

where $$m = \nu_t \frac{\Sigma_{tc}^f}{D_{fc}}$$

$$u_p = \frac{-m C_1}{B_{fc}^2 + B_{tc}^2} \sinh(B_{tc} r)$$

and the complete solution is:

$$u(r) = C_3 \sin(B_{tc} r) + C_4 \cos(B_{fc} r) - \frac{m C_1}{B_{fc}^2 + B_{tc}^2} \sinh(B_{tc} r)$$

$$(28)\quad \phi_{fc}(r) = C_3 \frac{\sin(B_{fc} r)}{r} + C_4 \frac{\cos(B_{fc} r)}{r} - \frac{m}{B_{fc}^2 + B_{tc}^2} \phi_{tc}(r)$$

for $\phi_{fc}(r)$ finite as $r \to 0$,

$$C_4 \equiv 0$$

$$\lim_{r \to 0} \frac{\sin(B_{fc} r)}{r} = \frac{0}{0}$$

$$\lim_{r \to 0} B_{fc} \frac{\cos(B_{fc} r)}{1} = B_{fc}$$

$$(18)\quad \phi_{fc}(r) = C_3 \frac{\sin(B_{fc} r)}{r} - \frac{m}{B_{fc}^2 + B_{tc}^2} \phi_{tc}(r)$$

Now, solving for the homogeneous part of equation (16a),

$$\frac{d^2u}{dr^2} - k_{tR}^2 u = 0$$

where $$k_{tR}^2 = \frac{\Sigma_{tR}^a}{D_{tR}} ,$$

$$u_h(r) = E_1 e^{+k_{tR} r} + E_2 e^{-k_{tR} r}$$

$$\frac{d^2u}{dr^2} - k_{tR}^2 u = -m' A_2 e^{-k_{fR} r}$$

where $$m' = \frac{\Sigma_{fR}^{s,re}}{D_{tR}}$$

$$u_p(r) = \frac{m' A_2}{k_{tR}^2 - k_{fR}^2} e^{-k_{fR} r}$$

and the complete solution is

$$u(r) = E_1 e^{+k_{tR} r} + E_2 e^{-k_{tR} r} + \frac{m' A_2}{k_{tR}^2 - k_{fR}^2} e^{-k_{fR} r}$$

(29) $$\phi_{tR}(r) = E_1 \frac{e^{k_{tR} r}}{r} + E_2 \frac{e^{-k_{tR} r}}{r} + \frac{m'}{k_{tR}^2 - k_{fR}^2} \phi_{fR}(r)$$

For $\phi_{tR}(r)$ finite as $r \to \infty$,

$$E_1 \equiv 0$$

(20) $$\phi_{tR}(r) = E_2 \frac{e^{-k_{tR} r}}{r} + \frac{m'}{k_{tR}^2 - k_{fR}^2} \phi_{fR}(r)$$

Now the boundary conditions of continuity of flux and current at the core-reflector interface (r_o) may be applied.

$$\phi_{fc}(r_o) = \phi_{fR}(r_o)$$

$$\phi_{tc}(r_o) = \phi_{tR}(r_o)$$

(30)

$$-D_{fc}\left[\frac{d}{dr}\ \phi_{fc}\right]_{r_o} = -D_{fR}\left[\frac{d}{dr}\ \phi_{fR}\right]_{r_o}$$

$$-D_{tc}\left[\frac{d}{dr}\ \phi_{tc}\right]_{r_o} = -D_{tR}\left[\frac{d}{dr}\ \phi_{tR}\right]_{r_o}$$

If the following substitutions are made,

$$\rho_1 = \frac{D_{fR}}{D_{fc}}$$

$$\rho_2 = \frac{D_{tR}}{D_{tc}}$$

$$X = \frac{\sinh(B_{tc}r)}{r}$$

$$V = \frac{\sin(B_{fc}r)}{r}$$

$$Z_1 = \frac{e^{-k_{fR}r}}{r}$$

$$Z_2 = \frac{e^{-k_{tR}r}}{r}$$

$$h_1 = \frac{m}{B_{fc}^2 + B_{tc}^2}$$

$$h_2 = \frac{m'}{k_{tR}^2 - k_{fR}^2}$$

the continuity equations become

$$C_3\left[Y\right] - C_1 h_1\ \left[X\right] = A_2\left[Z_1\right]$$

$$C_1 \left[X\right] = E_2 \left[Z_2\right] + A_2 h_2 \left[Z_1\right]$$

(30a)

$$C_3 \left[Y'\right] - C_1 h_1 \left[X'\right] = \rho_1 A_2 \left[Z_1'\right]$$

$$C_1 \left[X'\right] = \rho_2 E_2 \left[Z_2'\right] + A_2 h_2 \left[Z_1'\right]$$

where [ ] indicates evaluation at r_o.

These are a set of four homogeneous equations in four unknowns, A_2, C_1, C_3, and E_2. For a nontrivial solution the determinant of their coefficients must equal zero. Defining

$$\alpha = \left[\frac{X'}{X}\right] = B_{tc} \coth(B_{tc} r_o) - \frac{1}{r_o}$$

$$\beta = \left[\frac{Y'}{Y}\right] = B_{fc} \cot(B_{fc} r_o) - \frac{1}{r_o}$$

(31)

$$\gamma = \left[\frac{Z_1'}{Z_1}\right] = -k_{fR} - \frac{1}{r_o}$$

$$\delta = \left[\frac{Z_2'}{Z_2}\right] = -k_{tR} - \frac{1}{r_o}$$

Rearranging the rows, the determinant of the coefficients becomes

$$\Delta = \begin{vmatrix} 1 & 0 & -h_2 & -1 \\ h_1 & -1 & 1 & 0 \\ \alpha & 0 & -\rho_2 h_2 \gamma & -\rho_2 \delta \\ h_1 \alpha & -\beta & \rho_1 \gamma & 0 \end{vmatrix} = 0 ,$$

which is the critical condition. Expanding the determinant gives

$$\Delta = (h_2 \rho_2 \delta h_1 \alpha - \alpha \rho_1 \gamma - h_1 \alpha \rho_2 h_2 \gamma + \rho_1 \gamma \rho_2 \delta)$$

$$+ \beta(-\rho_2 \delta + h_1 \rho_2 h_2 \gamma + \alpha - \rho_2 \delta h_1 h_2) = 0$$

Letting $F_1 = \rho_2 h_1 h_2$ and solving for β,

(32)

$$\beta = \frac{F_1 \alpha(\delta - \gamma) + \rho_1 \gamma(\rho_2 \delta - \alpha)}{\rho_2 \delta - \alpha - F_1(\gamma + \delta)} ,$$

and this equation may be solved for the critical radius, r_o.

Once r_o is determined, the set of equations (30a) may be solved for three of the unknown constants in terms of the fourth (say C_1).

$$A_2 = C_1 \left[X\right] (a - \rho_2 \delta) / \rho_2 k_{tc} \left[Z_1\right] (\gamma - \delta)$$

$$C_3 = (C_1 k_{fc} \left[X\right] + A_2 \left[Z_1\right]) / \left[Y\right] \tag{33}$$

$$E_2 = (C_1 \left[X\right] - A_2 k_{tc} \left[Z_1\right]) / \left[Z_2\right]$$

Now, for any arbitrary value of C_1, the flux distribution in the reactor may be determined by the use of equations (17 - 20), which are repeated below.

$$\phi_{tc}(r) = C_1 \frac{\sinh (B_{tc} r)}{r} \tag{17}$$

$$\phi_{fc}(r) = C_3 \frac{\sin (B_{fc} r)}{r} - \frac{m}{B_{fc}^2 + B_{tc}^2} \phi_{tc}(r) \tag{18}$$

$$\phi_{fR}(r) = A_2 \frac{e^{-k_{fR} r}}{r} \tag{19}$$

$$\phi_{tR}(r) = E_2 \frac{e^{-k_{tR} r}}{r} + \frac{m'}{k_{tR}^2 - k_{fR}^2} \phi_{fR}(r) \tag{20}$$

If fast parasitic capture in the core is re-introduced into equation (13a), then

$$B_{fc}^2 = (\nu_f - 1) \frac{\Sigma_{fc}^f}{D_{fc}} - \frac{\Sigma_{fc}^c}{D_{fc}} , \tag{34}$$

and the other equations remain the same. This step was added to the computer program as an option, and results in appreciably greater radii but no substantial change in the flux distribution. For $\epsilon = 0.6$, RUN = 0.03 and RALN = 0.02, the critical radius is 22.3 cm. without fast parasitic capture, and 25.2 cm. with fast parasitic capture. All

the results presented in the section on reactor calculations included the terms for fast parasitic capture.

Input Data

The input data for the reactor calculations program consisted of both fast and thermal group microscopic cross sections and nuclei densities in the core and reflector. Both cross sections and nuclei densities for the reflector were constant values for all calculations using 1.125 eV energy cutoff. Only the cross sections for this cutoff are listed in the following three pages.

The first row of numbers in each set is the voidage, the radius of the UN particle in centimeters and the thickness of the AlN coating. The second row is the nuclei density of U^{235}, aluminum and nitrogen in the core, followed by the densities of aluminum and nitrogen in the reflector. Rows three through five are cross sections, appearing in the exact order as called for in the program listing. The final row in each group contains the fast parasitic capture cross sections of U^{235}, aluminum and nitrogen which are optional in the program (typed input data).

BLANK PAGE

```
0.4      .03      .02
.4432E-02    .40378E-01   .26959E-01    .4789E-01   .4789E-01
.25095E+01   .17808E+01   .82059E+01    .257E+03    .315E+03    .305E+03
.28841E+01   .2213E+01    .149E+01      .2724E-02   .11E+00
.31746E+01   .54633E+01   .1016E+02     .35513E-01  .64E+00
.21541E-00   .63289E-02   .29354E-01

0.5      .03      .02
.36930E-02   .41086E-01   .22463E-01    .4789E-01   .4789E-01
.25073E+01   .17933E+01   .82855E+01    .257E+03    .315E+03    .305E+03
.28716E+01   .22130E+01   .149E+01      .2724E-02   .11E+00
.32018E+01   .54633E+01   .1016E+02     .35513E-01  .64E+00
.22085E-00   .63765E-02   .28678E-01

0.6      .03      .02
.2955E-02    .41794E-01   .17973E-01    .4789E-01   .4789E-01
.25051E+01   .18036E+01   .83686E+01    .257E+03    .315E+03    .305E+03
.28609E+01   .2213E+01    .149E+01      .2724E-02   .11E+00
.3228E+01    .54633E+01   .1016E+02     .35513E-01  .64E+00
.22514E-00   .6417E-02    .27964E-01

0.7      .03      .02
.2216E-02    .42502E-01   .1348E-01     .4789E-01   .4789E-01
.25033E+01   .18061E+01   .84414E+01    .257E+03    .315E+03    .305E+03
.28565E+01   .22130E+01   .149E+01      .2724E-02   .11E+00
.32465E+01   .54633E+01   .1016E+02     .35513E-01  .64E+00
.22548E-00   .64312E-02   .27266E-01

0.8      .03      .02
.1477E-02    .4321E-01    .8986E-02     .4789E-01   .4789E-01
.25029E+01   .17847E+01   .84585E+01    .257E+03    .315E+03    .305E+03
.28704E+01   .2213E+01    .149E+01      .2724E-02   .11E+00
.32374E+01   .54633E+01   .1016E+02     .35513E-01  .64E+00
.21424E-00   .6367E-02    .26754E-01
```

```
0.4      .03      .01
.8656E-02    .34462E-01   .25268E-01    .4789E-01   .4789E-01
.25358E+01   .15815E+01   .7447E+01     .257E+03    .315E+03    .305E+03
.29806E+01   .2213E+01    .149E+01      .2724E-02   .11E+00
.28628E+01   .54633E+01   .1016E+02     .35513E-01  .64E+00
.12294E-00   .54308E-02   .34933E-01

0.5      .03      .01
.7214E-02    .36156E-01   .21057E-01    .4789E-01   .4789E-01
.25321E+01   .15952E+01   .75333E+01    .257E+03    .315E+03    .305E+03
.29646E+01   .2213E+01    .149E+01      .2724E-02   .11E+00
.28965E+01   .54633E+01   .1016E+02     .35513E-01  .64E+00
.12875E-00   .55011E-02   .33934E-01

0.6      .03      .01
.5771E-02    .3785E-01    .16845E-01    .4789E-01   .4789E-01
.25278E+01   .16119E+01   .7641E+01     .257E+03    .315E+03    .305E+03
.29475E+01   .2213E+01    .149E+01      .2724E-02   .11E+00
.29373E+01   .54633E+01   .1016E+02     .35513E-01  .64E+00
.13577E-00   .55871E-02   .32766E-01

0.7      .03      .01
.4328E-02    .39544E-01   .12634E-01    .4789E-01   .4789E-01
.2523E+01    .16313E+01   .77747E+01    .257E+03    .315E+03    .305E+03
.29306E+01   .2213E+01    .149E+01      .2724E-02   .11E+00
.29856E+01   .54633E+01   .1016E+02     .35513E-01  .64E+00
.14387E-00   .56877E-02   .31405E-01


0.6      .03      .04
.1077E-02    .44423E-01   .18725E-01    .4789E-01   .4789E-01
.24787E+01   .23101E+01   .96905E+01    .257E+03    .315E+03    .305E+03
.27154E+01   .22130E+01   .149E+01      .2724E-02   .11E+00
.36759E+01   .54633E+01   .1016E+02     .35513E-01  .64E+00
.4872E-00    .70646E-02   .23349E-01
```

```
 0.4      .03                .05
 .1082E-02          .45069E-01          .28301E-01          .4789E-01          .4789E-01
 .24682E+01         .27653E+01          .10554E+02          .257E+03           .315E+03          .305E+03
 .26384E+01         .22130E+01          .149E+01            .2724E-02          .11E+00
 .39106E+01         .54633E+01          .1016E+02           .35513E-01         .64E+00
 .74074E-00         .71545E-02          .2235E-01

 0.5      .03                .05
 .902E-03           .44995E-01          .23584E-01          .4789E-01          .4789E-01
 .24689E+01         .27172E+01          .10495E+02          .257E+03           .315E+03          .305E+03
 .26455E+01         .22138+01           .149E+01            .2724E-02          .11E+00
 .38892E+01         .54633E+01          .1016E+02           .35513E-01         .64E+00
 .71407E-00         .71531E-02          .22262E-01

 0.6      .03                .05
 .721E-03           .44921E-01          .18867E-01          .4789E-01          .4789E-01
 .24705E+01         .26265E+01          .10351E+02          .257E+03           .315E+03          .305E+03
 .26637E+01         .2213E+01           .149E+01            .2724E-02          .11E+00
 .38408E+01         .54633E+01          .1016E+02           .35513E-01         .64E+00
 .66433E-00         .71292E-02          .22311E-01

 0.7      .03                .05
 .541E-03           .44847E-01          .1415E-01           .4789E-01          .4789E-01
 .24745E+01         .2/496E+01          .10019E+02          .257E+03           .315E+03          .305E+03
 .27050E+01         .2213E+01           .149E+01            .2724E-02          .11E+00
 .37329E+01         .54633E+01          .1016E+02           .35513E-01         .64E+00
 .56825E-00         .70378E-02          .22761E-01

 0.6      .03                .025
 .222E-02           .42823E-01          .18267E-01          .4789E-01          .4789E-01
 .24967E+01         .19147E+01          .87107E+01          .257E+03           .315E+03          .305E+03
 .28191E+01         .2213E+01           .149E+01            .2724E-02          .11E+00
 .33571E+01         .54633E+01          .1016E+02           .35513E-01         .64E+00
 .28003E-00         .66838E-02          .26342E-01
```

Flow Chart. This flow chart details the major steps in an AFIT FORTRAN program which computes the critical radius and fast and thermal flux distribution for an infinitely reflected spherical geometry.

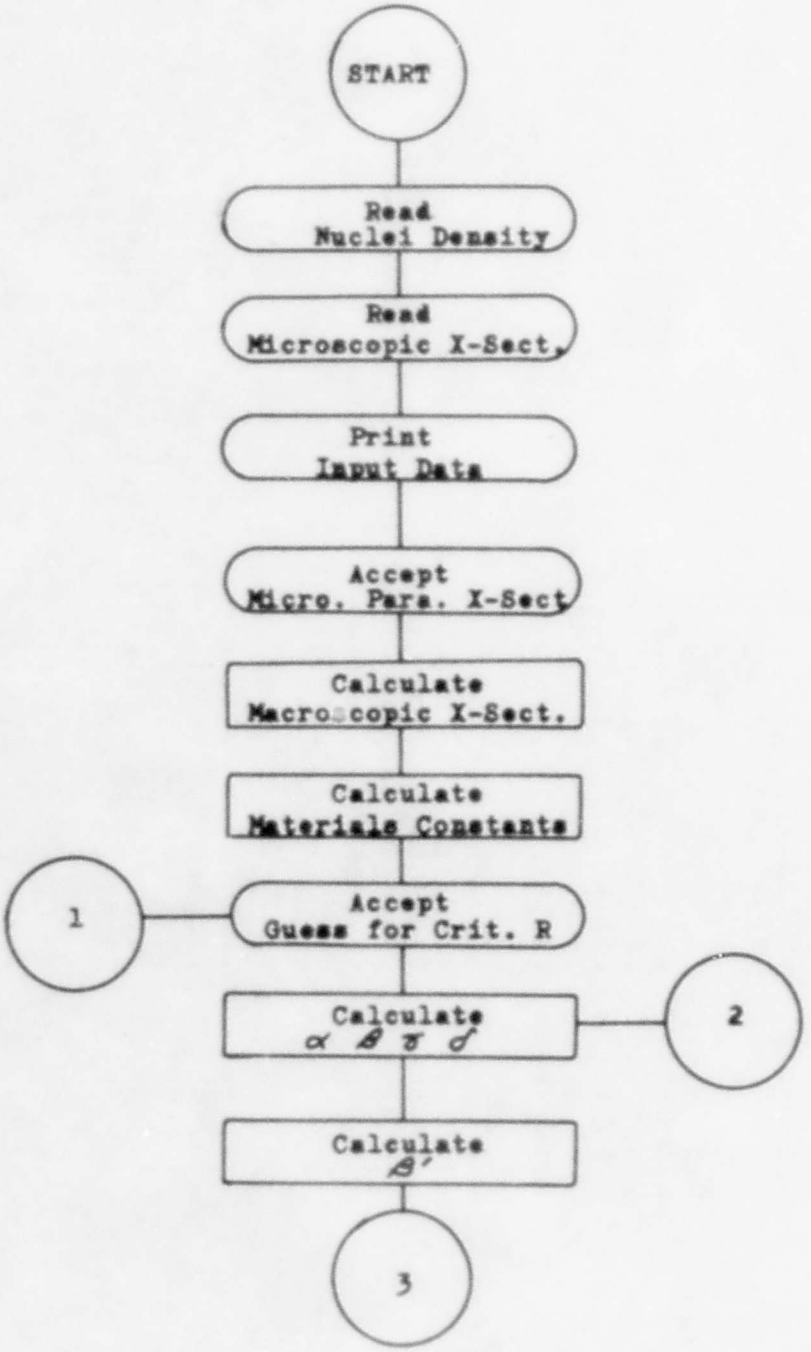

BLANK PAGE

```
0.4      .03
 .1082E-02    .45069E-01   .28301E-01   .4789E-01    .4789E-01
 .24682E+01   .27653E+01   .10554E+02   .257E+03     .315E+03     .305E+03
 .26384E+01   .22130E+01   .149E+01     .2724E-02    .11E+00
 .39106E+01   .54633E+01   .1016E+02    .35513E-01   .64E+00
 .74074E-00   .71545E-02   .2235E-01

0.5      .03      .05
 .902E-03     .44995E-01   .23584E-01   .4789E-01    .4789E-01
 .24689E+01   .27172E+01   .10495E+02   .257E+03     .315E+03     .305E+03
 .26455E+01   .2213E+01    .149E+01     .2724E-02    .11E+00
 .38892E+01   .54633E+01   .1016E+02    .35513E-01   .64E+00
 .71407E-00   .71531E-02   .22262E-01

0.6      .03      .05
 .721E-03     .44921E-01   .18867E-01   .4789E-01    .4789E-01
 .24705E+01   .26265E+01   .10351E+02   .257E+03     .315E+03     .305E+03
 .26637E+01   .2213E+01    .149E+01     .2724E-02    .11E+00
 .38408E+01   .54633E+01   .1016E+02    .35513E-01   .64E+00
 .66433E-00   .71292E-02   .22311E-01

0.7      .03      .05
 .541E-03     .44847E-01   .1415E-01    .4789E-01    .4789E-01
 .24745E+01   .2/496E+01   .10019E+02   .257E+03     .315E+03     .305E+03
 .27050E+01   .2213E+01    .149E+01     .2724E-02    .11E+00
 .37329E+01   .54633E+01   .1016E+02    .35513E-01   .64E+00
 .56825E-00   .70378E-02   .22761E-01

0.6      .03      .025
 .222E-02     .42823E-01   .18267E-01   .4789E-01    .4789E-01
 .24967E+01   .19147E+01   .87107E+01   .257E+03     .315E+03     .305E+03
 .28191E+01   .2213E+01    .149E+01     .2724E-02    .11E+00
 .33571E+01   .54633E+01   .1016E+02    .35513E-01   .64E+00
 .28003E-00   .66838E-02   .26342E-01
```

Flow Chart. This flow chart details the major steps in an AFIT FORTRAN program which computes the critical radius and fast and thermal flux distribution for an infinitely reflected spherical geometry.

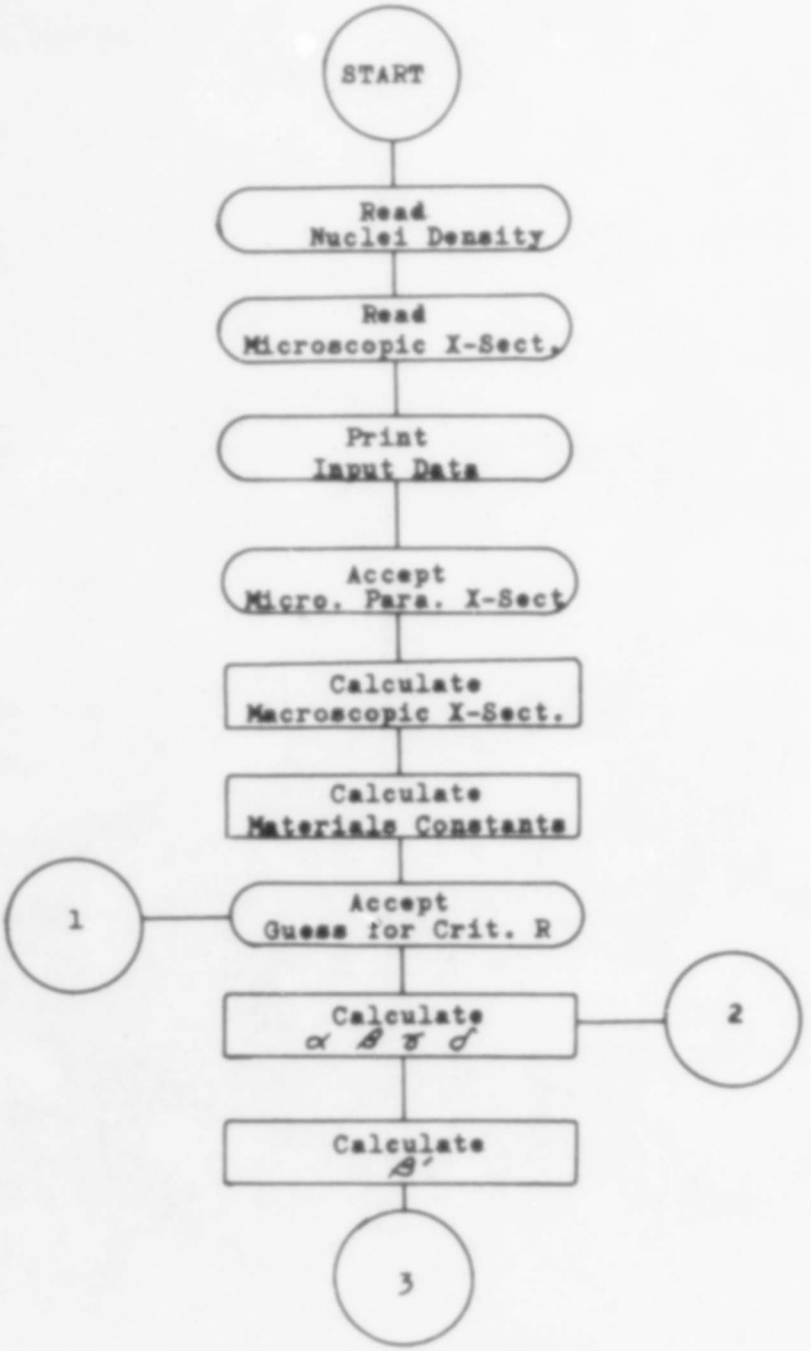

BLANK PAGE

```
0.4      .03      .05
.1082E-02    .45069E-01   .28301E-01   .4789E-01    .4789E-01
.24682E+01   .27653E+01   .10554E+02   .257E+03     .315E+03    .305E+03
.26384E+01   .22130E+01   .149E+01       .2724E-02  .11E+00
.39106E+01   .54633E+01   .1016E+02      .35513E-01 .64E+00
.74074E-00   .71545E-02   .2235E-01

0.5      .03      .05
.902E-03     .44995E-01   .23584E-01   .4789E-01    .4789E-01
.24689E+01   .27172E+01   .10495E+02   .257E+03     .315E+03    .305E+03
.26455E+01   .2213E+01    .149E+01     .2724E-02    .11E+00
.38892E+01   .54633E+01   .1016E+02    .35513E-01   .64E+00
.71407E-00   .71531E-02   .22262E-01

0.6      .03      .05
.721E-03     .44921E-01   .18867E-01   .4789E-01    .4789E-01
.24705E+01   .26265E+01   .10351E+02   .257E+03     .315E+03    .305E+03
.26637E+01   .2213E+01    .149E+01     .2724E-02    .11E+00
.38408E+01   .54633E+01   .1016E+02    .35513E-01   .64E+00
.66433E-00   .71292E-02   .22311E-01

0.7      .03      .05
.541E-03     .44847E-01   .1415E-01    .4789E-01    .4789E-01
.24745E+01   .24496E+01   .10019E+02   .257E+03     .315E+03    .305E+03
.27050E+01   .2213E+01    .149E+01     .2724E-02    .11E+00
.37329E+01   .54633E+01   .1016E+02    .35513E-01   .64E+00
.56825E-00   .70378E-02   .22761E-01

0.6      .03      .025
.222E-02     .42823E-01   .18267E-01   .4789E-01    .4789E-01
.24967E+01   .19147E+01   .87107E+01   .257E+03     .315E+03    .305E+03
.28191E+01   .2213E+01    .149E+01     .2724E-02    .11E+00
.33571E+01   .54633E+01   .1016E+02    .35513E-01   .64E+00
.28003E-00   .66838E-02   .26342E-01
```

Flow Chart. This flow chart details the major steps in an AFIT FORTRAN program which computes the critical radius and fast and thermal flux distribution for an infinitely reflected spherical geometry.

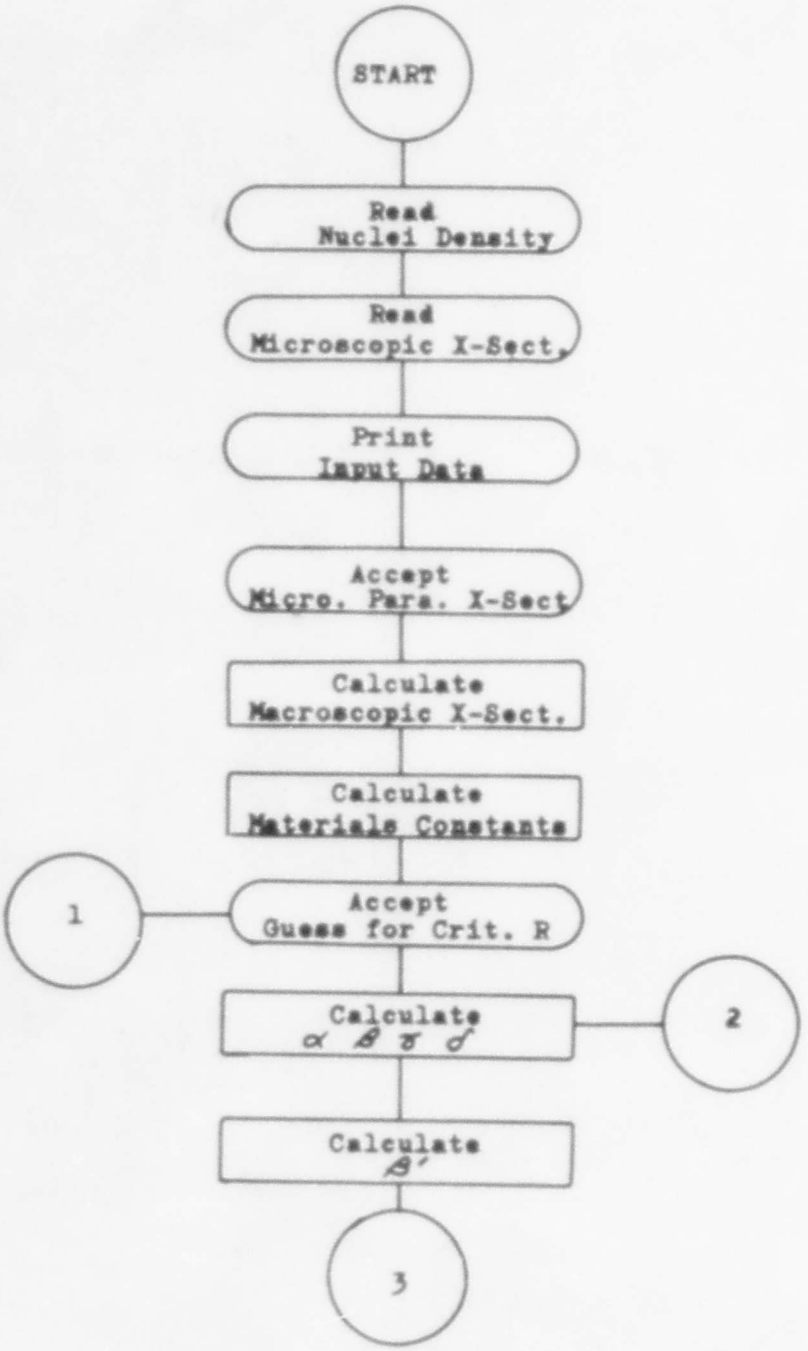

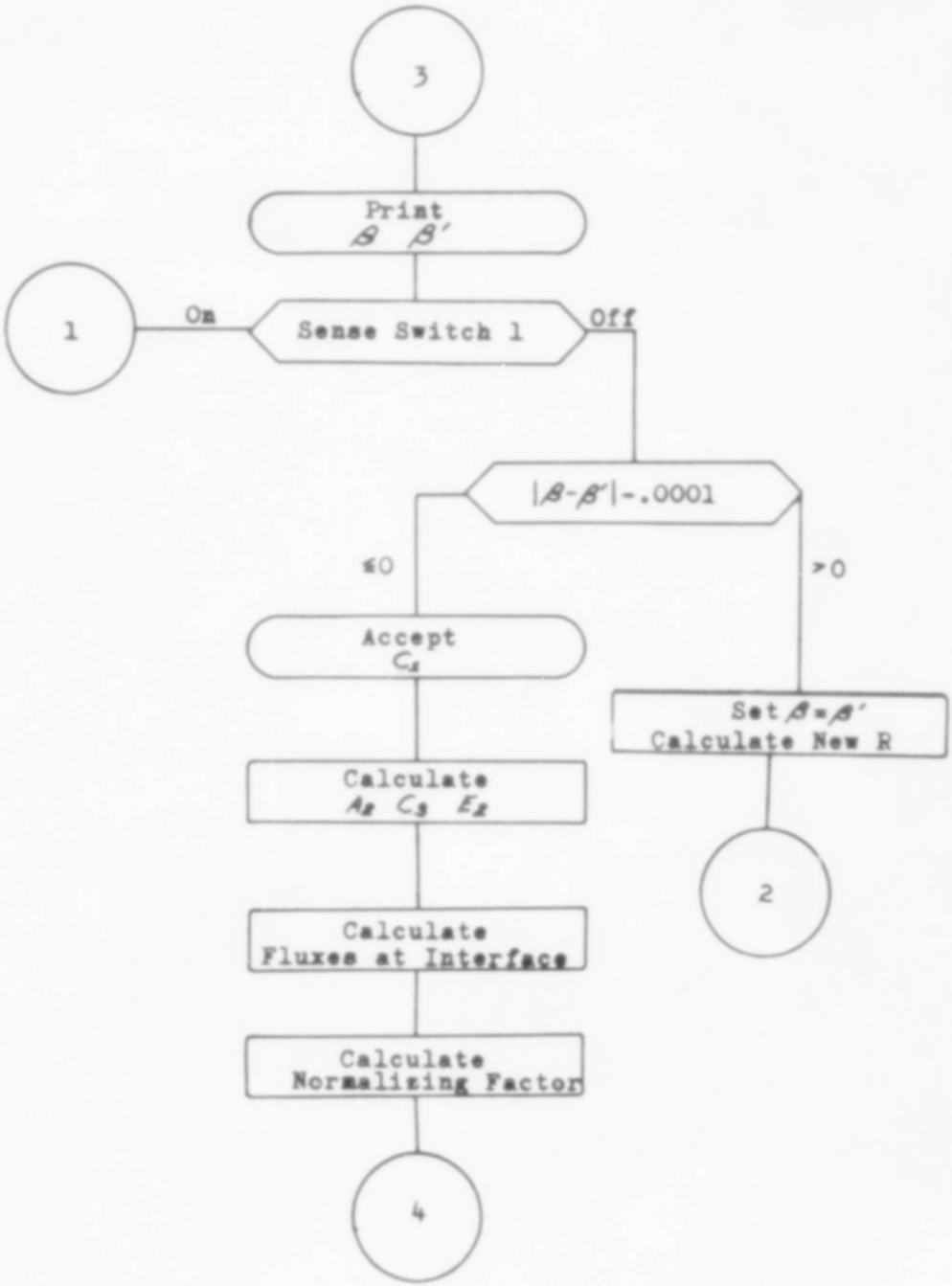
3
Print
β β'
1
On
Sense Switch 1
Off
|β-β'|-.0001
≤0
>0
Accept
C_z
Set β=β'
Calculate New R
Calculate
A_z C_3 E_z
2
Calculate
Fluxes at Interface
Calculate
Normalizing Factor
4

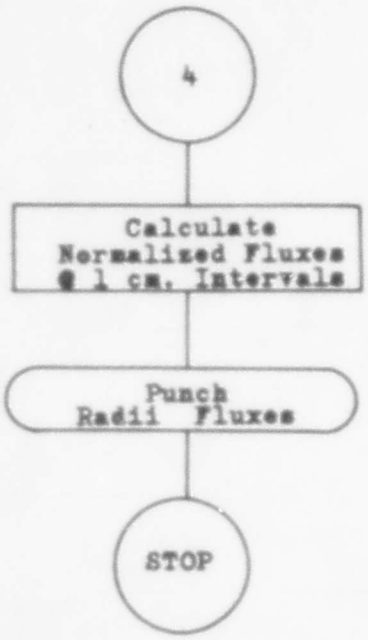
4
Calculate
Normalized Fluxes
@ 1 cm. Intervals
Punch
Radii Fluxes
STOP

BLANK PAGE

```
C       AFIT FORTRAN PROGRAM TO DETERMINE CRITICAL RADIUS AND NORMALIZED
C       FLUX DISTRIBUTION FOR AN INFINITELY REFLECTED SPHERICAL GEOMETRY
C       USING TWO-GROUP DIFFUSION THEORY      31 MARCH 1964


        PRINT 500
        PRINT 501
        PRINT 502
   10   READ, CU, CAL, CN, RAL, RN
C       CU=ATOM DENSITY OF U IN CORE PER BARN-CUBIC CENTIMETER
C       CAL=ATOM DENSITY OF AL IN CORE PER BARN-CUBIC CENTIMETER
C       CN=ATOM DENSITY OF N IN CORE PER BARN-CUBIC CENTIMETER
C       RAL=ATOM DENSITY OF AL IN REFLECTOR PER BARN-CUBIC CENTIMETER
C       RN=ATOM DENSITY OF N IN REFLECTOR PER BARN-CUBIC CENTIMETER
        READ, FV235, FF235, FT235, TF235, TT235, TC235
C       FV235=AVERAGE NUMBER OF NEUTRONS PER FAST FISSION
C       FF235=MICRO FAST FISSION CROSS SECTION FOR U235
C       FT235=MICRO FAST TRANSPORT CROSS SECTION FOR U235, BARNS
C       TF235=MICRO THERMAL FISSION CROSS SECTION FOR U235
C       TT235=MICRO THERMAL TRANSPORT CROSS SECTION FOR U235, BARNS
C       TC235=MICRO THERMAL TOTAL ABSORPTION CROSS SECTION FOR U235
        READ, CFTAL, RFTAL, TTAL, RFSAL, TCAL
C       CFTAL=MICRO FAST TRANS CROSS SECTION FOR AL IN CORE, BARNS
C       RFTAL=MICRO FAST TRANS CROSS SECTION FOR AL IN REFLECTOR, BARNS
C       TTAL=MICRO THERMAL TRANS CROSS SECTION FOR ALUMINUM
C       RFSAL=MICRO FAST REMOVAL (SCATTER) CROSS SECTION FOR AL IN REFLECTOR
C       TCAL=MICRO THERMAL TOTAL ABSORPTION CROSS SECTION FOR ALUMINUM
        READ, CFTN, RFTN, TTN, RFSN, TCN
C       CFTN=MICRO FAST TRANS CROSS SECTION FOR N IN CORE, BARNS
C       RFTN=MICRO FAST TRANS CROSS SECTION FOR N IN REFLECTOR, BARNS
C       TTN=MICRO THERMAL TRANS CROSS SECTION FOR NITROGEN
C       RFSN=MICRO FAST REMOVAL (SCATTER) CROSS SECTION FOR N IN REFLECTOR
C       TCN=MICRO THERMAL TOTAL ABSORPTION CROSS SECTION FOR NITROGEN
        PRINT 504, CU,CAL,CN,RAL,RN,FV235,FF235,FT235,TF235,TT235,TC235
        PRINT 504, CFTAL,RFTAL,TTAL,RFSAL,TCAL,CFTN,RFTN,TTN,RFSN,TCN
        PRINT 518
        ACCEPT 519, FC235, CFCAL, CFCN
C       FC235=MICRO FAST NONFISSION ABSORPTION CROSS SECTION FOR U235
C       CFCAL=MICRO FAST ABSORPTION CROSS SECTION FOR ALUMINUM
C       CFCN=MICRO FAST ABSORPTION CROSS SECTION FOR NITROGEN
   20   CTSGC=CU*TC235+CAL*TCAL+CN*TCN
C       CTSGC=MACRO THERMAL TOTAL ABSORPTION CROSS SECTION IN CORE
        CTDIK=1./(3.*(CU*TT235+CAL*TTAL+CN*TTN))
C       CTDIK=THERMAL DIFFUSION COEFFICIENT IN CORE
        RTSGC=RAL*TCAL+RN*TCN
C       RTSGC=MACRO THERMAL TOTAL ABSORPTION CROSS SECTION IN REFLECTOR
        RTDIK=1./(3.*(RAL*TTAL+RN*TTN))
C       RTDIK=THERMAL DIFFUSION COEFFICIENT IN REFLECTOR
        CFSGC=CU*FC235+CAL*CFCAL+CN*CFCN
C       CFSGC=MACRO FAST ABSORPTION (NONFISSION) CROSS SECTION IN CORE
        FSGFI=CU*FF235
C       FSGFI=MACRO FAST FISSION CROSS SECTION (U235 IN CORE)
        CFDIK=1./(3.*(CU*FT235+CAL*CFTAL+CN*CFTN))
C       CFDIK=FAST DIFFUSION COEFFICIENT IN CORE
        RFSGS=RAL*RFSAL+RN*RFSN
C       RFSGS=MACRO FAST REMOVAL (SCATTER) CROSS SECTION IN REFLECTOR
        RFDIK=1./(3.*(RAL*RFTAL+RN*RFTN))
C       RFDIK=FAST DIFFUSION COEFFICIENT IN REFLECTOR
```

```
      TSGFI=CU*TF235
C     TSGFI=MACRO THERMAL FISSION CROSS SECTION (U235 IN CORE)
      PRINT 505, CTSGC, CTDIK, RTSGC, RTDIK, CFSGC
      PRINT 505, FSGFI, CFDIK, RFSGS, RFDIK, TSGFI

C     SECTION OF PROGRAM TO COMPUTE CRITICAL RADIUS

   30 XK1R=SQRT(RFSGS/RFDIK)
      XK2R=SQRT(RTSGC/RTDIK)
      XB1C=SQRT(((FV235-1.)*FSGFI-CFSGC)/CFDIK)
      XB2C=SQRT(CTSGC/CTDIK)
      RHO1=RFDIK/CFDIK
      RHO2=RTDIK/CTDIK
      XM=RFSGS/RTDIK
      XMP=2.43*TSGFI/CFDIK
      XH1=XMP/(XB1C**2+XB2C**2)
      XH2=XM/(XK2R**2-XK1R**2)
      XE1=RHO2*XH1*XH2
   38 PRINT 520
      ACCEPT 521, RAD
   40 Z3=EXPF(XB2C*RAD)
      Z4=1./Z3
      ALPHA=XB2C*((Z3+Z4)/(Z3-Z4))-1./RAD
      GAMMA=-XK1R-1./RAD
      DELTA=-XK2R-1./RAD
      Z5=XE1*ALPHA*(DELTA-GAMMA)+RHO1*GAMMA*(RHO2*DELTA-ALPHA)
      Z6=RHO2*DELTA-ALPHA-XE1*(GAMMA+DELTA)
      PRIME=Z5/Z6
      BETA=XB1C*COSF(XB1C*RAD)/SINF(XB1C*RAD)-1./RAD
      PRINT 515, BETA, PRIME
C     SELECT RAD LESS THAN CRITICAL RADIUS BEFORE ATTEMPTING TO CONVERGE
            IF(SENSE SWITCH 1)38,44
   44 IF(ABS(BETA-PRIME)-.0001)60,60,45
C     NEWTON-RAPHSON SOLUTION FOR TRANSCENDENTAL EQUATION
   45 BETA=PRIME
   50 Z7=(XB1C*COSF(XB1C*RAD)/SINF(XB1C*RAD))-(1./RAD)-BETA
      Z8=-(XB1C**2)*((1./SINF(XB1C*RAD))**2)+(1./(RAD**2))
      XRAD=RAD-Z7/Z8
      PRINT 516, RAD, XRAD
C     NEW VALUE OF RADIUS MAY BE ENTERED IF SOLUTION DIVERGES
            IF(SENSE SWITCH 2)54,53
   54 PRINT 520
       ACCEPT 521, XRAD
      GO TO 55
   53 IF(ABS(XRAD-RAD )-.0001)40,40,55
   55 RAD=XRAD
      GO TO 50
```

```
C       SECTION OF PROGRAM TO COMPUTE FLUX DISTRIBUTION IN CORE AND REFLECTOR

   60   X=.5*(Z3-Z4)/RAD
        Y=SINF(XB1C*RAD)/RAD
        Z1=EXPF(-XK1R*RAD)/RAD
        Z2=EXPF(-XK2R*RAD)/RAD
        PRINT 590
        ACCEPT 521, C1
C       C1=POWER LEVEL VARIABLE AT CRITICALITY
        A2=C1*X*(ALPHA-RHO2*DELTA)/RHO2*XH2*Z1*(GAMMA-DELTA)
        A4=(C1*X-A2*XH2*Z1)/Z2
        C3=(C1*XH1*X+A2*Z1)/Y
C       VALUES OF CONSTANTS IN DIFFUSION EQUATIONS, IN TERMS OF C1
        TFLC=C1*X
C       TFLC=THERMAL FLUX IN CORE
        XNORM=TFLC
C       XNORM=NORMALIZATION FACTOR FOR ALL FLUXES
        FFLC=C3*Y-XH1*TFLC
C       FFLC=FAST FLUX IN CORE
        FFLR=A2*Z1
C       FFLR=FAST FLUX IN REFLECTOR
        TFLR=A4*Z2+XH2*FFLR
C       TFLR=THERMAL FLUX IN REFLECTOR
        PRINT 600, A2, A4, C3
        PRINT 601
        PRINT 605, RAD, FFLC, FFLR, TFLC, TFLR
        RAD=0.0
  120           IF(SENSE SWITCH 1)110,115
  110   RAD=RAD+0.05
        GO TO 130
  115   RAD=RAD+1.0
  130   Z3=EXPF(XB2C*RAD)
        Z4=1./Z3
        X=.5*(Z3-Z4)/RAD
        Y=SINF(XB1C*RAD)/RAD
        Z1=EXPF(-XK1R*RAD)/RAD
        Z2=EXPF(-XK2R*RAD)/RAD
        TFLC=(C1*X)/XNORM
        FFLC=((C3*Y)/XNORM)-XH1*TFLC
        FFLR=(A2*Z1)/XNORM
        TFLR=((A4*Z2)/XNORM)+XH2*FFLR
              IF(SENSE SWITCH 2)150,140
  140   PRINT 605, RAD, FFLC, FFLR, TFLC, TFLR
        GO TO 160
  150   PUNCH 606, RAD, FFLC, FFLR, TFLC, TFLR
```

```
500 FORMAT(/8X,49HAFIT FORTRAN PROGRAM TO DETERMINE CRITICAL RADIUS)
501 FORMAT(/8X,49HAND FLUX DISTRIBUTION FOR AN INFINITELY REFLECTED/)
502 FORMAT(7X,51HSPHERICAL GEOMETRY USING TWO-GROUP DIFFUSION THEORY/)
504 FORMAT(/(E15.8))
505 FORMAT(/(E20.8))
515 FORMAT(/5HBETA=F10.6,4X,6HPRIME=F10.6/)
516 FORMAT(/4HRAD=F10.4,4X,5HXRAD=F10.4/)
518 FORMAT(/39HENTER FC235, CFCAL, CFCN, FORMAT 3E15.8)
519 FORMAT(3E15.8)
520 FORMAT(//41HENTER RADIUS IN CENTIMETERS, FORMAT F10.4)
521 FORMAT(F10.4)
590 FORMAT(/36HENTER C1 (POWER LEVEL), FORMAT F10.4)
600 FORMAT(/3HA2=E14.8,4X,3HA4=E14.8,4X,3HC3=E14.8/)
601 FORMAT(/6X,3HRAD,12X,4HFFLC,11X,4HFFLR,11X,4HTFLC,11X,4HTFLR/)
605 FORMAT(5E15.8/)
606 FORMAT(5E15.8)
160          IF(SENSE SWITCH 3)10,120
    END
```

```
        AFIT FØRTRAN PRØGRAM TØ DETERMINE CRITICAL RADIUS
        AND FLUX DISTRIBUTIØN FØR AN INFINITELY REFLECTED
       SPHERICAL GEØMETRY USING TWØ-GRØUP DIFFUSIØN THEØRY

   .29550000E-02
   .41794000E-01
   .17973000E-01
   .47890000E-01
   .47890000E-01
   .25051000E+01
   .18036000E+01
   .83686000E+01
   .25700000E+03
   .31500000E+03
   .30500000E+03
   .28609000E+01
   .22130000E+01
   .14900000E+01
   .27240000E-02
   .11000000E+00
   .32280000E+01
   .54633000E+01
   .10160000E+02
   .35513000E-01
   .64000000E+00
ENTER FC235, CFCAL, CFCN, FØRMAT 3E15.8
  .22514E-00      .6417E-02       .27964E-01
        .91737506E+00
        .28351814E+00
        .35917500E-01
        .59745882E+00
        .14360777E-02
        .53296380E-02
        .16475998E+01
        .18311699E-02
        .90673833E+00
        .75943500E+00

ENTER RADIUS IN CENTIMETERS, FØRMAT F10.4
     5.0
BETA=  -.006706     PRIME=  -.1313..

ENTER RADIUS IN CENTIMETERS, FØRMAT F10.4
     1.0
BETA=  -.001332     PRIME=  -.587785

ENTER RADIUS IN CENTIMETERS, FØRMAT F10.4
    10.0
BETA=  -.013692     PRIME=  -.074958

ENTER RADIUS IN CENTIMETERS, FØRMAT F10.4
    15.0
BETA=  -.021296     PRIME=  -.056224

ENTER RADIUS IN CENTIMETERS, FØRMAT F10.4
    20.0
```

```
BETA=  -.030002     PRIME=  -.046867

ENTER RADIUS IN CENTIMETERS, FORMAT F10.4
    25.0
BETA=  -.040617     PRIME=  -.041257

ENTER RADIUS IN CENTIMETERS, FORMAT F10.4
    30.0
BETA=  -.054697     PRIME=  -.037518

ENTER RADIUS IN CENTIMETERS, FORMAT F10.4
    25.0
BETA=  -.040617     PRIME=  -.041257

RAD=    25.0000     XRAD=    25.2670

RAD=    25.2670     XRAD=    25.2650

RAD=    25.2650     XRAD=    25.2650

BETA=  -.041257     PRIME=  -.041022

RAD=    25.2650     XRAD=    25.1683

RAD=    25.1683     XRAD=    25.1680

RAD=    25.1680     XRAD=    25.1680

BETA=  -.041022     PRIME=  -.041107

ENTER C1 (POWER LEVEL), FORMAT F10.4
     1.0
A2= .13820585E+15     A4= .10977285E+23     C3= .79312047E+19

        RAD              FFLC             FFLR             TFLC             TFLR
 .25168078E+02   .17700000E+13   .17720547E+13   .91128345E+18   .91128337E+18
 .10000000E+01   .54987858E+00   .14499606E-03   .32245173E-17   .94266569E+04
 .20000000E+01   .54877996E+00   .69312158E-04   .10008729E-16   .36884502E+04
 .30000000E+01   .54695195E+00   .44177530E-04   .40347244E-16   .19242829E+04
 .40000000E+01   .54439881E+00   .31677137E-04   .18284916E-15   .11293964E+04
 .50000000E+01   .54112673E+00   .24228087E-04   .88387811E-15   .70705408E+03
 .60000000E+01   .53714350E+00   .19302836E-04   .44506197E-14   .46109204E+03
 .70000000E+01   .53245867E+00   .15818220E-04   .23050619E-13   .30928374E+03
 .80000000E+01   .52708343E+00   .13232713E-04   .12187089E-12   .21177825E+03
 .90000000E+01   .52103061E+00   .11245521E-04   .65457045E-12   .14758436E+03
 .10000000E+02   .51431466E+00   .96762119E-05   .35596579E-11   .10375376E+03
```

Appendix E

Temperature Distribution in the Fuel Particles

Before the probable integrity of the fuel particles can be determined, it is necessary to know the temperatures which will exist in the particles. These temperatures will depend on both the rate of heat generation in the fluidized bed and the temperature of the fluid. If it is assumed that the film coefficient of heat transfer in the bed is effectively infinite, then the surface of the particles will be at the same temperature as the surrounding fluid. Without specifying a fluid temperature, it is possible to determine the rise in temperature in the particles (above fluid temperature) on the basis of the rate of volumetric heat generation in the fuel section of the particles.

To obtain the volumetric heat generation rate, the thermal power in the bed and the volume of UN in the bed must be known (assuming all heating is in the UN part of the particles). For fuel particles with a UN core 0.06 cm. in diameter, and an 0.02 cm. AlN coating, the thermal power in the bed is between 1.2 Mwt/ ft^2 and 6.8 Mwt/ ft^2 for a voidage of between 0.5 and 0.8 (see Appendix C).

If a reactor core radius of 25 cm. is assumed, giving a cross-sectional area of 2.2 ft^2, the thermal power out of the bed will be between 2.6 and 15.0 Mwt, or between 6.2×10^5 and 36×10^5 cal/ sec. The critical mass of U^{235} for this radius is about 80 kg, as given in Figure 6. With a uranium density in UN of 13.52 g/ cc (17:2) there will be 6.3×10^3 cm^3 of UN in the bed. Allowing for a 10% heat loss in the bed, the volumetric heat generation rate will be between 1.08×10^2 and 6.4×10^2 cal/ cm^3 sec.

The temperature in a homogeneous sphere with a uniform volumetric heat production rate, q^1, is given by

$$t(r) = t_i + \frac{q^1}{6 k_1} (r^2_i - r^2) \tag{35}$$

where r_i and t_i are the radius and surface temperature of the sphere. The temperature at the inner (r_i) and outer (r_s) radii of a hollow spherical shell with constant heating on the inside is given by

$$t_i = t_s + \frac{q^1 r^3_i}{k_2} \left(\frac{1}{r_i} - \frac{1}{r_s} \right) \tag{36}$$

These two equations may be written as

$$t_o = t_i + \frac{q^1}{6k_1} r^2_i \qquad t_o = t(r = o) \tag{37}$$

$$t_i = \frac{q^1 r_i^3}{k_2} \left(\frac{1}{r_i} - \frac{1}{r_s} \right) \tag{38}$$

which will give the increase in temperature in the particles at the interface and the center, above the fluid temperature

No values of the thermal conductivity of either UN (k_1) or AlN (k_2) at temperatures above about 800°C are available, so extrapolated values were used. k_1 was taken as 0.08 cgs units and k_2 as 0.02 cgs units for an average temperature of about 2000°C. k_1 is an increasing function of temperature and k_2 is a decreasing function of temperature.

Using equations (37) and (38), with r_i = .03 cm., r_s = .05 cm. and $q' = 1.08 \times 10^2$ cal/ cm^3 sec, t_i = 2°C and t_s = 2.5°C. For $q' = 6.4 \times 10^2$ cal/ cm^3 sec, t_i = 12°C and t_s = 15°C. For thermal conductivities an order of magnitude less, or q' an order of magnitude greater, the values for the maximum q' are t_i = 120°C, t_s = 150°C.

For fuel particles of constant density, an increase in diameter will decrease the voidage at a given mass flow rate. Thus to achieve higher power in the reactor for the same critical mass, it might be possible to go to fewer, larger particles. An increase in the fuel pellet radius from 0.03 to 0.3 cm. would result in a temperature at the center of the particle 50°C above the temperature at the interface (for $q^1 = 1.08 \times 10^2$ cal/ cm^3 sec). If the AlN coating was also increased in thickness from 0.02 to 0.2 cm., the temperature rise from the particle surface to the interface would be 60°C, and thus the total rise would be 110°C.

If a maximum temperature increase of 100°C in the particles is specified as a safe value, it is obvious that increases in particle size to increase power per gram of U^{235} will be limited by the temperature rise in the particles themselves. It appears that a probable upper limit on particle size, for reasonable power levels, is between 0.1 cm and 1.0 cm in diameter.

The problem of maximum power generation per gram of U^{235} is also effected by the cross-sectional area of the core. For radii between 12 and 100 cm., the critical mass, M_c, is given in terms of the critical radius, R_c, by

$$M_c = 20 + 4.45 (R_c - 12) \text{ kg} \tag{39}$$

as can be seen in Figure 6. Thus the cross-sectional area decreases faster that the critical mass ($A = \pi R_c^2$). For a given flow rate and entrance-exit temperature drop, power is a direct function of the cross-sectional area, and so there is probably a minimum core radius for the efficient production of thermal power (assuming that

the real core configuration gives values corresponding to those for the spherical one).

Vita

Kenneth Robert Hooks [redacted] He graduated in 1957 from Washington-Lee High School in Arlington, Virginia. After receiving a Bachelor of Arts degree in Physics from the University of Colorado in 1962, he received his commission as a Second Lieutenant in the USAF Reserve, with immediate assignment to the Air Force Institute of Technology.

[redacted]